Analyses and Historical Reconstruction of Groundwater Flow, Contaminant Fate and Transport, and Distribution of Drinking Water Within the Service Areas of the Hadnot Point and Holcomb Boulevard Water Treatment Plants and Vicinities, U.S. Marine Corps Base Camp Lejeune, North Carolina

Chapter A–Supplement 4
Simulation of Three-Dimensional Groundwater Flow

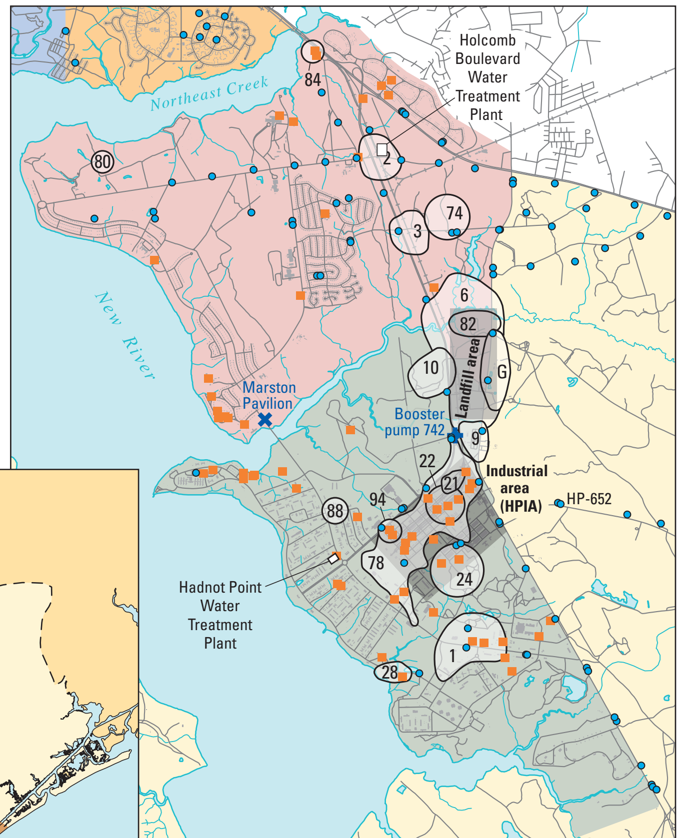

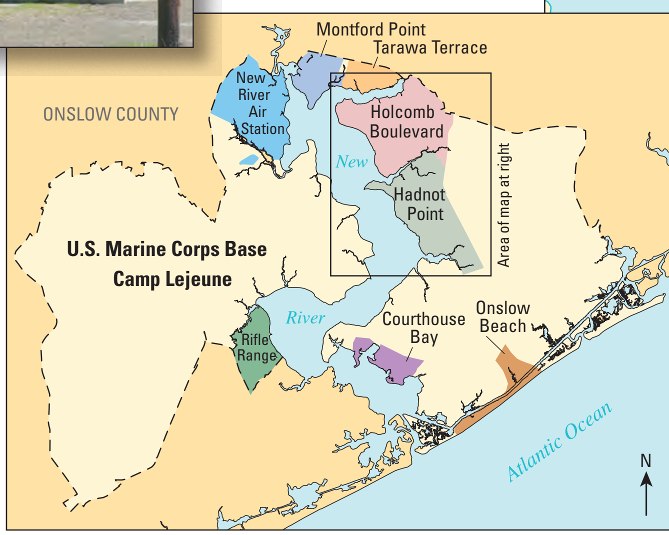

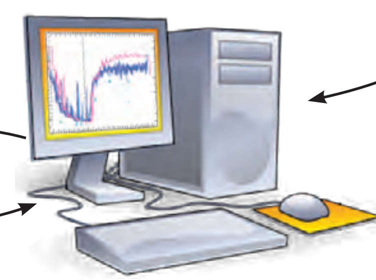

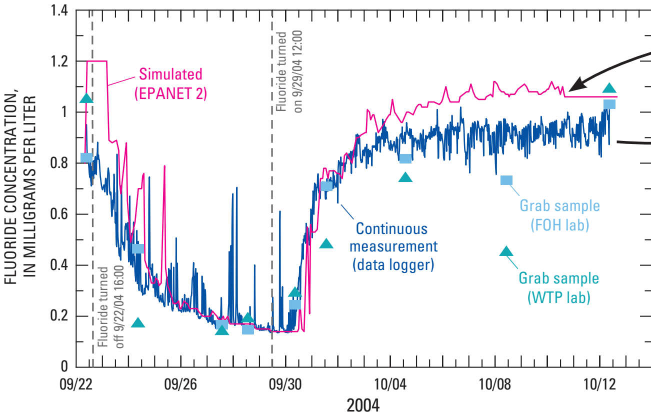

ATSDR
AGENCY FOR TOXIC SUBSTANCES
AND DISEASE REGISTRY

DEPARTMENT OF HEALTH & HUMAN SERVICES · USA

Atlanta, Georgia – March 2013

Front cover: Historical reconstruction process using data, information sources, and water-modeling techniques to estimate historical contaminant concentrations.

Maps: U.S. Marine Corps Base Camp Lejeune, North Carolina; Holcomb Boulevard and Hadnot Point areas showing extent of sampling at Installation Restoration Program sites (white numbered areas), above-ground and underground storage tank sites (orange squares), and water-supply wells (blue circles).

Photograph (upper): Hadnot Point water treatment plant (Building 20).

Photograph (lower): Well house building for water-supply well HP-652.

Graph: Measured fluoride data and simulation results for Paradise Point elevated storage tank (S-2323) for tracer test of the Holcomb Boulevard water-distribution system, September 22–October 12, 2004; simulation results obtained using EPANET 2 water-distribution system model assuming last-in first-out plug flow (LIFO) storage tank mixing model. [WTP lab, water treatment plant water-quality laboratory; FOH lab, Federal Occupational Health Laboratory]

Analyses and Historical Reconstruction of Groundwater Flow, Contaminant Fate and Transport, and Distribution of Drinking Water Within the Service Areas of the Hadnot Point and Holcomb Boulevard Water Treatment Plants and Vicinities, U.S. Marine Corps Base Camp Lejeune, North Carolina

Chapter A–Supplement 4
Simulation of Three-Dimensional Groundwater Flow

By René J. Suárez-Soto, L. Elliott Jones, and Morris L. Maslia

Agency for Toxic Substances and Disease Registry
U.S. Department of Health and Human Services
Atlanta, Georgia

March 2013

Authors

René J. Suárez-Soto, MSEnvE, EIT
Environmental Health Scientist
Agency for Toxic Substances and Disease Registry
Division of Community Health Investigations
Atlanta, Georgia

L. Elliott Jones, MS, PE
Hydrologist
U.S. Geological Survey
Georgia Water Science Center
Atlanta, Georgia

Morris L. Maslia, MSCE, PE, D.WRE, DEE
Research Environmental Engineer and Project Officer
Agency for Toxic Substances and Disease Registry
Division of Community Health Investigations
Exposure-Dose Reconstruction Project
Atlanta, Georgia

For additional information write to:

Project Officer
Exposure-Dose Reconstruction Project
Division of Community Health Investigations
Agency for Toxic Substances and Disease Registry
4770 Buford Highway, Mail Stop F-59
Atlanta, Georgia 30341-3717

Suggested citation

Suárez-Soto RJ, Jones LE, and Maslia, ML. Simulation of Three-Dimensional Groundwater Flow—Supplement 4. In: Maslia ML, Suárez-Soto RJ, Sautner JB, Anderson BA, Jones LE, Faye RE, Aral MM, Guan J, Jang W, Telci IT, Grayman WM, Bove FJ, Ruckart PZ, and Moore SM. Analyses and Historical Reconstruction of Groundwater Flow, Contaminant Fate and Transport, and Distribution of Drinking Water Within the Service Areas of the Hadnot Point and Holcomb Boulevard Water Treatment Plants and Vicinities, U.S. Marine Corps Base Camp Lejeune, North Carolina—Chapter A: Summary and Findings. Atlanta, GA: Agency for Toxic Substances and Disease Registry; 2013.

Contents

Figures

Tables (Tables S4.6 and S4.8 are in back of report)

See the Chapter A report for conversion factors and definitions of terms and abbreviations used throughout this supplement.

Analyses and Historical Reconstruction of Groundwater Flow, Contaminant Fate and Transport, and Distribution of Drinking Water Within the Service Areas of the Hadnot Point and Holcomb Boulevard Water Treatment Plants and Vicinities, U.S. Marine Corps Base Camp Lejeune, North Carolina

Chapter A–Supplement 4 Simulation of Three-Dimensional Groundwater Flow

By René J. Suárez-Soto,[1] L. Elliott Jones,[2] and Morris L. Maslia[1]

Introduction

The purpose of the study described in this supplement of Chapter A (Supplement 4) is to construct, simulate, and calibrate a groundwater-flow model that represents the hydrogeologic framework and related groundwater-flow conditions described by Faye (2012) and Faye et al. (2013) within the vicinity of the Hadnot Point–Holcomb Boulevard (HPHB) study area, U.S. Marine Corp Base (USMCB) Camp Lejeune (Figure S4.1). Multiple variants of the groundwater-flow model were constructed and are described herein. The models simulate groundwater-flow conditions in the Brewster Boulevard, Tarawa Terrace, and Upper and Middle Castle Hayne aquifer systems from January 1942 to June 2008. Much of the discussion and analyses described herein parallel and partially duplicate methods and approaches described in similar reports of groundwater-flow investigations at Tarawa Terrace (TT) and vicinity by Faye and Valenzuela (2007). Model results were eventually used within several contaminant fate and transport models described by Jones et al. (2013) and Jang et al. (2013) for the historical reconstruction of finished-water[3] concentrations within the service areas of the Hadnot Point and Holcomb Boulevard water treatment plants (HPWTP and HBWTP, respectively). This supplement focuses on the description of groundwater-flow model geometry, boundaries, hydraulic properties, calibration, and sensitivity analyses.

---

[1] Agency for Toxic Substances and Disease Registry, Atlanta, Georgia.

[2] U.S. Geological Survey, Georgia Water Science Center, Atlanta, Georgia.

[3] For this study, finished water is defined as groundwater (or raw water) that has undergone treatment at a WTP and is delivered to a person's home or other facility.

Background

A study and reconstruction of historical contamination events in finished water at USMCB Camp Lejeune, North Carolina, is being conducted by the Agency for Toxic Substances and Disease Registry (ATSDR). USMCB Camp Lejeune has been used as a military training facility since 1942 and is located in Onslow County in the central part of the North Carolina Coastal Plain. The Base is located south of the City of Jacksonville and about 70 miles northeast of the City of Wilmington (Figure S4.1).

The historical reconstruction of contaminant fate and transport in groundwater of the TT base housing area of USMCB Camp Lejeune and historical finished-water concentrations supplied by the TT water treatment plant have been extensively studied by ATSDR. Those studies, analyses, and results are described in previous reports (Maslia et al. 2007, 2009a; Faye and Green 2007; Jang and Aral 2008). Current studies (2010 and thereafter) focus on historical reconstruction of contaminant concentrations in groundwater and finished water in the HPWTP and HBWTP service areas (also referred to herein as the HPHB study area). This reconstruction process requires gathering information about the groundwater system, characterization of contaminant sources and simulation of contaminant fate and transport in groundwater and in finished water. The water treatment plants serving these areas of the Base obtained groundwater from 96 water-supply wells (hereafter referred to as wells or supply wells) distributed in these areas and the east side of USMCB Camp Lejeune (Figure S4.1). Therefore, information on the historical operational schedules of these wells is a prerequisite for the simulation of groundwater flow, contaminant fate

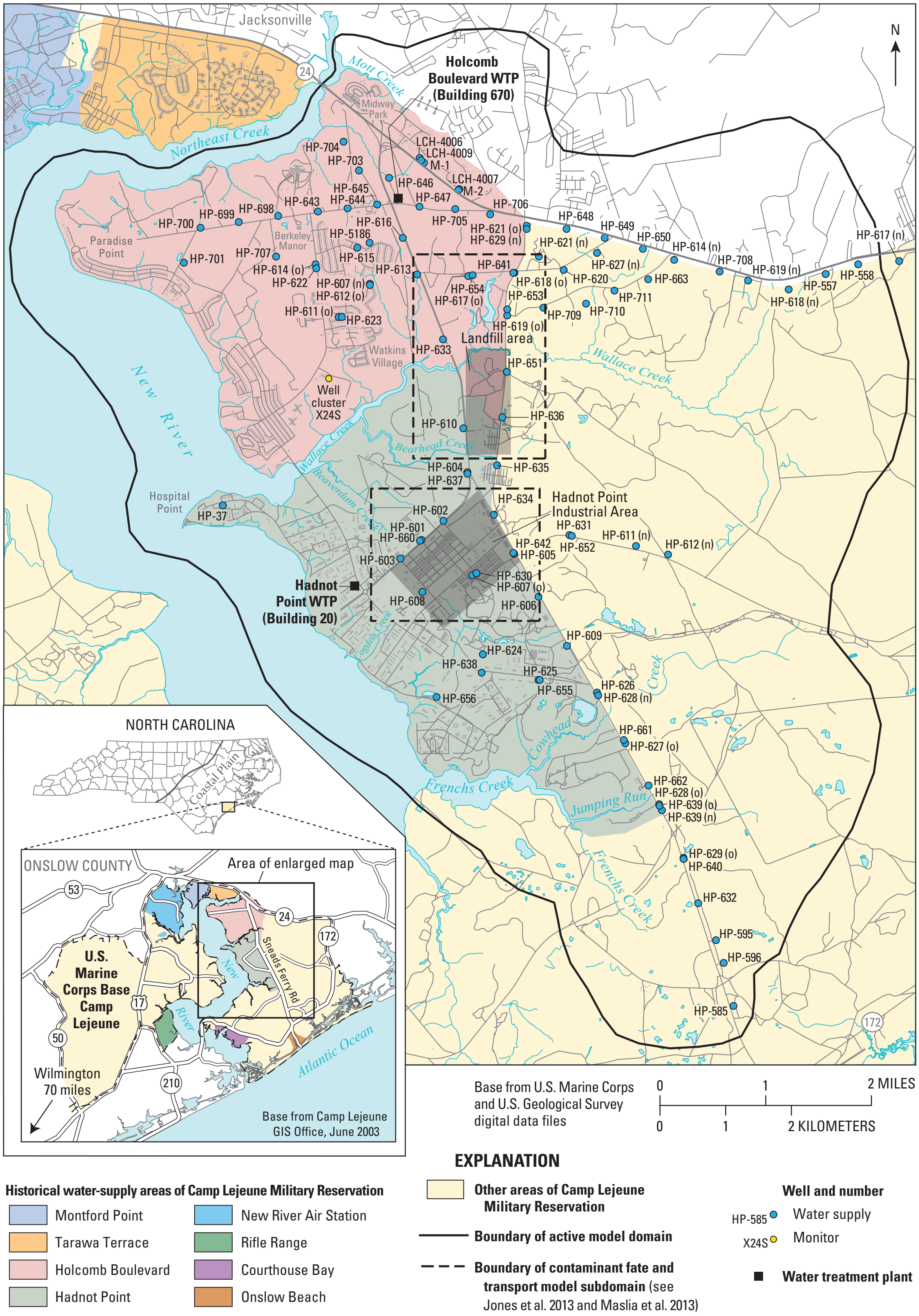

Figure S4.1. Hadnot Point–Holcomb Boulevard study area showing active groundwater-flow model boundary, contaminant fate and transport model subdomain boundaries, and selected monitor and water-supply wells, Hadnot Point–Holcomb Boulevard study area, U.S. Marine Corps Base Camp Lejeune, North Carolina.

and transport, and the distribution of finished water in the HPHB study area. Refer to Sautner et al. (2013) and Telci et al. (2013) for a detailed discussion of historical operation of water-supply wells.

Several groundwater-flow models have been constructed in or around the study area and have been summarized in reports published by Giese et al. (1997), Faye and Valenzuela (2007), and Baker Environmental, Inc. (1998a,b). The analyses and three-dimensional numerical groundwater-flow models described in these references range from regional to local.

Giese et al. (1997) developed and calibrated a groundwater-flow model of the entire North Carolina Coastal Plain as part of the U.S. Geological Survey (USGS) Regional Aquifer-System Analysis (RASA) program. The purpose of this study was to develop an understanding of regional groundwater-flow systems and support better management of groundwater resources; therefore, the simulated information relevant to the USMCB Camp Lejeune area is highly generalized (Faye and Valenzuela 2007).

The groundwater-flow models described by Baker Environmental, Inc. (1998a,b) generally coincide with the area of interest described in Maslia et al. (2013). Under the Basewide Remediation Assessment Groundwater Study (BRAGS), the BRAGS model—described by Baker (1998a)—was constructed to evaluate the effects of various groundwater remediation projects. As part of the BRAGS model, several local models were developed for multiple sites—including Sites 73 and 82—using a variably spaced grid and particle-tracking analysis[4] to assess remediation efforts (Baker Environmental, Inc. 1998a,b).

Model simulations of groundwater flow at and in the vicinity of TT (Figure S4.1) were described by Faye and Valenzuela (2007). The model domain for the TT study is slightly north of the HPHB study area, and many of the hydrogeologic features apply to the current study. Much of the analyses described by Faye and Valenzuela (2007) parallel the analyses applied at the HPHB study area or served as guidelines for the development and calibration of the groundwater-flow model described in this supplement. Ultimately, the goal of the current study was to estimate historical monthly contaminant concentrations at multiple sites within the HPHB study area and specifically within the Hadnot Point Industrial Area (HPIA) and the Hadnot Point landfill (HPLF) area[5] (Figure S4.1); therefore, models discussed previously were not appropriate for this purpose. However, the information presented in these reports was used as guidelines to develop the numerical models presented herein.

[4] See Maslia et al. (2013) for sites 73 and 82 locations; see Faye et al. (2010) for details on site histories.

[5] The Hadnot Point Industrial Area (HPIA) is a formally designated name and acronym used in many Camp Lejeune references [e.g., Baker Environmental, Inc. (1994), CH2M HILL (2006)], and the ATSDR Hadnot Point–Holcomb Boulevard Chapter reports and Chapter A supplements follow this naming convention. The acronym HPLF is used in the ATSDR Hadnot Point–Holcomb Boulevard report series for brevity and convenience to identify the Hadnot Point landfill.

Hydrogeologic Framework

Fourteen aquifers and confining units were identified within the HPHB study area and were named after local cultural features where the units were first identified or as subdivisions of the Castle Hayne Formation (Harned et al. 1989; Geophex, Ltd. 1994, 2001, 2002; Faye 2012). Named hydrogeologic units are correlated with geologic units, and respective groundwater-flow model layers are in Table S4.1. Sediments correlated with the Brewster Boulevard aquifer and confining unit by Faye (2012) between Northeast and Wallace Creeks (Figure S4.1) thicken considerably south of Wallace Creek and were subdivided, for purposes of this study, into two aquifers and two confining units, all assigned to the Brewster Boulevard aquifer system and model layer 1. With the exception of the Brewster Boulevard aquifer system, hydrogeologic units listed in Table S4.1 correspond, with minor changes, one-to-one to units previously identified and described by Faye (2012) between Northeast and Wallace Creeks. The name of the TT confining unit described by Faye (2007) was changed in Faye (2012) to the "Upper Castle Hayne confining unit," which is the name also used in this report.

The base of the Lower Castle Hayne aquifer is at the top of the Beaufort confining unit and corresponds, within most of the study area, to the base of freshwater flow. Freshwater is defined herein as water containing a concentration of total dissolved solids less than 5,000 milligrams per liter. The top of freshwater flow occurs everywhere at the water table, which fluctuates seasonally over a range of about 10 feet (ft) or less. Depending on location, whether north or south within the study area or highland or lowland, the water table generally occurs in the lower or upper part of the Brewster Boulevard aquifer system, respectively, or within the TT aquifer.

Aquifers of the Castle Hayne aquifer system comprise the major water-bearing units of the study area and are composed largely of fine silty and clayey sand and sandy limestone. Confining units are clay, sandy clay, or silty clay. For detailed descriptions of framework geometry and well, borehole, and geophysical data used to define the hydrogeologic framework of the study area, refer to Faye (2012).

Table S4.1. Hydrogeologic units, unit thicknesses, and corresponding model layers, Hadnot Point–Holcomb Boulevard study area, U.S. Marine Corps Base Camp Lejeune, North Carolina (modified from Faye 2012 and Maslia et al. 2013).

[DEM, digital elevation model; —, not applicable]

Geologic units			Hydrogeologic units	Abbreviation	Thickness range, in feet	Model layer	Number of data points used to define top of layer
System	**Series**	**Formation**					
Quaternary	Holocene Pleistocene	Undifferentiated	Brewster Boulevard upper aquifer	BBUAQ	4 to 42	1	DEM and bathymetry data [1]
Tertiary	Pliocene	Absent	Absent			1	DEM and bathymetry data [1]
Tertiary	Miocene	Pungo River Formation, undifferentiated	Brewster Boulevard upper confining unit	BBUCU	1 to 22	1	DEM and bathymetry data [1]
Tertiary	Miocene	Pungo River Formation, undifferentiated	Brewster Boulevard lower aquifer	BBLAQ	4 to 48	1	DEM and bathymetry data [1]
Tertiary	Miocene	Belgrade Formation, undifferentiated	Brewster Boulevard lower confining unit	BBLCU	2 to 30	2	132
Tertiary	Miocene	Belgrade Formation, undifferentiated	Tarawa Terrace aquifer (upper part)	TTAQ	8 to 86	3	61
Tertiary	Oligocene	River Bend Formation, undifferentiated	Tarawa Terrace aquifer (middle and lower parts)	TTAQ	8 to 86	3	61
Tertiary	Oligocene	River Bend Formation, undifferentiated	Upper Castle Hayne confining unit [previously designated Tarawa Terrace confining unit in Faye (2007)]	UCHCU	4 to 40	4	76
Tertiary	Late Eocene	Unnamed	Upper Castle Hayne aquifer–River Bend unit	UCHRBU	16 to 70	5	35
Tertiary	Middle Eocene	Castle Hayne Formation	Local confining unit	Local CU	8 to 23	5	35
Tertiary	Middle Eocene	Castle Hayne Formation	Upper Castle Hayne aquifer–Lower unit	UCHLU	10 to 48	5	35
Tertiary	Middle Eocene	Castle Hayne Formation	Middle Castle Hayne confining unit	MCHCU	12 to 27	6	42
Tertiary	Middle Eocene	Castle Hayne Formation	Middle Castle Hayne aquifer	MCHAQ	62 to 122	7	21
Tertiary	Middle Eocene	Castle Hayne Formation	Lower Castle Hayne confining unit	LCHCU	18 to 38	Base of model	6
Tertiary	Middle Eocene	Castle Hayne Formation	Lower Castle Hayne aquifer	LCHAQ	64 to 86	Base of model	6
Tertiary	Paleocene	Beaufort Formation, undifferentiated	Beaufort confining unit	Beaufort CU	—	Base of model	6

[1] 1/9-arc resolution digital elevation model from the National Elevation Dataset (USGS 2010) and bathymetry data (NOAA 2008) were used to define the top of layer 1

Horizontal Hydraulic Conductivity

Results of more than 200 aquifer and slug tests accomplished at multiple locations throughout the study area were analyzed and reported by Faye (2012) and are used herein to describe the hydraulic characteristics of several hydrogeologic units included in the groundwater-flow model. Hydrogeologic unit names, abbreviated names and corresponding model layers are listed in Table S4.1. Reported horizontal hydraulic conductivities for the Brewster Boulevard upper confining unit, Brewster Boulevard lower aquifer, and Brewster Boulevard lower confining unit—model layer 1—ranged from 0.1 foot per day (ft/d) to 87 ft/d (Table S4.2) and averaged 12 ft/d. Similarly, horizontal hydraulic conductivities for the TT aquifer—model layer 3—ranged from 1.0 ft/d to 62 ft/d (Table S4.3) and averaged 17 ft/d. Corresponding horizontal hydraulic conductivities for the Upper Castle Hayne aquifer–River Bend unit, Local confining unit, and Upper Castle Hayne aquifer–Lower unit—model layer 5— ranged from 1.6 ft/d to 79 ft/d (Table S4.4) and averaged 28 ft/d. Only three aquifer tests were available for model layer 7 (Middle Castle Hayne aquifer), and the horizontal hydraulic conductivity ranged from 10 ft/d to 33 ft/d. The geometric means for horizontal hydraulic conductivities of model layers 1, 3, and 5 are 4.0 ft/d, 10 ft/d, and 24 ft/d, respectively.

Table S4.2. Horizontal hydraulic conductivity data used during parameter estimation of cell-by-cell array for the Brewster Boulevard aquifer system (model layer 1), Hadnot Point–Holcomb Boulevard study area, U.S. Marine Corps Base Camp Lejeune, North Carolina (from Faye 2012).

[BBUAQ, Brewster Boulevard upper aquifer; BBUCU, Brewster Boulevard upper confining unit; BBLAQ, Brewster Boulevard lower aquifer]

Site name	Horizontal hydraulic conductivity, in feet per day	Contributing aquifer or confining unit
03-MW05	6.1	BBUCU, BBLAQ
03-MW06	0.6	BBUAQ, BBUCU, BBLAQ
03-MW07	6.1	BBUAQ
03-MW08	3	BBUAQ, BBUCU
06-GW2S	0.7	BBUAQ, BBUCU, BBLAQ
22-RW01	3.4	BBUAQ, BBUCU, BBLAQ
22-RW02	3.1	BBUAQ, BBUCU, BBLAQ
74-GW06	6.3	BBUAQ, BBUCU
75-GW08	3.5	BBUAQ, BBUCU
78-Bldg902RW1	2.3	BBUAQ, BBUCU
84-MW18 (Baker)	0.8	BBLAQ
88-MW03IW	6.8	BBLAQ
88-MW04	16	BBUAQ, BBUCU, BBLAQ
88-MW04IW	65	BBLAQ
88-MW05	0.8	BBUAQ, BBUCU, BBLAQ
88-MW07	30	BBUAQ, BBUCU, BBLAQ
88-MW07IW	61	BBLAQ
88-MW09	0.4	BBUAQ, BBUCU, BBLAQ
88-MW09IW	87	BBLAQ
Bldg21_DW03	57	BBLAQ
Bldg21_MW07	0.1	BBUAQ
BldG-MW09	0.2	BBUAQ, BBUCU
Bldg33_MW11	2.8	BBLAQ
Bldg331_PW16	20	BBLAQ
Bldg645_MW05	5.7	BBLAQ
Bldg645_MW06	10.4	BBLAQ
Bldg1115_MW16	9.3	BBLAQ
Bldg1613_MW01	1.6	BBUAQ
Bldg1613_MW02	13	BBUAQ
Bldg1613_MW08	22	BBUAQ
Bldg1856_MW02	6.3	BBUAQ
Bldg1856_MW07	3.1	BBUAQ
Bldg1856_MW12	7.9	BBUAQ
BldgFC201E_PW01	18	BBUAQ
BldgFC251_MW08	21	BBUAQ, BBUCU, BBLAQ
BldgFC263_MW16	8.1	BBUAQ, BBUCU, BBLAQ
BldgH28_MW03	3.1	BBLAQ
BldgH28_MW05	2.7	BBLAQ
BldgLCH4022_MW01	4.9	BBLAQ
BldgLCH4022_MW06	3.2	BBLAQ
BldgLCH4022_MW07	3.9	BBLAQ
BldgLCH4022_MW19	5.2	BBLAQ
BldgPT5_MW16	40	BBUAQ, BBUCU, BBLAQ
BldgS2633_MW04	0.5	BBLCU
BldgS2633_MW05	1.4	BBLCU
G-BP07	0.9	BBLAQ(?)
G-BP10(?)	1	BBLAQ(?)
G-MW03S	0.5	BBUCU, BBLAQ(?)
G-MW04	0.7	BBUCU, BBLAQ(?)
G-MW06	1.5	BBUAQ, BBUCU
G-MW07	1.1	BBUAQ, BBUCU
G-MW08	0.6	BBUAQ, BBUCU
G-MW09	3	BBUAQ
HP-585	64	BBUCU, BBLAQ

The reported horizontal hydraulic conductivities are not normally distributed, as indicated by the differences between the respective geometric means and average values. Both the average and geometric mean of hydraulic conductivity values increase with depth.

Aquifer-test results were also used to determine the spatial variability of horizontal hydraulic conductivity. Faye (2012) used the results of aquifer- and slug-test data (Tables S4.2 and S4.4) to present highly generalized maps of horizontal hydraulic conductivity for the Brewster Boulevard aquifer system (model layer 1) and the Upper Castle Hayne aquifer (model layer 5; Figures S4.2–S4.3). Areas of higher than average horizontal hydraulic conductivity occur west of the HPIA and in the HPLF area in the Brewster Boulevard aquifer system (Figure S4.2). In the same way, aquifer-test results for the Upper Castle Hayne aquifer indicate areas of higher than average horizontal hydraulic conductivity values in the HPLF (Figure S4.3).

The average and geometric mean of horizontal hydraulic conductivity presented in this section were used as guidelines during calibration of the hydraulic conductivity arrays of the groundwater-flow model. Additional aquifer and slug-test data were available for multi-aquifer wells (Faye 2012); however, data representing single aquifers were the focus of this section.

Table S4.3. Horizontal hydraulic conductivity data used during parameter estimation of cell-by-cell array for the Tarawa Terrace aquifer (model layer 3), Hadnot Point–Holcomb Boulevard study area, U.S. Marine Corps Base Camp Lejeune, North Carolina (from Faye 2012).

[TTAQ, Tarawa Terrace aquifer]

Site name	Horizontal hydraulic conductivity, in feet per day	Contributing aquifer
03-MW02IW	4.1	TTAQ
78-GW32-2	22	TTAQ
82-DP01	23	TTAQ
84-MW16 (Baker)	1.0	TTAQ
88-MW03DW	6.2	TTAQ
Bldg645_MW09	3.3	TTAQ
HP-595	15	TTAQ
HP-621 (old)	62	TTAQ
HPFF_MW75	27	TTAQ
Tank_S781_MW10	9.3	TTAQ

Table S4.4. Horizontal hydraulic conductivity data used during parameter estimation of cell-by-cell array for the Upper Castle Hayne aquifer system (model layer 5), Hadnot Point–Holcomb Boulevard study area, U.S. Marine Corps Base Camp Lejeune, North Carolina (from Faye 2012).

[UCHRBU, Upper Castle Hayne aquifer–River Bend unit; UCHRBU&LU, Upper Castle Hayne aquifer–River Bend and Lower units; Local CU, Local confining unit; TTCU, Tarawa Terrace confining unit]

Site name	Horizontal hydraulic conductivity, in feet per day	Contributing aquifer or confining unit
78-642-1	14	UCHRBU&LU, Local CU, MCHCU
78-642-2	18	UCHRBU&LU, Local CU, MCHCU
80-MW03IW	1.6	UCHRBU
82-DRW01	18	UCHCU(?), UCHRBU
HP-611 (new)	12	UCHRBU&LU, Local CU, MCHCU
HP-612 (new)	24	UCHRBU&LU, Local CU
HP-614 (new)	28	UGHRBU&LU, Local CU
HP-621 (new)	26	UCHRBU&LU
HP-638	19	TTAQ, UCHRBU
HP-650	39	UCHRBU&LU
HP-652	62	UCHRBU&LU
HP-662	15	TTAQ, UCHRBU&LU
HP-663	30	UCHRBU&LU, Local CU
HP-698	18	UCHRBU&LU, Local CU
HP-699	24	UCHRBU&LU, Local CU
HP-700	23	UCHRBU&LU
HP-701	61	UCHRBU&LU
HP-703	79	UCHRBU&LU
HP-704	36	UCHRBU&LU, Local CU
HP-705	36	UCHRBU&LU, Local CU
HP-706	12	UCHRBU&LU, Local CU
HP-707	11	UCHRBU&LU, Local CU
HP-708	39	UCHRBU&LU, Local CU
HP-708 observation well #1A	37	UCHRBU (?)
HP-708 observation well #2	40	UCHRBU (?)
HP-709	28	UCHRBU&LU, Local CU
HP-710	16	UCHRBU&LU
HP-711	25	TTCU, UCHRBU
HP-5186	42	UCHRBU&LU
LCH-4009	19	UCHRBU, Local CU
S190A	30	UCHRBU, Local CU

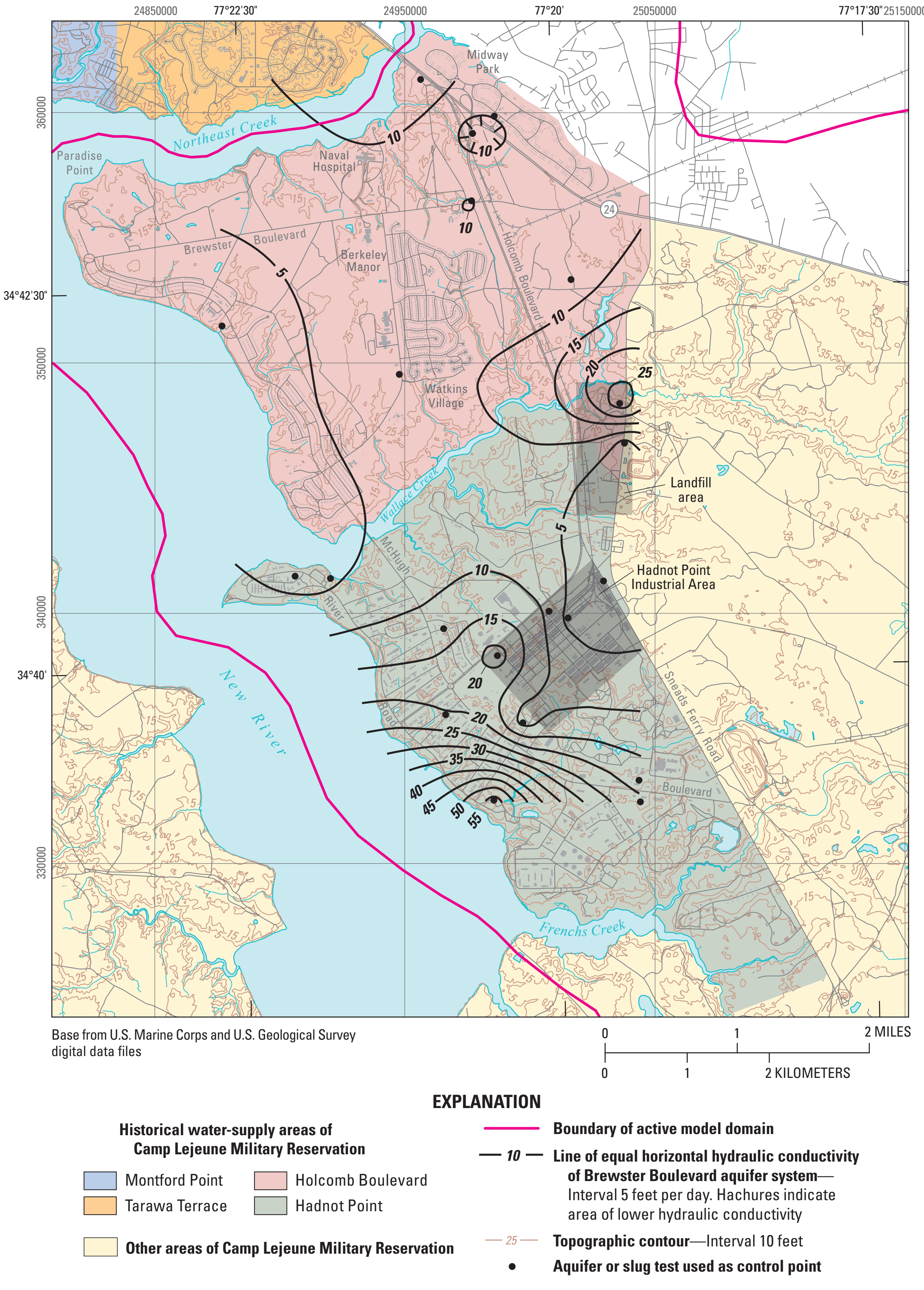

Figure S4.2. Horizontal hydraulic conductivity of the Brewster Boulevard aquifer system—model layer 1, Hadnot Point–Holcomb Boulevard study area, U.S. Marine Corps Base Camp Lejeune, North Carolina (modified from Faye 2012).

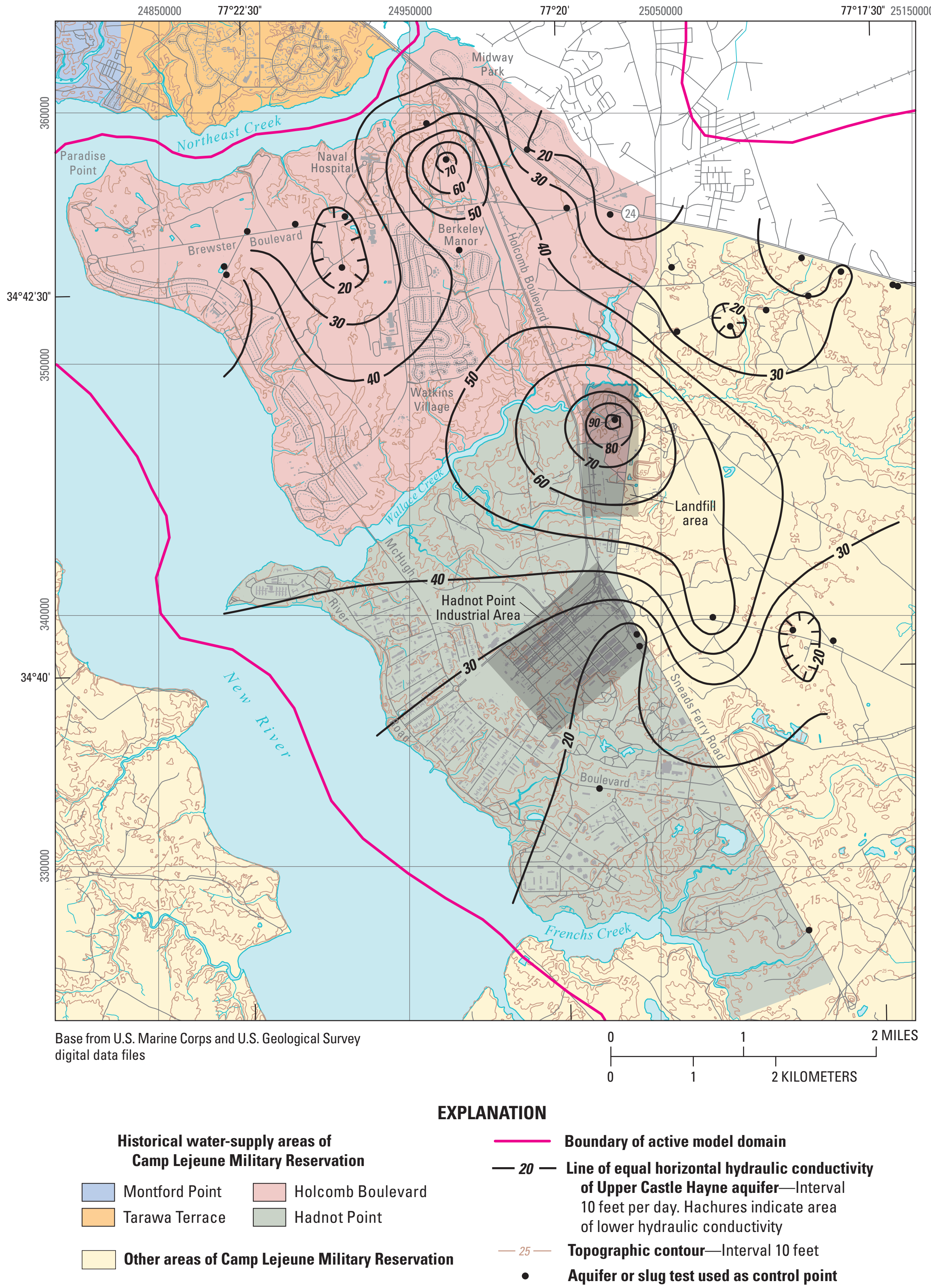

Figure S4.3. Horizontal hydraulic conductivity of the Upper Castle Hayne aquifer—model layer 5, Hadnot Point–Holcomb Boulevard study area, U.S. Marine Corps Base Camp Lejeune, North Carolina (modified from Faye 2012).

Potentiometric Surface

More than 13,000 water-level measurements were obtained from well-data files and reports published to document and summarize the results of Comprehensive Environmental Response, Compensation, and Liability Act (CERCLA) and Resource Conservation and Recovery Act (RCRA) groundwater contaminant investigations and were assembled and organized into spreadsheets and a database. From all measurements, water-level data at 551 locations in the study area collected in monitor wells open to the Brewster Boulevard aquifer system are considered representative of predevelopment water-table conditions. These data along with stream surface altitudes estimated from a digital elevation model (DEM; U.S. Geological Survey 2010) of the study area were used to construct an estimated predevelopment potentiometric surface of the Brewster Boulevard aquifer system (model layer 1; Figure S4.4). Contours of equal potentiometric levels generally conform to surface topography, and groundwater flows from highland to lowland areas toward major rivers and streams.

Conceptual Model of Groundwater Flow

Specific details pertinent to the development of the conceptual model of groundwater flow are described in Faye et al. (2013). For completeness, the conceptual model is also described below. To better integrate the numerous and disparate water-level data available within the study area into a general understanding of hydrologic processes, a conceptual model that addresses groundwater flow, occurrences of recharge, and stream-aquifer relations was developed and based on similar descriptions and analyses by Freeze and Witherspoon (1966, 1967), Hubbard (1940), and Toth (1962, 1963).

The spatial configuration of the water table prior to development of groundwater supply (predevelopment) in the study area probably closely resembled a subdued replica of surface topography (Faye et al. 2013). Except in areas of supply-well or remediation pumping, a similar configuration probably occurs to the present day (2013). Recharge to the Brewster Boulevard aquifer system occurs originally as infiltration of precipitation to the water table. Where topography is substantially high, such as in the northern and western parts of the study area, groundwater-flow gradients at the highest altitude are substantially downward, possibly through most or all of the Middle Castle Hayne aquifer. Generally, maximum rates of recharge occur within highland areas and progressively decline toward lowlands and stream valleys. Consequently, groundwater within the unconfined and poorly confined parts of the Brewster Boulevard aquifer system flows laterally from highland to lowland areas and eventually discharges to the New River, Northeast, Wallace, and Frenchs Creeks, and smaller streams and tributaries. Downstream reaches of major streams such as Wallace, Northeast, and Frenchs Creeks and the New River are probably incised within the Tarawa Terrace aquifer and possibly within the Castle Hayne aquifer as well. Where incision is incomplete, substantial vertical continuity of permeable sediments is likely maintained across relatively thick sections of paleochannel sands (Faye 2012). Accordingly, groundwater flow within the Tarawa Terrace and Castle Hayne aquifers probably mimics, to a large degree, flow within the Brewster Boulevard aquifer system, with an exception occurring in the immediate vicinity of the large streams mentioned previously where flow directions are upward and discharge occurs as diffuse upward leakage. Discharge from the Middle and Lower Castle Hayne aquifers also occurs as diffuse upward leakage, probably largely within the western and southwestern parts of the study area.

Faye and Valenzuela (2007) described groundwater-flow conditions in the TT area following the onset of pumping at water-supply wells which are applicable to the HPHB study area. This is because most of the hydrogeologic characteristics of both sites are similar. With minor changes, similar descriptions probably apply to the HPHB study area. With the routine operation of supply wells, groundwater flow that was entirely directed toward streams and rivers under predevelopment conditions was partially diverted to pumping wells. As a consequence, (1) predevelopment potentiometric levels in the vicinity of pumping wells declined in all water-bearing units contributing to the wells, (2) predevelopment flow directions changed preferentially toward pumping wells and away from natural points of discharge such as Wallace Creek, and (3) potentiometric levels near the predevelopment flow boundaries possibly declined, causing the boundaries to migrate further away from the study area. Declines in potentiometric levels in the vicinity of New River and tidally affected reaches of Northeast and Wallace Creeks possibly caused a reversal from upward to downward vertical flow, creating the possibility of inducing salt or brackish water landward into actively pumped aquifers.

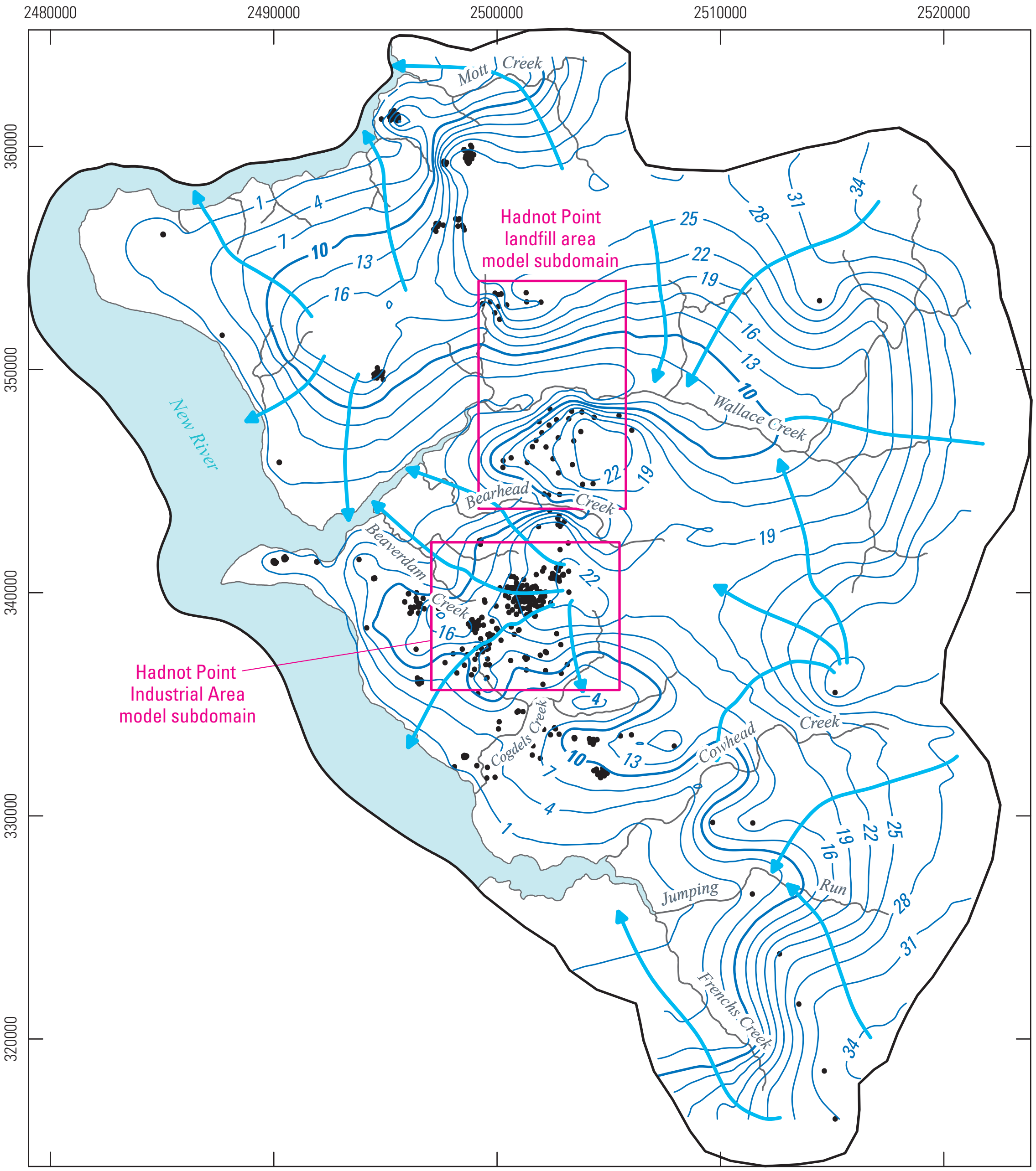

Base from U.S. Marine Corps and U.S. Geological Survey digital data files
Map coordinates are North Carolina State Plane coordinates
North American Datum of 1983

0 1 2 MILES
0 1 2 KILOMETERS

EXPLANATION

Boundary of active model domain

Boundary of contaminant fate and transport model subdomain (see Jones et al. 2013 and Maslia et al. 2013)

10 **Potentiometric contour**—Shows altitude at which water level would have stood in tightly cased wells, predevelopment. Contour interval 3 feet. Datum is NGVD 29

Generalized direction of groundwater flow

• **Water measurement used as control point**

Figure S4.4. Estimated predevelopment (steady-state) potentiometric surface and generalized direction of groundwater flow, Brewster Boulevard aquifer system, Hadnot Point–Holcomb Boulevard study area, U.S. Marine Corps Base Camp Lejeune, North Carolina.

Mathematics of Three-Dimensional Groundwater Flow

A partial differential equation based on the principles of mass balance can be used to describe the groundwater-flow system previously described in the conceptual model. The derivation of the generalized governing equation of groundwater flow in saturated media has been described in many references including those by Bear (1978), Anderson and Woessner (1992), Kresic (1997), and Schwartz and Zhang (2003). The partial differential equation can be written as:

$$\frac{\partial}{\partial x}\left(K_{xx}\frac{\partial h}{\partial x}\right)+\frac{\partial}{\partial y}\left(K_{yy}\frac{\partial h}{\partial y}\right)+\frac{\partial}{\partial z}\left(K_{zz}\frac{\partial h}{\partial z}\right)+W=S_s\frac{\partial h}{\partial t} \quad \text{(S4.1)}$$

where

K_{xx}, K_{yy}, and K_{zz}	equal horizontal hydraulic conductivity along the x, y, and z axes [LT^{-1}];
h	equals the potentiometric head [L];
W	equals sources or sinks of water (volumetric rate per unit volume) [$L^3 T^{-1} L^{-3}$];
S_s	equals the specific storage of the porous media [L^{-1}]; and
t	equals time [T][6].

Predevelopment (or steady-state) conditions are represented by setting the right-hand side of Equation S4.1 to zero.

[6] L represents length units; T represents time units.

Equation S4.1 is subjected to the following boundary and initial conditions.

Boundary Conditions

Type 1. Specified head boundary (Dirichlet condition) in which the hydraulic head or potentiometric level is specified. When the hydraulic head is a constant value, such as a boundary representing sea level, this boundary is also referred to as *constant-head* boundary condition.

Type 2. Specified flow boundary (Neumann condition) in which the gradient of the head (or flux) across a boundary is given. When the flux is specified as zero, this represents a *no-flow* boundary condition.

Type 3. Head-dependent flow boundary (Cauchy or mixed boundary) in which the flux over a boundary is calculated given a head-value at the boundary. This boundary condition type is also known as a generalized-head boundary in model applications.

Initial Conditions

Under steady-state conditions (right-hand side of Equation S4.1 is zero), initial conditions do not need to be specified. For transient or unsteady-state conditions, initial conditions supply the hydraulic head or potentiometric level everywhere within the domain of interest at some initial time such as steady-state (e.g., time = 0). In the case where water-supply wells are pumping, initial conditions are represented by predevelopment or steady-state conditions existing prior to the onset of pumping.

The system represented by Equation S4.1 and the respective boundary conditions can be solved using analytical and numerical methods. Analytical solutions are only available for simple systems, while complex systems require numerical methods (e.g., finite-difference or finite-element methods). The numerical code used in this study (e.g., MODFLOW-2005) uses a finite-difference method to solve Equation S4.1 along with associated boundary and initial conditions. Details of the solution methodology are described in Harbaugh (2005)[7].

[7] MODFLOW is a family of three-dimensional groundwater-flow models developed by the U.S. Geological Survey. Specific MODFLOW model codes (e.g. MODFLOW-2005) applied to the HPHB study area are described herein. When used generically herein, MODFLOW refers to all variants of the family of MODFLOW groundwater-flow model codes.

Three-Dimensional Groundwater-Flow Model

The codes used for groundwater-flow simulation and model calibration included MODFLOW-2000, MODFLOW-2005, MODFLOW-ASP, and PEST 12. MODFLOW-2000, -ASP, and -2005 (Harbaugh et al. 2000; Harbaugh 2005; Doherty 2010) are based on the original modular finite-difference groundwater-flow model developed by McDonald and Harbaugh (1984). These codes all simulate groundwater flow in a three-dimensional, heterogeneous, anisotropic porous media. MODFLOW-ASP and PEST 12 are computer codes used for parameter estimation and model calibration were developed or modified by Doherty (2010, 2011). The model grid and arrays were constructed and manipulated using the graphical user interface software Groundwater Modeling System (GMS) version 8 (U.S. Army Engineer and Research Development Center 2008) and ModelMuse version 2 (Winston 2009).

Documented herein are (1) development and steady-state (predevelopment) calibration results of a uniform grid model; (2) development and transient-state calibration results using historical and predicted pumpage data (Telci et al. 2013); (3) development and simulation results of two variably spaced grid models for the HPIA and HPLF areas; and (4) sensitivity analyses. The calibrated steady-state (predevelopment) model represents long-term average groundwater-flow conditions prior to the onset of pumping for water supply within the HPHB study area; the transient model represents the onset of pumping and resulting conditions from 1942 to 2008.

Table S4.5. Location coordinates of the groundwater-flow model grid (total model domain), Hadnot Point–Holcomb Boulevard study area, U.S. Marine Corps Base Camp Lejeune, North Carolina.

Position	Location coordinates[1]	
	East	North
Northwestern corner[2]	2478760	365640
Northeastern corner	2524360	365640
Southeastern corner	2524360	314040
Southwestern corner	2478760	314040

[1] Location coordinates are North Carolina State Plane coordinates, North American Datum of 1983

[2] Origin of the model grid (domain)

Domain and Discretization

The active domain of the HPHB study area flow model is bounded in the north by the mid-channel of Northeast Creek, in the east by State Route (SR) 172, in the south by the intersection of Sneads Ferry Road and SR 172, and in the west by the mid-channel of New River (Figure S4.1). The total model domain and active model domain areas are 84 square miles (mi^2) and 50 mi^2, respectively. Location coordinates of the total model domain are listed in Table S4.5. The total model domain was subdivided into 152 columns and 172 rows, corresponding to a finite difference grid consisting of 300-ft (per side) square cells.

Vertical discretization consists of 7 layers representing 11 hydrogeologic units (Table S4.1). Odd-numbered model layers (1, 3, 5, and 7) are considered water-bearing units representing aquifers, and even-numbered model layers (2, 4, and 6) represent confining units. Several hydrogeologic units were combined in layers 1 and 5. Model-layer and hydrogeologic-unit correspondence is listed in Table S4.1. Layer thicknesses were derived from stratigraphic data—geophysical and electric logs—obtained from about 900 locations across the model domain and described by Faye (2012). The altitude at the top of layer 1 was obtained using 1/9-arc resolution DEM and bathymetry data obtained from the National Elevation Dataset (U.S. Geological Survey 2010) and the National Geophysical Data Center (National Oceanic and Atmospheric Administration 2008), respectively. The altitude data for each hydrogeologic unit were interpolated in GMS and used to build the model grid. The number of data points available to interpolate the top of each unit ranged from 6 to 132 and decreased with depth (Table S4.1). Contours showing the top altitude along with thickness ranges for each model layer are shown in Figure S4.5. Layer 1 contains the water table, and the bottom of layer 7 corresponds to the top of the Lower Castle Hayne confining unit.

Temporal discretization of the transient groundwater-flow model consists of 798 monthly stress periods starting in January 1942 and ending in June 2008 (Table S4.6, back of report). For groundwater-flow simulations, one time step per stress period was used; therefore, each stress period had a length of 28, 29, 30, or 31 days.

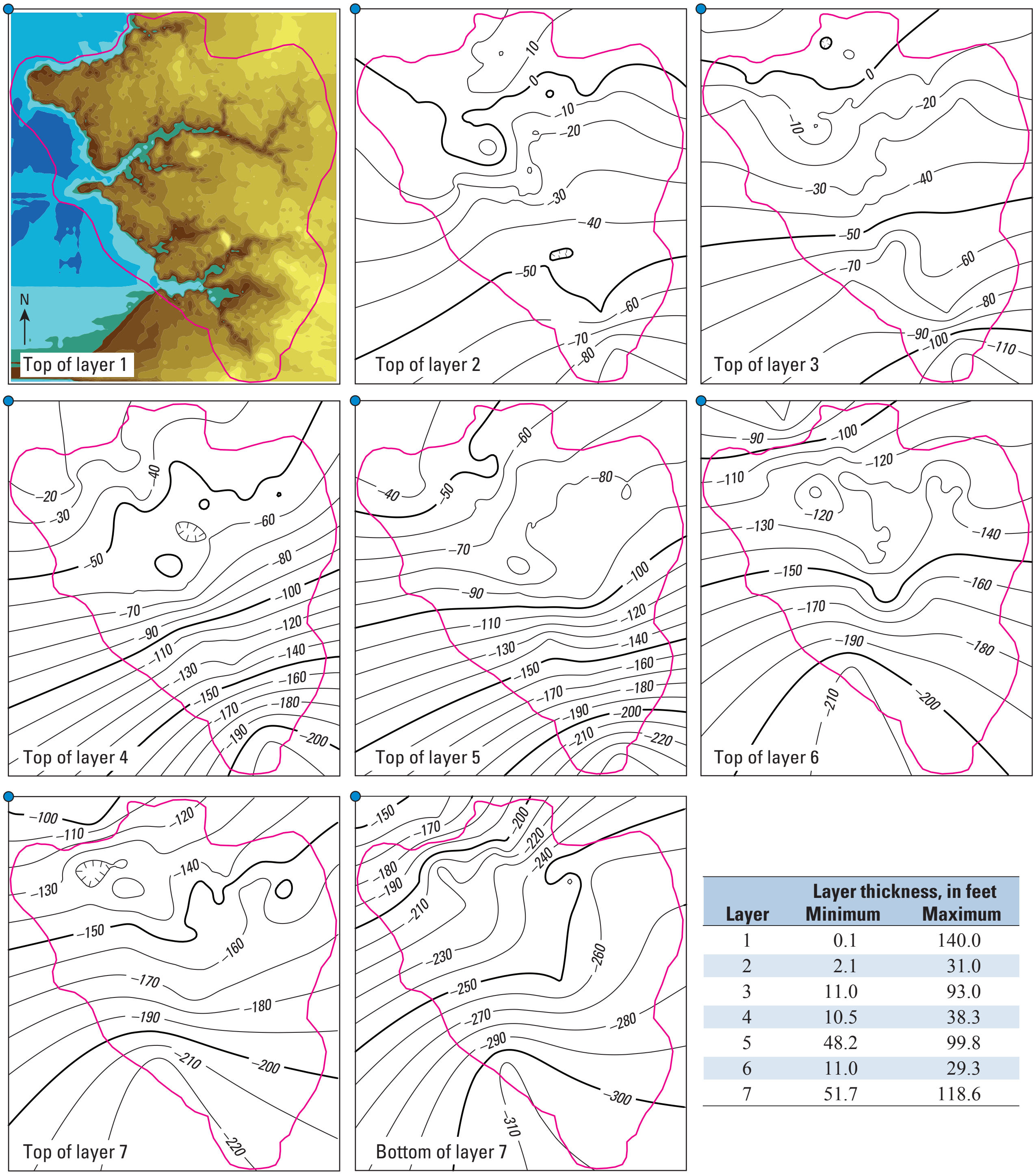

Layer	Layer thickness, in feet Minimum	Maximum
1	0.1	140.0
2	2.1	31.0
3	11.0	93.0
4	10.5	38.3
5	48.2	99.8
6	11.0	29.3
7	51.7	118.6

EXPLANATION

Land-surface altitude, in feet above or below NGVD 29

–20 –10 0 10 20 30 40 50

–200 **Structure contour**—Shows altitude of top or bottom of layer. Hachures indicate depression. Contour interval 10 feet. Datum is NGVD 29

Boundary of active model domain

Origin of model grid—See Table S4.5 for coordinate values

Figure S4.5. Model layer altitude and thickness of groundwater-flow model, Hadnot Point–Holcomb Boulevard study area, U.S. Marine Corps Base Camp Lejeune, North Carolina.

Boundary and Initial Conditions

The boundary conditions of the groundwater-flow model, shown in Figure S4.6, include no-flow and specified-head boundaries. Boundary conditions are explained in further detail in subsequent sections of this report. Initial conditions for the transient model—initial or starting heads—were obtained from the steady-state model and represent predevelopment conditions. For transient simulations, the first stress period is defined as steady-state.

Specified Head

The surfaces of New River and adjoining tidally influenced inlets to Northeast, Wallace, and Frenchs Creeks correspond to sea level; therefore, a specified head of 0 ft in layer 1 was assigned (Figure S4.1), as was similarly done for the TT study area by Faye and Valenzuela (2007). An assumption was made that the long-term sea-level change for the duration of the model simulation was insignificant. Specified head can be simulated in MODFLOW using the time-variant specified head (CHD) package and is represented by a Type 1 or Dirichlet boundary condition. The CHD package allows the use of temporal changes in the specified-head boundary; however, sea level was considered to be constant.

No-Flow

No-flow conditions represent a zero flux across the active model domain boundary (Type 2 or Neumann boundary condition). These conditions represent impermeable bedrock or a fault zone, a groundwater divide, and in some cases, the freshwater/saltwater interface in coastal aquifers (Anderson and Woessner 1992). The base and the perimeter of the groundwater-flow model correspond to a no-flow boundary. The perimeter of the model—excluding New River and Northeast Creek areas—generally follows a topographic divide and is considered to be a groundwater divide for the aquifers of interest to this study; therefore, a no-flow boundary was assigned for all model layers. The base of the groundwater-flow model corresponds to the top of the Lower Castle Hayne confining unit and is considered the base of freshwater flow.

Drains

MODFLOW uses the drain (DRN) package to represent head-dependent conditions for hydrologic features where water is removed from the model (Harbaugh et al. 2000). Drains can only remove water from the aquifer and are commonly used to represent gaining perennial and ephemeral (intermittent) streams. Several drains were assigned in layer 1 using geographic information system (GIS) layers for creeks and tributaries. Creeks simulated as drains in the groundwater-flow model are Mott Creek, Beaverdam Creek, Bearhead Creek, Wallace Creek, Cogdels Creek, Cowhead Creek, Frenchs Creek, Jumping Run, and other unnamed creeks or streams (Figure S4.6).

The inputs required to describe drain features in MODFLOW are drain altitude and conductance. To obtain the altitude of the drains, 5-ft-interval altitude contours were traced from USGS topographic maps using GMS 8. Then, a triangulated irregular network was created and used to interpolate the altitude at each drain cell.

Conductance values for the drains cells can be approximated using the following equation.

$$C = (K_h LW) / t, \qquad \text{(S4.2)}$$

where

- C equals conductance [$L^2 T^{-1}$],
- K_h equals the hydraulic conductivity of the streambed material [LT^{-1}],
- L equals the length of the stream [L],
- W equals the width of the stream [L], and
- t equals the thickness of the streambed [L].

Assuming a hydraulic conductivity of 1 ft/d, a length of 300 ft (length of the cell), and a width of 10 ft results in an initial estimate for drain conductance of 3,000 square feet per day (ft^2/d). The calibrated value of 1,000 ft^2/d was determined during initial trial-and-error calibration.

Recharge

Recharge was assigned to the uppermost active cell and varied cell-by-cell. Recharge is modeled in MODFLOW with a flux condition using the RCH package. The recharge array was obtained during the steady-state model calibration. Using a dataset of more than 13,000 water-level measurements, a set of 849 measurements was selected to represent predevelopment conditions. These water-level measurements were used in a regression analysis by using similar methods to those described by Faye (2012). The resulting equation was used to generate 540 water-level observations—spaced every 1,500 ft—which were used for calibration within PEST. Parameterization for recharge was performed using a set of 970 pilot points (Doherty et al. 2010). Pilot points were uniformly distributed within the active model domain. To stabilize the numerical problem, regularization and singular value decomposition were implemented. Each pilot point was assigned a preferred value for recharge based on the U.S. Department of Agriculture (USDA) soil survey map shown in Figure S4.7. Pilot points lying within the poorly and very poorly drained areas were assigned a preferred value of 0.001 ft/d [4 inches per year (in/yr)] while the rest of the points were assigned a value of 0.0023 ft/d (10 in/yr). Optimization of the recharge array against the water-level measurement dataset representing predevelopment conditions resulted in the spatial distribution of recharge shown in Figure S4.8.

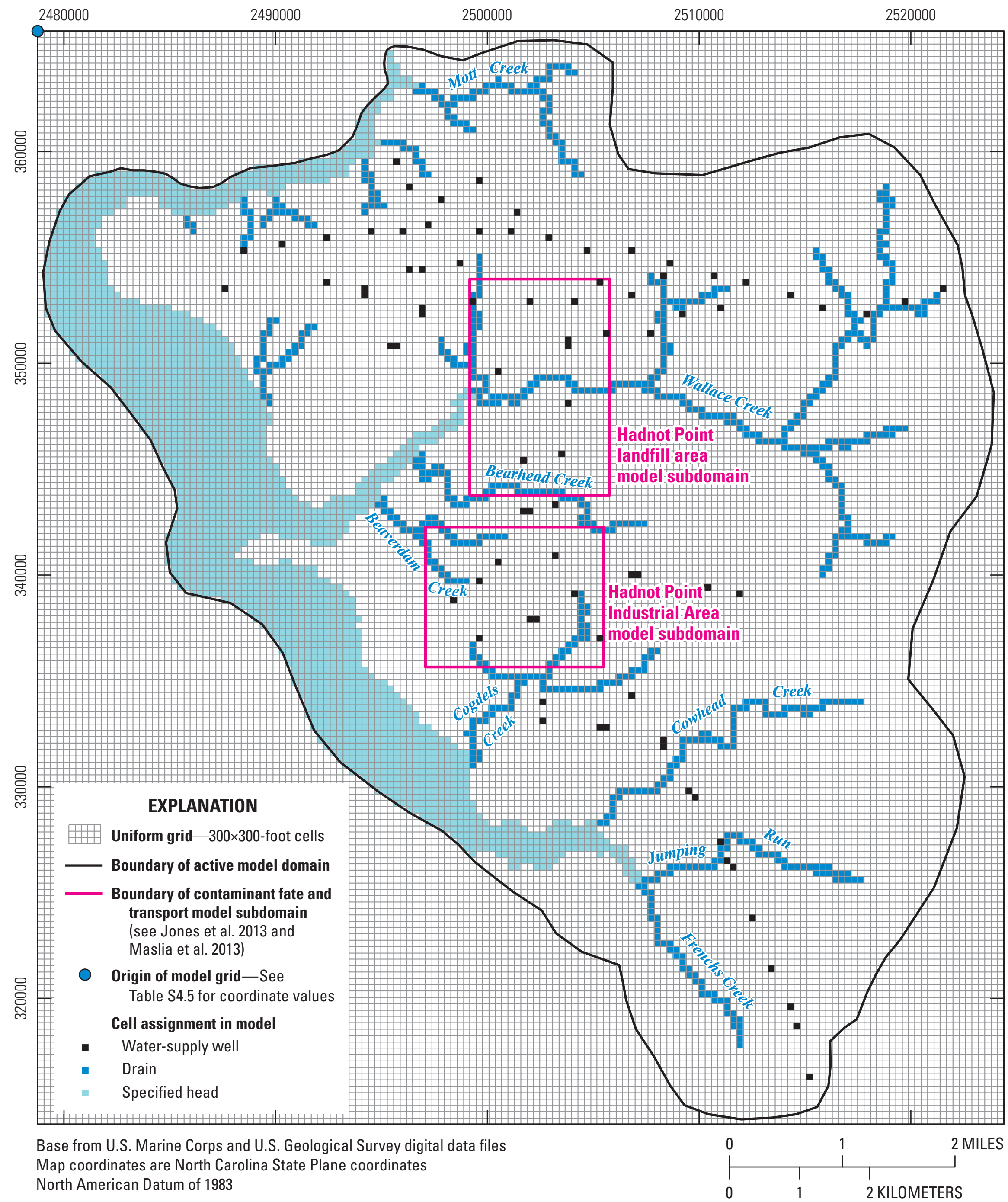

Figure S4.6. Groundwater-flow model grid and boundaries, Hadnot Point–Holcomb Boulevard study area, U.S. Marine Corps Base Camp Lejeune, North Carolina.

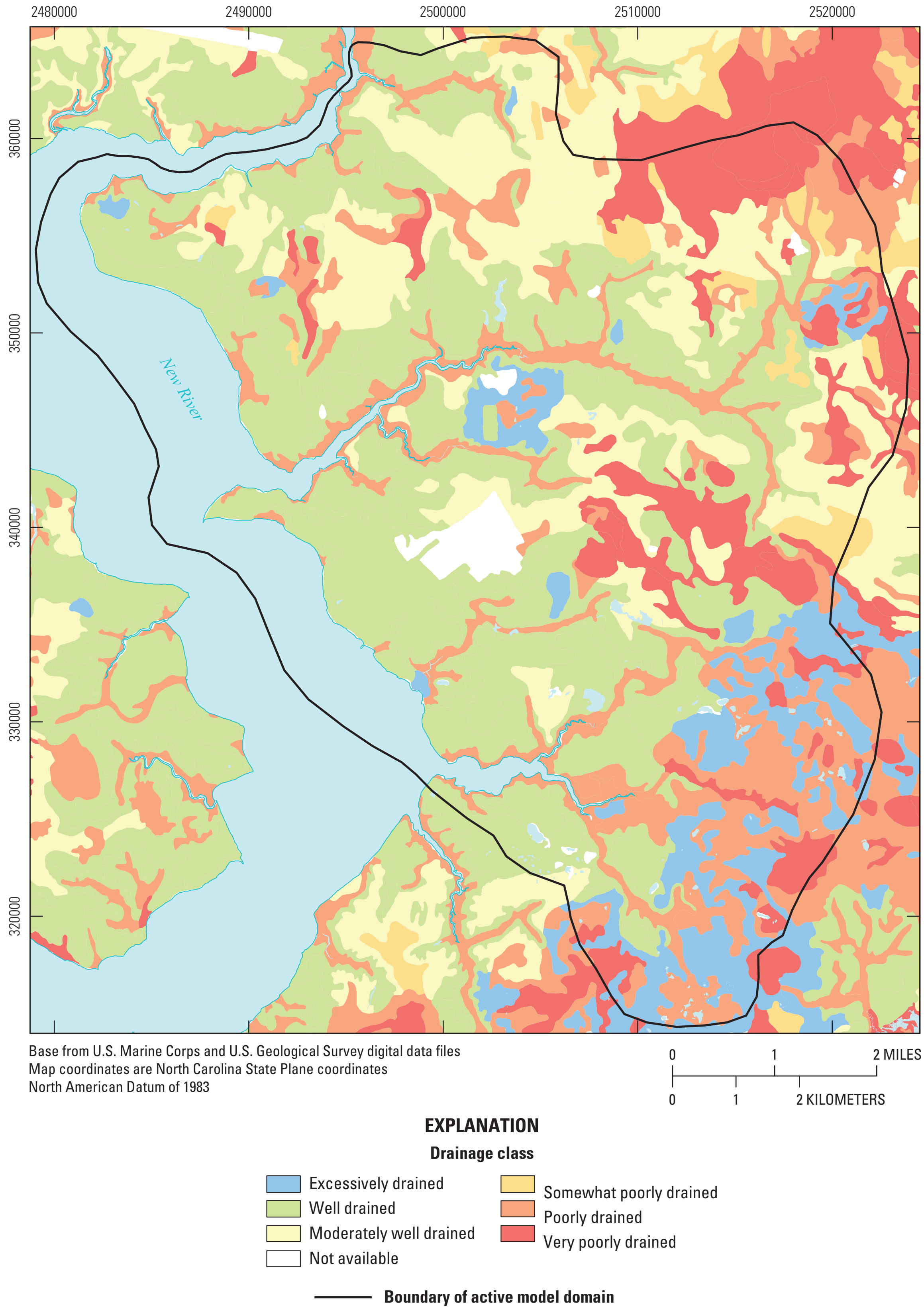

Figure S4.7. Soil drainage classes used for parameter estimation, Hadnot Point–Holcomb Boulevard study area, U.S. Marine Corps Base Camp Lejeune, North Carolina (source: USDA Soil Survey 2009 data for Onslow County; data processed using USDA Soil Data Viewer; aggregation method across map units is by dominant soil condition).

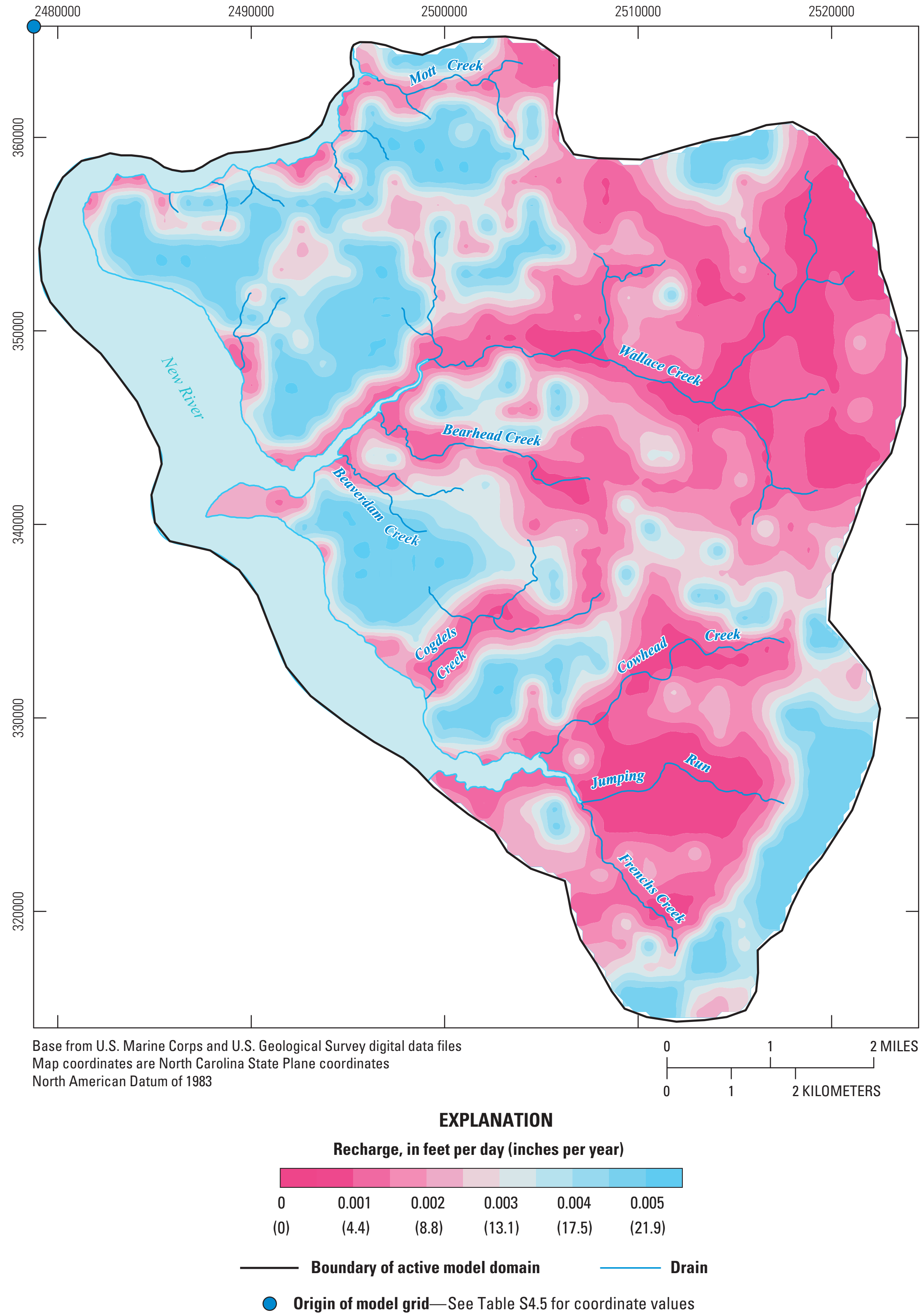

Figure S4.8. Recharge values assigned to the groundwater-flow model, Hadnot Point–Holcomb Boulevard study area, U.S. Marine Corps Base Camp Lejeune, North Carolina.

Groundwater infiltration or recharge probably changed continuously due to fluctuations in precipitation and evapotranspiration. During the transient-flow simulation, the steady-state recharge model array was multiplied each month by an adjustment factor to account for variations in groundwater infiltration. To calculate the adjustment factor, the following procedure was used:

1. Precipitation information from January 1942 through June 2008 was obtained for the Hoffmann/Maysville weather station from the National Climatic Data Center.
2. Long-term average and average daily precipitation for each month—using all available daily data—were calculated. The long-term precipitation was 57.2 in/yr.
3. Average daily precipitation for each month was divided by the long-term average to calculate an adjustment factor for each month in the simulation period.

The recharge adjustment factors are shown in Figure S4.9.

Wells

Historically, 96 water-supply wells operated in the study area. Pumpage from supply wells was simulated using the Revised Multi-Node Well (MNW2) package (Konikow et al. 2009). The input data required to simulate pumping wells includes location, pumping rate, well-screen information, and skin effects information (i.e., thickness of the skin and hydraulic conductivity of the skin).

Pumping wells were placed in the groundwater-flow model using georeferenced maps or reported coordinates from the driller's report. Well-construction information was used to determine the numbers of screens and screen length for each well (Faye et al. 2010, 2013). Data obtained from pumping records varied substantially. Available data included well capacities and daily operation schedules for some wells, while in other cases only a design capacity was available (Sautner et al. 2013). A historical reconstruction of the pumping (operational) schedules of wells supplying water to the HPWTP and HBWTP is described by Telci et al. (2013).

The first supply wells at USMCB Camp Lejeune were constructed during 1941 and early 1942 and were probably in operation by the summer of 1942 (Sautner et al. 2013). Accordingly, supply wells assigned to the groundwater-flow model began operation during June 1942. The MNW2 package automatically proportions the flow between layers using the transmissivity assigned to each layer contributing to well flow (Konikow et al. 2009). After initial simulation and calibration of the transient model, the supply wells were simulated using the WEL package in MODFLOW to overcome compatibility issues with the model code being used to simulate contaminant fate and transport (Jones et al. 2013). The MNW2 package was used to obtain the required input files for the WEL package.

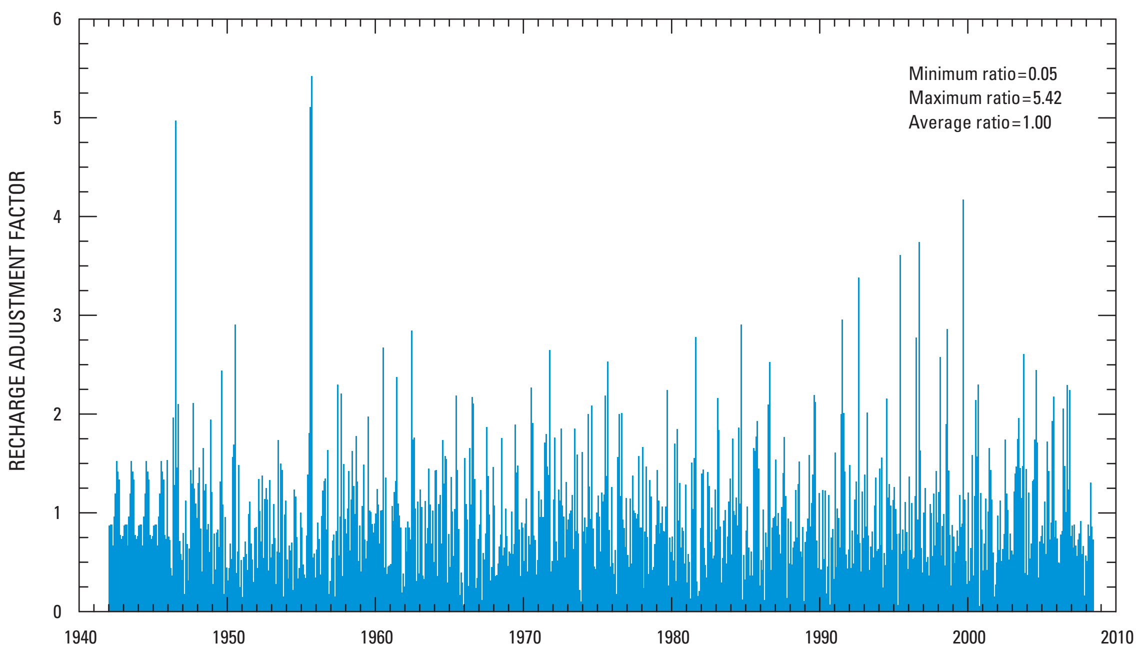

Figure S4.9. Recharge adjustment factors, Hadnot Point–Holcomb Boulevard study area, U.S. Marine Corps Base Camp Lejeune, North Carolina.

During the grid refinement process used to create the variably spaced grid models,[8] ModelMuse (Winston 2009) automatically assigns cells for pumping wells by using the original pumping-cell location. However, specific model cells assigned to pumping wells within the HPIA and HPLF contaminant fate and transport subdomains (Figure S4.1) were adjusted using location coordinates of the wells. The cells—row and column—assigned for pumping wells in the HPIA and HPLF are listed in Table S4.7. In addition, Table S4.7 shows the percentage of layer flow to total flow for each respective well. The majority of water-supply wells pump mostly from model layer 5 (Upper Castle Hayne aquifer system).

Hydraulic Properties

Hydraulic properties in the groundwater-flow model were defined using the MODFLOW layer property flow (LPF) package (Harbaugh, 2005). All layers are specified as convertible; therefore, the layer can switch between confined and unconfined flow depending on the flow conditions. Specific yield and storativity were assigned similar values to those used by Faye and Valenzuela (2007). A specific yield of 0.05 was assigned uniformly to layer 1. Cell-by-cell specific storage was assigned based on an assumed storage coefficient (storativity) of 0.0004.

Horizontal hydraulic conductivity values previously described in the Horizontal Hydraulic Conductivity section of this supplement were used to assign initial values to each layer representing an aquifer—layers 1, 3, 5, and 7. Horizontal hydraulic conductivity values for layers 1, 3, and 5 were adjusted during the steady-state model calibration using parameter estimation with 970 pilot points per layer. Additional details about the calibration process are provided in the Approach to Model Calibration section of this supplement. The horizontal hydraulic conductivity for confining units—layers 2, 4, and 6—was uniformly assigned a value of 1 ft/d, derived from values used in Faye and Valenzuela (2007) for the TT study area. Cardinell et al. (1993) reported the existence of paleochannels underlying New River to depths of approximately 200 ft. Consequently, the horizontal hydraulic conductivity assigned to layers 2, 4, and 6 was increased during model calibration in selected areas described by Cardinell et al. (1993) to account for the occurrence of paleochannels. The calibrated horizontal hydraulic conductivity arrays for all layers are shown in Figure S4.10. Vertical hydraulic conductivity was defined using a ratio of horizontal to vertical hydraulic conductivity. The ratio is 10.0 for layers representing aquifers—layers 1, 3, 5, and 7—and 15.0 for layers representing confining units—layers 2, 4, and 6.

[8] The location and orientation of the HPIA and HPLF model subdomain areas (Figure S4.1) required two variably spaced grid models owing to computational requirements rather than using just one variably spaced grid.

Table S4.7. Water-supply well names, model coordinate locations, and ratios of model layer flow to total flow for selected water-supply wells within the HPIA and HPLF area, Hadnot Point–Holcomb Boulevard study area, U.S. Marine Corps Base Camp Lejeune, North Carolina.

[—, well does not pump from this model layer; HPIA, Hadnot Point Industrial area; HPLF, Hadnot Point landfill]

Water-supply well name	Location coordinates[1]		Ratio of model layer flow to total flow,[2] in percent						
	Row	Column	Layer 1	Layer 2	Layer 3	Layer 4	Layer 5	Layer 6	Layer 7
HP-601	132	115	3.0	1.7	2.3	0.8	92.3	—	—
HP-602	114	136	—	—	27.2	1.6	71.3	—	—
HP-603	151	94	—	—	25.8	1.2	73.0	—	—
HP-605	146	207	—	0.1	18.5	—	78.7	2.7	—
HP-606	189	231	—	—	50.0	—	50.0	—	—
HP-607 (old)	168	165	0.1	2.9	36.2	1.2	59.6	—	—
HP-608	184	115	0.8	1.3	67.9	0.7	29.2	—	—
HP-630	166	169	2.8	2.6	19.3	4.3	70.9	—	—
HP-634	107	187	—	0.1	26.0	0.9	73.0	—	—
HP-642	146	206	—	—	—	0.2	96.9	2.8	—
HP-660	133	113	—	—	—	3.6	96.4	—	—
HP-651	160	165	—	—	—	—	100.0	—	—

[1] Location coordinates are specific to each variably spaced grid model

[2] The ratios shown are temporal averages calculated for the model simulation period January 1942–June 2008

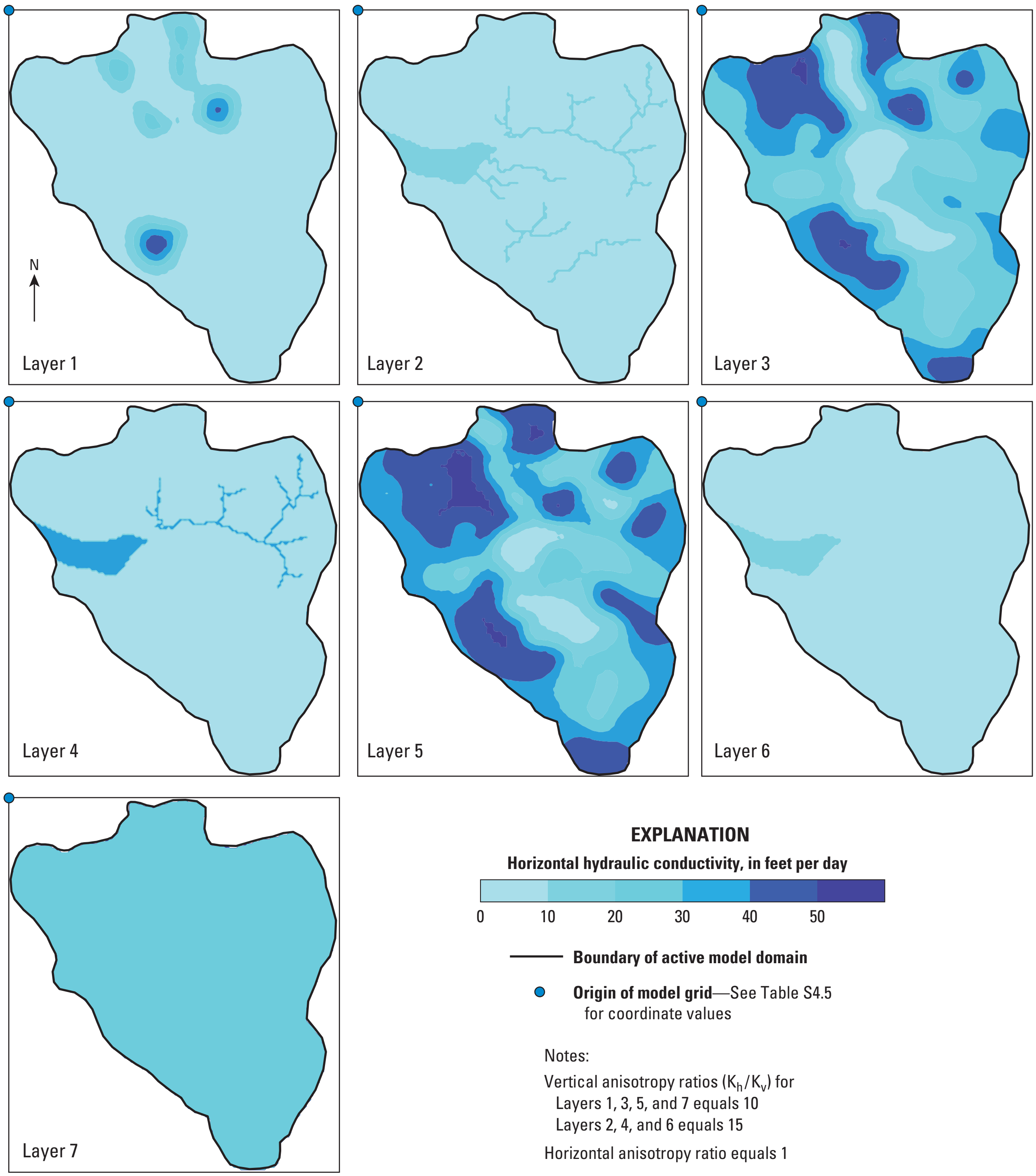

Figure S4.10. Calibrated horizontal hydraulic conductivity and vertical anisotropy assigned to the groundwater-flow model, Hadnot Point–Holcomb Boulevard study area, U.S. Marine Corps Base Camp Lejeune, North Carolina.

Model Results

Predevelopment and transient conditions were simulated by using the models described in the previous sections. Results for these models include residual analyses, simulated potentiometric levels for steady-state and transient conditions, and flow-budget analyses.

Approach to Model Calibration

Model calibration was accomplished by using a variety of approaches and tools that included trial-and-error and advanced parameter estimation. Calibration was performed in two stages or phases that included (1) steady-state flow model calibration and (2) transient-state flow model calibration.[9] Most of the field observations available for groundwater-flow model calibration included water-level measurements representing predevelopment conditions.

In phase 1, more than 700 water-level measurements were used to calibrate the steady-state model by using an automated parameter-estimation approach. A highly parameterized model—with more than 3,800 parameters—was calibrated using regularization and singular value decomposition. PEST 12 was used to conduct simulations and optimization. The parameters included 970 pilot points for each of four parameter groups—horizontal hydraulic conductivity for layers 1, 3, and 5 and recharge. A residual analysis was used to evaluate the goodness of the fit of the solution. Residual analysis includes a plot of observed potentiometric levels (heads or water-level measurements) versus residuals and a spatial analysis of the residuals.

Phase 2 included a trial-and-error approach in which hydrographs for multiple wells were compared against simulated water levels. The wells used for this comparison include the cluster in X24S (Figure S4.1). In this calibration phase, vertical anisotropy and temporal variation in recharge were adjusted to improve the match between observed and simulated water levels.

Steady-State (Predevelopment) Conditions

Observed water-level data presented in Table S4.8 (back of report) and described by Faye et al. (2013, Table S3.4) were used to evaluate the steady-state calibration results. Well-screen information was used to determine the most appropriate layer for comparing simulated water levels to measured water levels. The midpoint of the screen was used to determine the corresponding layer for each monitor well. Water-level measurements from supply wells with long or multiple screens were compared to flow-weighted (composite) simulated water levels. Flow-weighted water levels were obtained by adding the appropriate proportion of the simulated water levels from each model layer (Table S4.7). For example, the simulated water level for well HP-602 is obtained by adding about 27, 2, and 71 percent of the simulated level from layers 3, 4 and 5, respectively. Furthermore, simulated water levels for each well were spatially interpolated by using bilinear interpolation to facilitate direct comparisons to the location coordinates of the observation point. Simulated water levels were compared to observed values by calculating a residual to assess the goodness of fit of the calibration (Table S4.8). Residuals in this report are defined by using the equation:

$$r_i = o_i - s_i \, , \qquad \text{(S4.3)}$$

where

- r_i equals the residual for pair i [L],
- o_i equals the observed or measured water level i [L],and
- s_i equals the simulated water level paired to observation i [L].

Using the residual definition expressed in Equation S4.3, the average residual is 0.5 ft and the root-mean-square residual is 3.4 ft. Figure S4.11 shows simulated and observed results in a set of scatter plots. The results in these plots are shown for supply wells (blue circles) and other wells (orange circles). The minimum residual is –17.5 ft at well BldgSLCH4019_MW10, and the maximum residual is 11.5 ft at Bldg45_MW04 (Law).[10] Residuals for all layers were spatially plotted to determine the existence of any biases or trends (Figure S4.12). The majority (70 percent) of the residuals are between –2.5 ft and 2.5 ft. Some areas where the magnitude of the residuals tends to be higher include the Midway Park (LCH) area, Site 88, and Site 3 (See Maslia et al. 2013, Figure A1, for location).

Total simulated flow into the model domain was 3.1×10^6 cubic feet (ft^3). All of the flow coming into the model originates from recharge. Because the active domain is about 50 mi^2, the recharge rate will average about 9.7 in/yr. About 37 percent of the flow discharges to the specified-head boundaries, and about 63 percent discharges to the drains. The simulated flow to drains is about 0.45 ft^3 per second per square mile and represents long-term average annual baseflow. The flow-budget error between simulated inflow and outflow is –0.5 percent. By comparison, the long-term average recharge rate estimated for the TT study area was 13.3 in/yr over an active model domain area of about 2.1 mi^2 (Faye and Valenzuela 2007).

As indicated by the simulated potentiometric level, groundwater flows laterally from the highlands to the lowlands, discharging to the drains and specified-head boundaries (Figure S4.12). Simulated water levels range from 43.5 ft in the highland areas to less than 10 ft in the lowland areas to 0 ft along New River, Northeast Creek, and other tributaries; simulated water levels are similar for all layers. The simulated flow patterns and directions of groundwater flow shown in Figure S4.12 conform to the conceptual model and are in general agreement with those shown in Figure S4.4.

[9] A third stage for fate and transport model calibration is discussed in Jones et al. (2013).

[10] Refer to Faye et al. (2010, Plate 1) for building location.

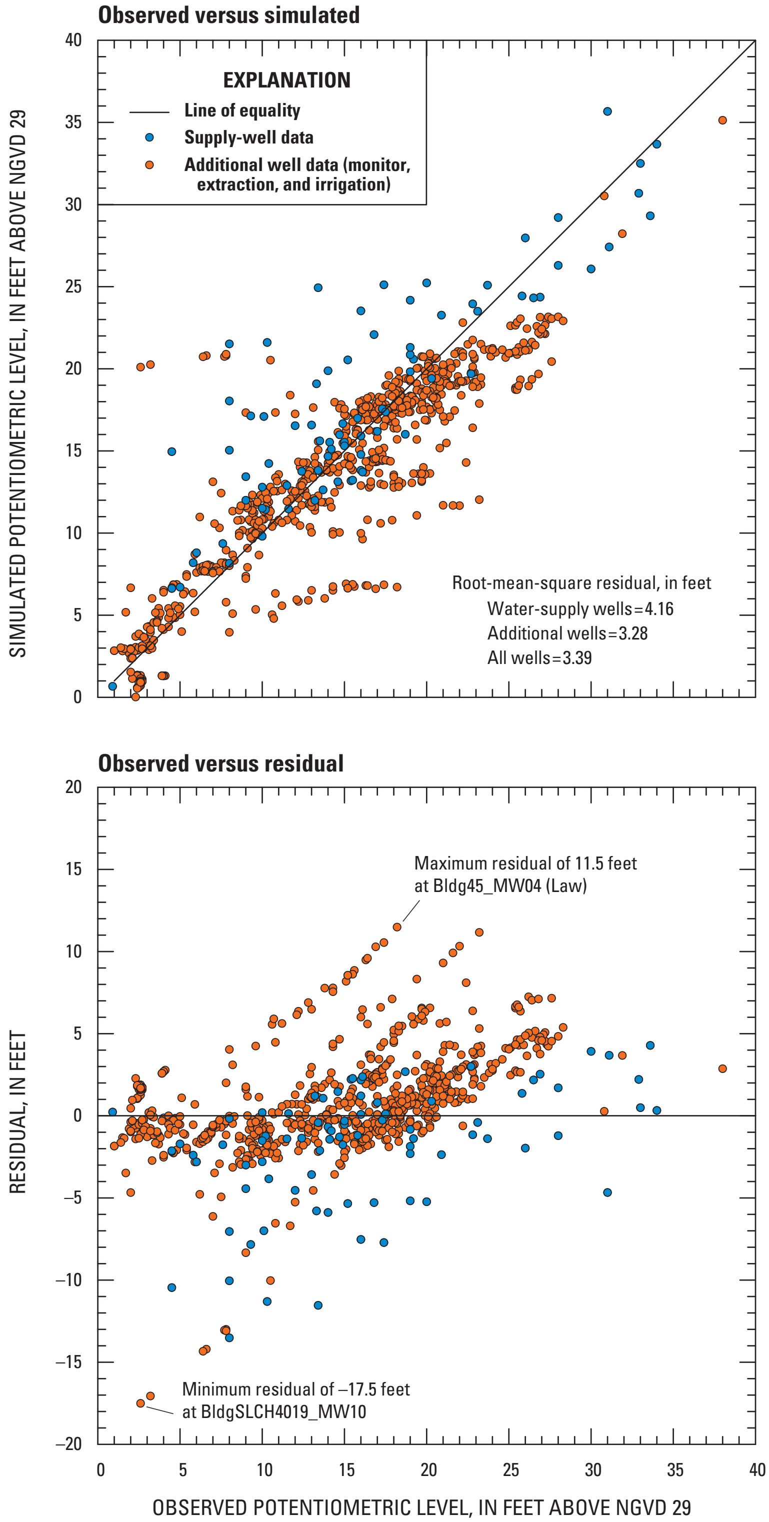

Figure S4.11. Steady-state groundwater-flow model results shown as observed and simulated potentiometric levels, and observed potentiometric levels and corresponding residuals, steady-state groundwater-flow model calibration, Hadnot Point–Holcomb Boulevard study area, U.S. Marine Corps Base Camp Lejeune, North Carolina.

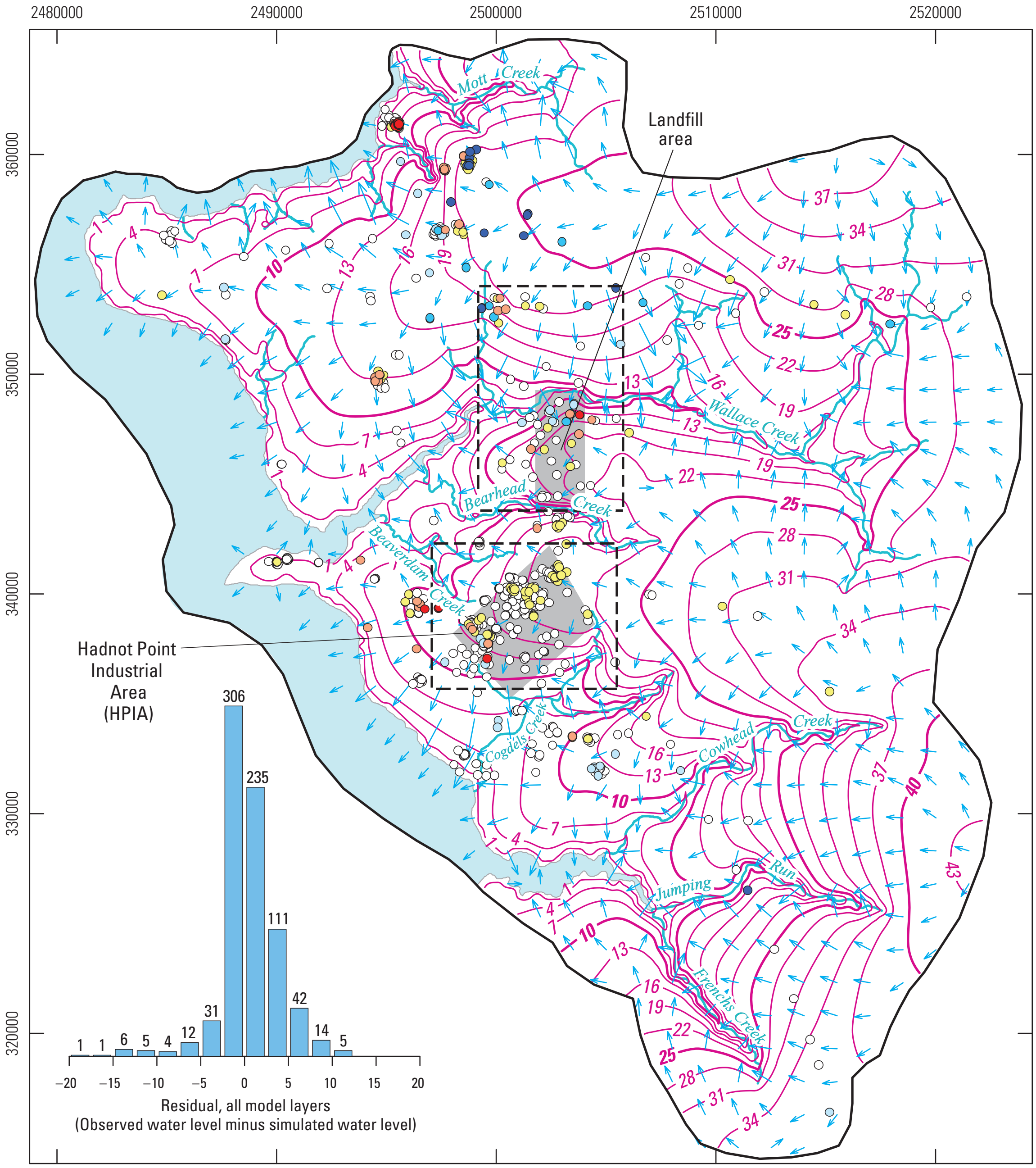

Base from U.S. Marine Corps and U.S. Geological Survey digital data files
Map coordinates are North Carolina State Plane coordinates
North American Datum of 1983

0 1 2 MILES
0 1 2 KILOMETERS

EXPLANATION

Active model domain

Contaminant fate and transport model subdomain

Simulation results

10 Potentiometric contour—Contour interval 3 feet. Datum is NGVD 29

Direction of groundwater flow

Residual

- >7.5
- 5 to 7.5
- 2.5 to 5
- 2.5 to –2.5
- –2.5 to –5
- –5 to –7.5
- <–7.5

Residual statistics, all model layers

Number of terms	773
Minimum	–17.5 feet
Maximum	11.5 feet
Average residual	0.5 feet
Standard deviation	3.34
Root-mean-square residual	3.39 feet

Figure S4.12. Simulated predevelopment (steady-state) potentiometric surface, directions of groundwater flow, and water-level residuals derived from the calibrated three-dimensional groundwater-flow model, Brewster Boulevard aquifer system, Hadnot Point–Holcomb Boulevard study area, U.S. Marine Corps Base Camp Lejeune, North Carolina.

Transient-State (Pumping) Conditions

The transient-state model simulates monthly conditions starting in January 1942 and ending in June 2008. Transient conditions include the effects of pumping from 96 supply wells that operated in the study area during different periods from 1942 to 2008 and the stress induced by variation in effective recharge. During July 1942, the first supply wells in the HPHB study area started pumping—wells HP-601, HP-602, HP-603, and HP-608 (Sautner et al. 2013). The groundwater-flow model readily simulates the effects of pumping wells in the HPIA where the simulated drawdown of the water table (Brewster Boulevard Aquifer system—model layer 1) is about 3–4 ft by July 1942 (Figure S4.13). In the HPLF, the wells operating at this time included HP-610 and HP-613, which produce a simulated water-table drawdown of about 6 ft (Figure S4.14). Most of the wells were pumping from the Upper Castle Hayne aquifer—model layer 5. Simulated potentiometric surface maps for model layer 5 during January 1951, January 1968, November 1984, and June 2008 are shown in Figure S4.15. Pumping for most of the supply wells in the HPIA began during 1942, causing the predevelopment potentiometric surface to change substantially. Pumping did not start until 1963 for some of the wells of interest in the HPIA (e.g., HP-634). By January 1968, some wells in the HPIA are pumping at lower rates due to the availability of additional supply wells; however, these wells still affected potentiometric levels (Figure S4.15). By November 1984, the influence of pumping at well HP-651 is prominent, and most of the wells in the HPIA area are pumping at a lower rate. By the end of the simulation period (June 2008), most supply wells in the HPIA and HPLF have been shut down, and the potentiometric surface returns to conditions similar to predevelopment conditions (Figure S4.12).

Only a few monitor wells in the study area contained continuous water-level data useful for assessment and calibration of the transient model. Continuous water levels for well cluster X24S, located southwest of Watkins Village, are particularly useful for this study (Figure S4.1). Three wells from this cluster (X24S7, X24S1, and X24S6) are open to aquifers represented in the groundwater-flow model, which are BBLAQ, UCHRBU, and UCHLU, respectively.[11] Groundwater-level response—potentiometric levels and trends—for wells X24S1, X24S7, and X24S6 is similar and was previously described by Faye et al. (2013). X24S6 was selected for comparison of simulated results to observed results. Preliminary transient model simulations did not include temporal variation of recharge. However, analyses for well cluster X24S indicated that groundwater levels at this well—and for the corresponding aquifer (Upper Castle Hayne aquifer–Lower unit [UCHLU])—were probably influenced by precipitation (Faye 2012). As previously described in the Three-Dimensional Groundwater-Flow Model section, the calibrated recharge array was multiplied by a monthly factor that mimics the effect of precipitation variability. Initial simulations of the transient groundwater-flow model were conducted without temporal variability of recharge.

Figure S4.16 shows monthly measured water-level altitudes for well X24S6 in feet above National Geodetic Vertical Datum of 1929 (NGVD 29). Measured monthly water-level altitude ranges from 3.6 ft to 9.1 ft NGVD 29. The average and standard deviation measured water-level altitudes are 5.8 ft and 1.2 ft, respectively. In conjunction with the measured water levels, the simulated water-level results at X24S6 from two transient groundwater-flow simulations—*cases a and b*—are shown in Figure S4.16. The simulated water levels for well X24S6 range from 4.5 ft to 5.6 ft for *case a* and from 2.6 ft to 9.1 ft for *case b*. The average simulated water levels for *cases a* and *b* are 5.0 ft and 5.1 ft, respectively. When comparing *case b* results and measured water levels qualitatively, there are periods during which simulated and observed water levels trend in the same direction, but in other periods, water levels trend in opposite directions. As shown in Figure S4.16, temporal variability of recharge could explain the variability in observed water levels at well X24S6. In this figure, *case a* shows the simulated water levels when recharge is constant over time. *Case b* represents temporal variability of recharge.

[11] See Table S4.1 for hydrogeologic unit abbreviations.

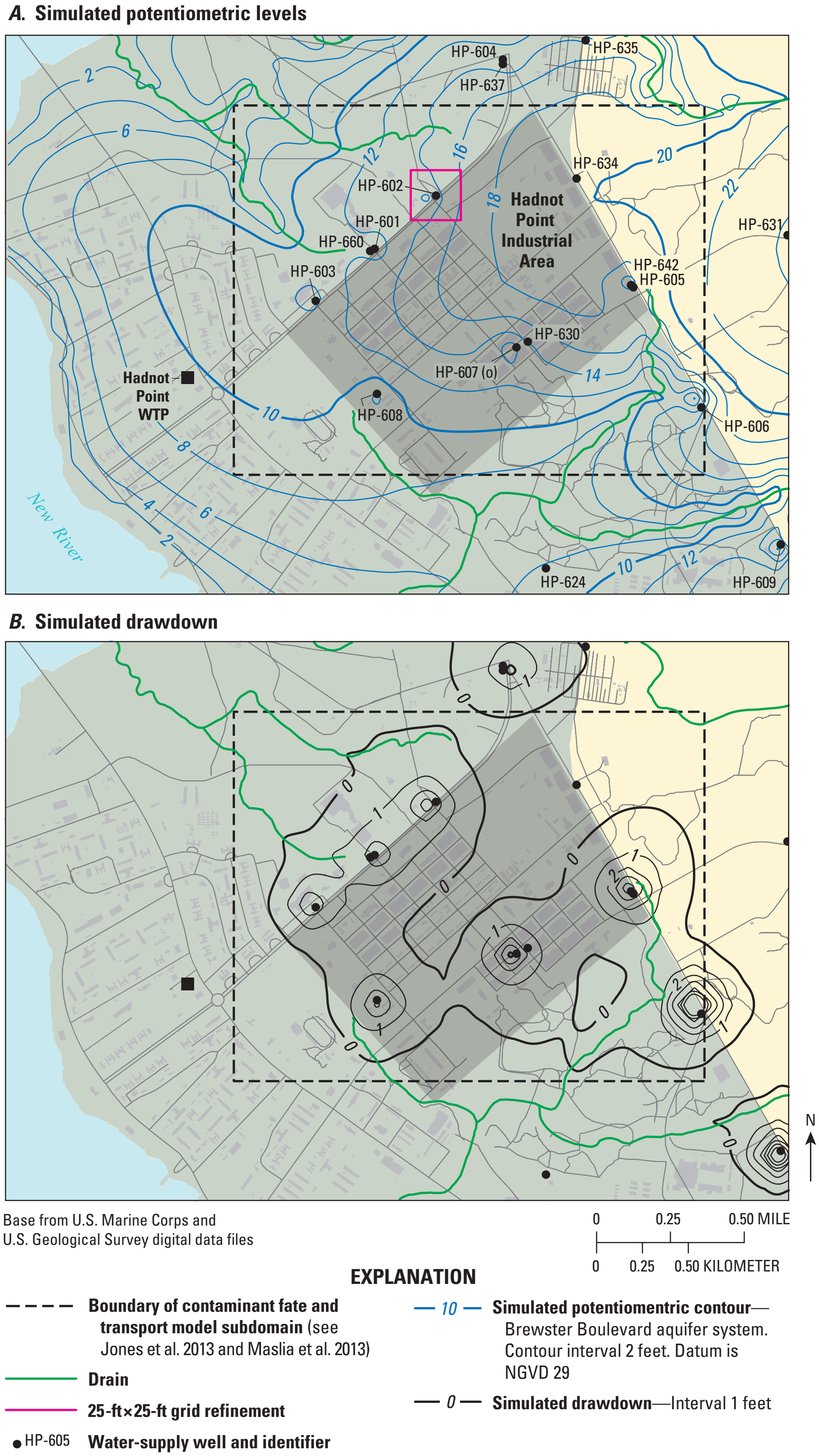

Figure S4.13. Simulated *(A)* potentiometric levels and *(B)* drawdowns, combined Brewster Boulevard aquifer, Brewster Boulevard upper confining unit, and Brewster Boulevard lower aquifer—model layer 1, stress period 7 (July 1942), Hadnot Point Industrial Area, Hadnot Point–Holcomb Boulevard study area, U.S. Marine Corps Base Camp Lejeune, North Carolina.

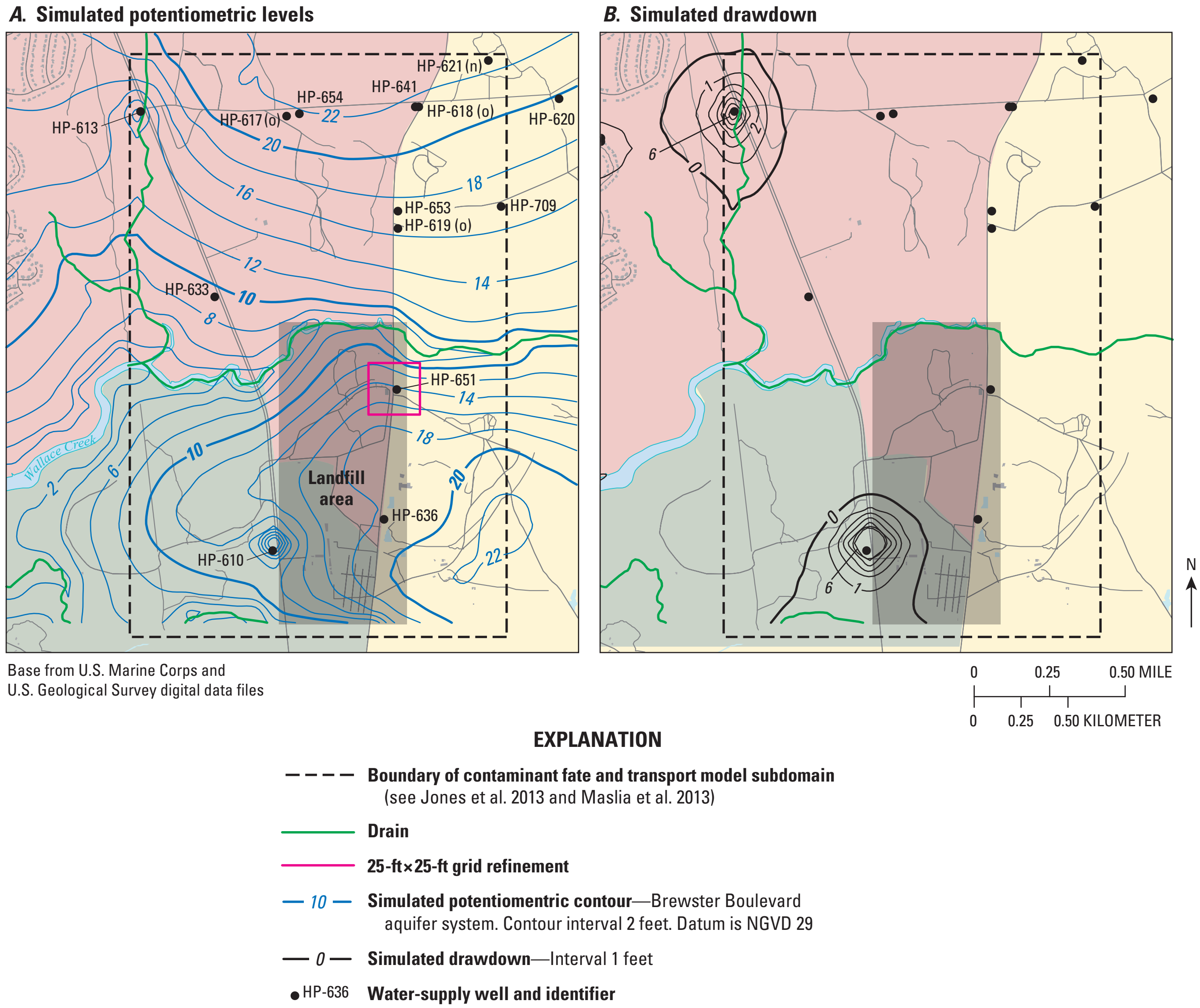

Figure S4.14. Simulated *(A)* potentiometric levels and *(B)* drawdowns, combined Brewster Boulevard aquifer, Brewster Boulevard upper confining unit, and Brewster Boulevard lower aquifer—model layer 1, stress period 7 (July 1942), Hadnot Point landfill area, Hadnot Point–Holcomb Boulevard study area, U.S. Marine Corps Base Camp Lejeune, North Carolina.

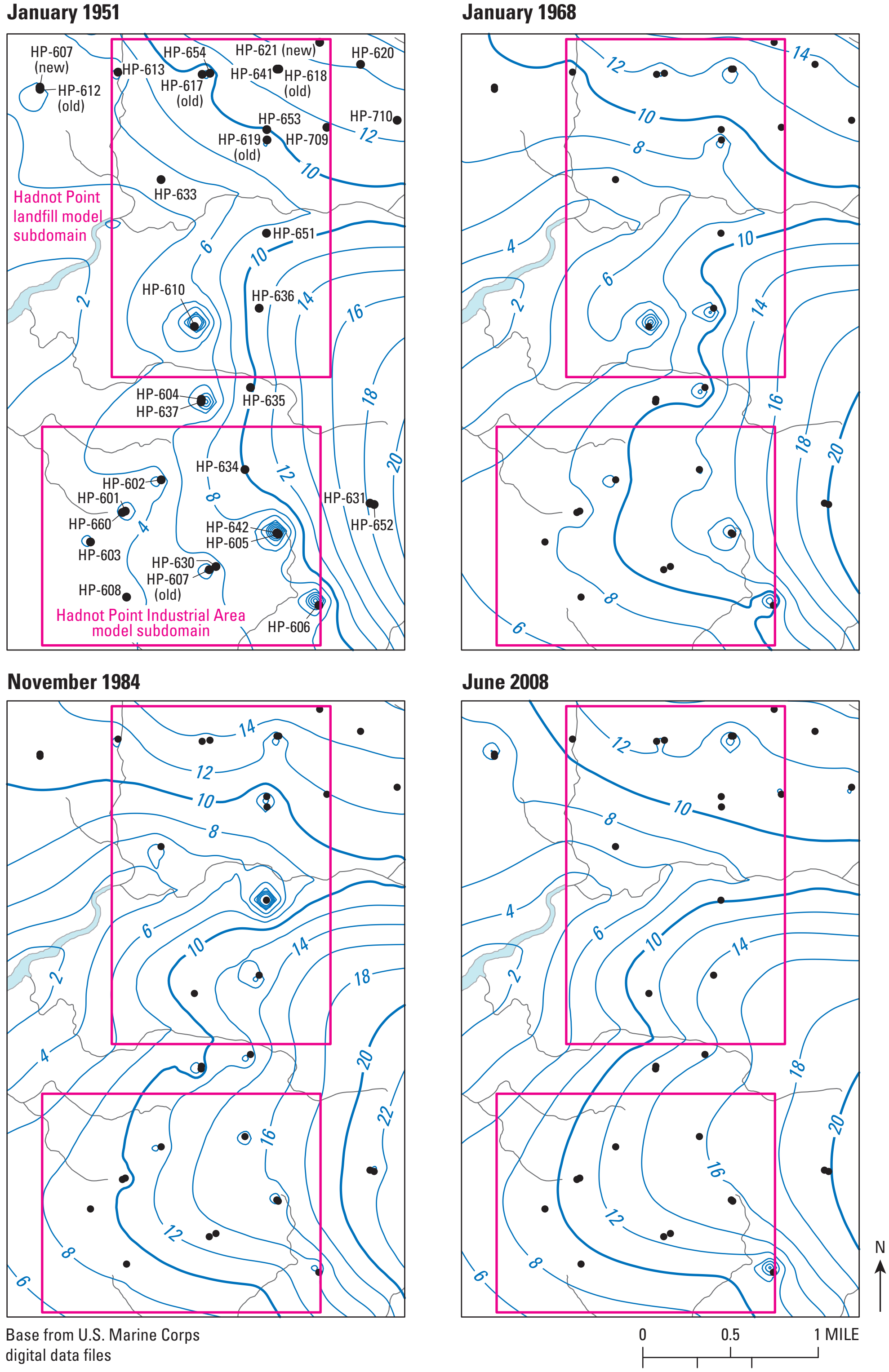

EXPLANATION

— 10 — **Simulated potentiometric contour**—Contour interval 2 feet. Datum is NGVD 29

Boundary of contaminant fate and transport model subdomain (see Jones et al. 2013 and Maslia et al. 2013)

HP-608 • **Water-supply well and identifier**

Figure S4.15. Simulated potentiometric levels for January 1951, January 1968, November 1984, and June 2008, combined Upper Castle Hayne aquifer–River Bend unit, Local confining unit, and Upper Castle Hayne aquifer–Lower unit—model layer 5, Hadnot Point–Holcomb Boulevard study area, U.S. Marine Corps Base Camp Lejeune, North Carolina.

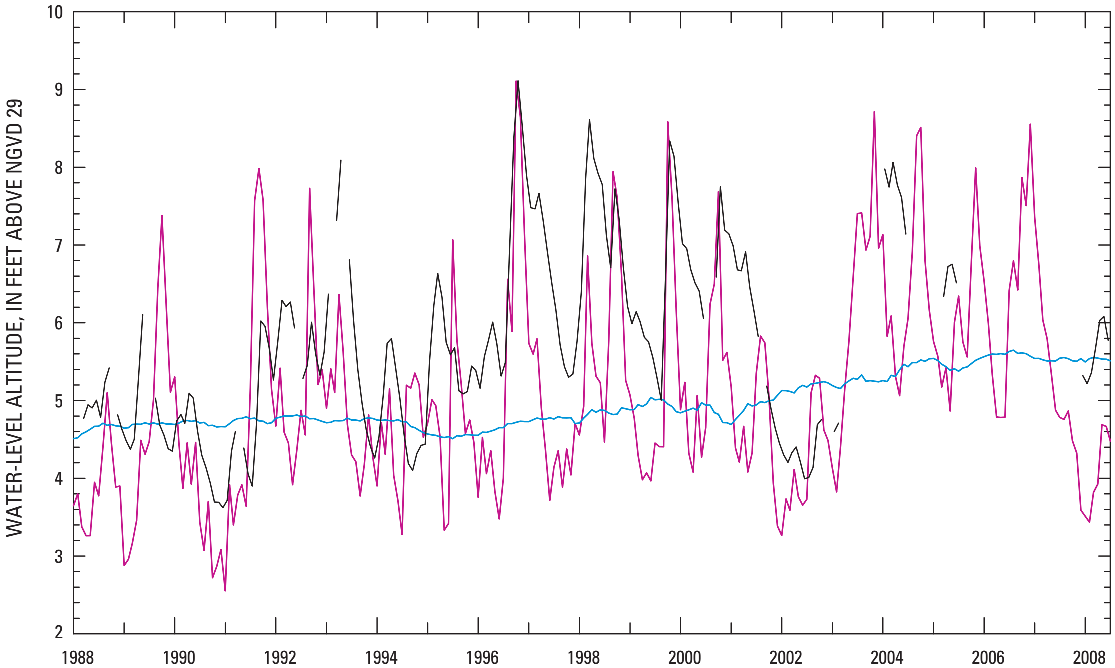

EXPLANATION

Measured water-level altitude (monthly)
Statistics:
Minimum=3.6 feet
Maximum=9.1 feet
Average=5.8 feet
Standard deviation=1.2 feet

***Case a*: Simulated water-level altitude (recharge: no temporal variability)**
Statistics:
Minimum = 4.5 feet
Maximum = 5.6 feet
Average = 5.0 feet
Standard deviation=0.3 foot

***Case b*: Simulated water-level altitude (recharge: temporal variability)**
Statistics:
Minimum = 2.6 feet
Maximum = 9.1 feet
Average = 5.1 feet
Standard deviation=1.3 feet

Figure S4.16. Comparison of observed water-level altitude and simulated water-level altitude for well X24S6 for two cases of the transient groundwater-flow model: *case a* with temporal variability of recharge, and *case b* without temporal variability of recharge, Hadnot Point–Holcomb Boulevard study area, U.S. Marine Corps Base Camp Lejeune, North Carolina. [Note: Date range for measured and simulated water-level altitude for *cases a* and *b* is March 1988 to June 2008.]

Sensitivity Analysis

Sensitivity analysis has been described as a method used to ascertain the dependency of a given model output (e.g., water level, hydraulic head, or concentration) on model input parameters (e.g., hydraulic conductivity, pumping rate, or specified concentration)(Maslia et al. 2009b). Numerous methods are described in the literature for conducting sensitivity analyses. One such method, referred to as one-at-a-time design or experiment, is conducted by changing calibrated model input parameter values, one at a time, and then assessing the resulting variation on model output (Saltelli et al. 2000). Thus, the purpose of this Supplement 4 report section is to present and discuss the characterization of the groundwater model output sensitivity (e.g., simulated water levels) due to model input parameter variability.

Input Parameter Sensitivity Analysis

For this study, the model input parameters included in the sensitivity analysis are horizontal hydraulic conductivity for layers 1–7, recharge, and pumping rate. Results of sensitivity analyses are commonly reported as a metric, such as the root-mean-square. The sensitivity analysis was conducted by multiplying the calibrated parameter arrays—one parameter at a time—by a parameter multiplier that ranged from 0.1 to 10. The root-mean-square and mean water-level residual are the specific sensitivity analysis metrics and were calculated for each model simulation using observed water levels from Table S4.8 and are shown graphically in Figure S4.17. The figure contains the results for sensitivity analyses for recharge and horizontal hydraulic conductivity for all layers combined and for each layer individually. The multiplier value of 1 on the abscissa indicates a calibrated model parameter value. Results indicate that horizontal hydraulic conductivity for all layers (combined) and recharge are the most sensitive parameters. The sensitivity analyses for changes to horizontal hydraulic conductivity for individual layers (1–7) indicate that layer 5 is the most sensitive of all individual layers for parameter multipliers greater than 1.0. For parameter multipliers less than 1.0, horizontal hydraulic conductivities in layers 1 and 5 are the most sensitive parameters. However, at the lower limit of the sensitivity analysis (multiplier of 0.1), horizontal hydraulic conductivities of layers 2 and 4 are as sensitive as layer 5.

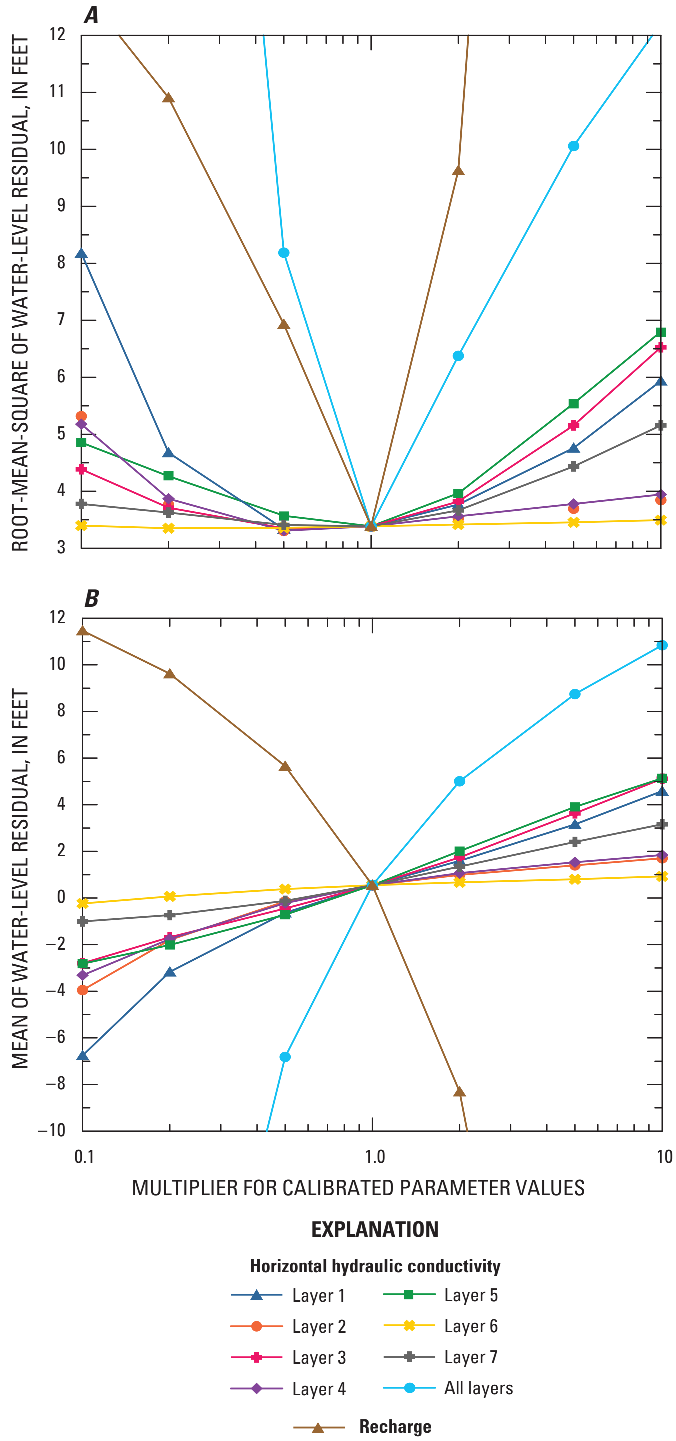

Figure S4.17. Sensitivity-analysis results for groundwater-flow model parameters in terms of *(A)* root-mean-square of water-level residual, and *(B)* mean of water-level residual, Hadnot Point–Holcomb Boulevard study area, U.S. Marine Corps Base Camp Lejeune, North Carolina.

Variably Spaced Grid Sensitivity Analysis

Simulations for the TT study area indicated a finite difference grid consisting of cells of 50 ft (per side) or less was required for fate and transport simulations to minimize numerical dispersion and oscillations (Faye 2008). Therefore, variably spaced grid models consisting of cells 50 ft (per side) for the HPIA and HPLF model subdomains (Figure S4.6) were developed; sensitivity analyses were conducted using the variably spaced grid models (50-ft per side cells). Results using the calibrated model grid size (300-ft per side cells) and the variably spaced grid models (50-ft per side cells in the HPIA and HPLF area) are described below.

The HPIA variably spaced model grid is subdivided into 288 rows, 298 columns, and 7 layers. This refinement represents an increase of 328 percent in the number of cells from the 300-ft uniform grid model. Similarly, the HPLF variably spaced model grid is subdivided into 348 rows, 268 columns, and 7 layers, representing an increase of 357 percent in the number of cells.[12] As with the calibrated model grid, the layers corresponded to the hydrogeologic units listed in Table S4.1. Variably spaced grid model properties (e.g., horizontal hydraulic conductivity, horizontal anisotropy, recharge) are identical to the 300-ft uniform grid model. Within the HPIA and HPLF subdomain areas (Figure S4.6), 36 cells (6 × 6) of 50 ft × 50 ft occupy one 300-ft × 300-ft cell of the calibrated model.

Individual variably spaced grid models for the HPIA and HPLF were created based on the 300-ft uniform grid model (Figure S4.6). Refinement for both models was performed to obtain a finite difference grid consisting of 50-ft (per side) square cells in the HPIA and HPLF areas. These areas are referred to as contaminant fate and transport subdomains in Maslia et al. (2013). Grid refinement was conducted to minimize the contrast in cell size between adjacent cells. The ratio of cell sizes for adjacent cells is 1.5 or less, except for a limited number of columns and rows where the ratio is 2. Grid refinement was accomplished using ModelMuse (Winston 2009).

Simulated potentiometric levels (heads) for the uniform and variably spaced grid models were compared to determine the equivalency of the model results. For the HPIA variably spaced grid model, the difference in simulated heads for most of the subdomain area is within 0.5 ft of the results obtained from the uniform grid model (Figure S4.18). The largest difference occurs near Cogdels Creek where the simulated heads for the HPIA variably spaced grid model are about 1–2 ft lower than the heads simulated by the uniform grid model for model layer 1. Similar differences occur for model layers 2–7. For the HPLF variably spaced grid model, the largest difference occurs in the upland areas along the southeastern boundary of the model at the headwaters of Frenchs Creek and its tributaries and in the extreme northeast boundary north of the headwaters of Wallace Creek (Figure S4.19). In those areas, simulated heads for the HPLF variably spaced grid model are nearly 4 ft lower than heads simulated by the uniform grid model. Elsewhere, the HPLF model simulated heads about 2 ft lower than the uniform grid model. Despite the aforementioned discrepancy, groundwater gradients are similar in magnitude and direction throughout the HPLF variably spaced grid model area (50-ft × 50-ft cells) when compared with the uniform grid model (300-ft × 300-ft cells) for the same area.

[12] See Maslia et al. (2013, Table A10) for a comprehensive listing of all model grid dimensions.

Cell-Size Sensitivity Analysis

A sensitivity analysis was conducted in the HPIA and HPLF subdomain areas to determine the effects of reducing cell sizes from 50 ft per side to 25 ft per side. For this analysis, refined model grids—within the HPIA and HPLF subdomain areas—consisting of 25 ft per side were used in the areas surrounding water-supply wells (Figure S4.1). The cell dimensions of the refined grid were 25 ft along each cell side (see Figures S4.13 and S4.14 for locations). Water levels simulated using the refined model grid (25-ft cells) were compared to water levels simulated using the variably spaced grid model (50-ft cells) at well HP-602 for the HPIA model subdomain and at well HP-651 for the HPLF model subdomain. Results are presented for January 1968 and November 1984 for water-supply well HP-602 and for July 1972 and November 1984 for well HP-651. Figure S4.20 shows that water levels simulated using the refined and variably spaced grid models (50-ft and 25-ft cells, respectively) are nearly identical. For example, during January 1968, the simulated water level at well HP-602 using the 50-ft model grid was 5.3 ft; for the 25-ft model grid, the simulated water level was 4.6 ft. Thus, sensitivity to a 50-percent reduction in cell dimension (75-percent reduction in cell area) within the model subdomain areas is apparent only in the immediate vicinity of a model cell with a pumping well, and the difference in simulated water levels at these cells is small compared to total simulated drawdown.

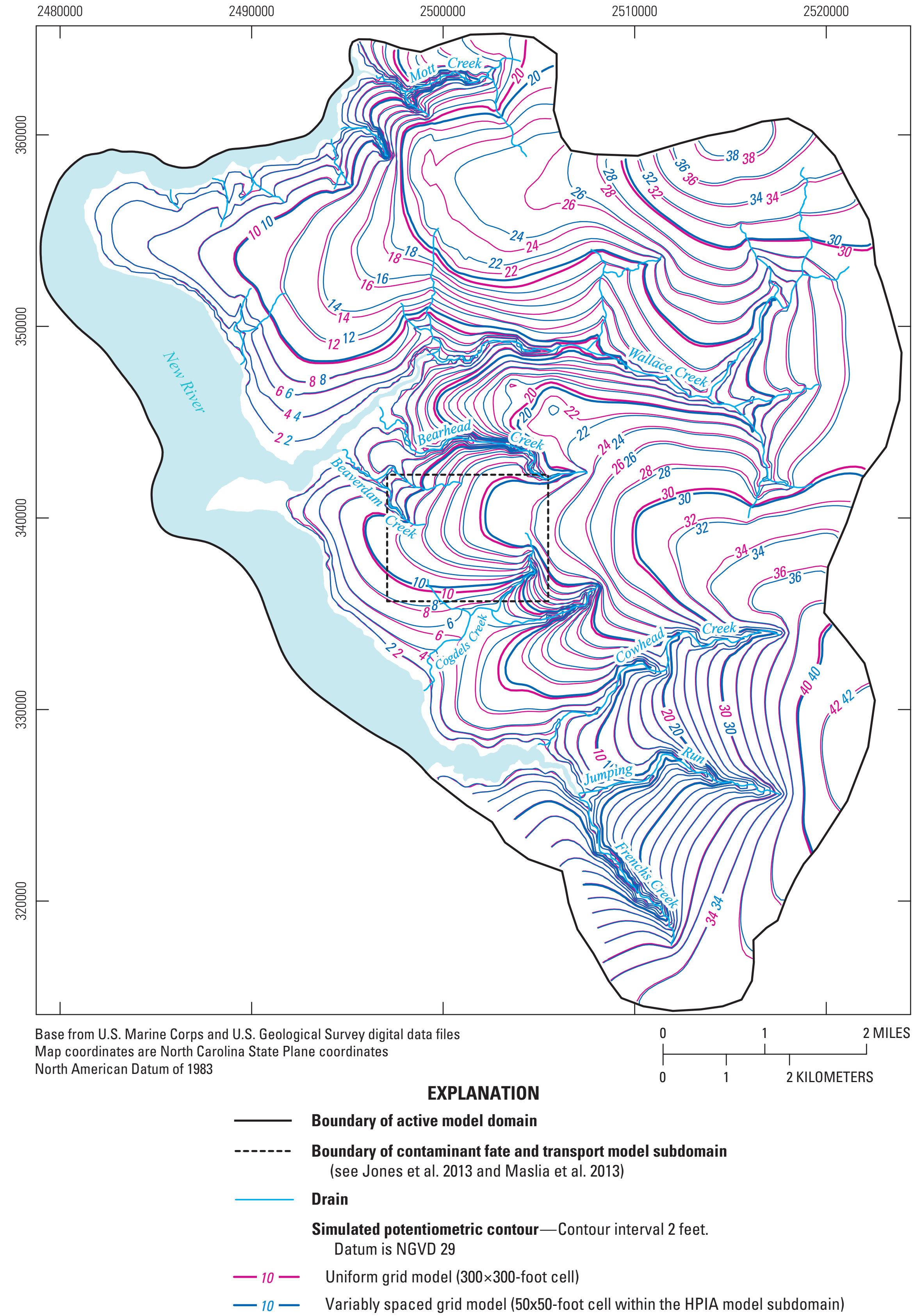

Figure S4.18. Simulated potentiometric levels for layer 1 for the uniform grid model and the Hadnot Point Industrial Area (HPIA) variably spaced grid model, Hadnot Point–Holcomb Boulevard study area, U.S. Marine Corps Base Camp Lejeune, North Carolina.

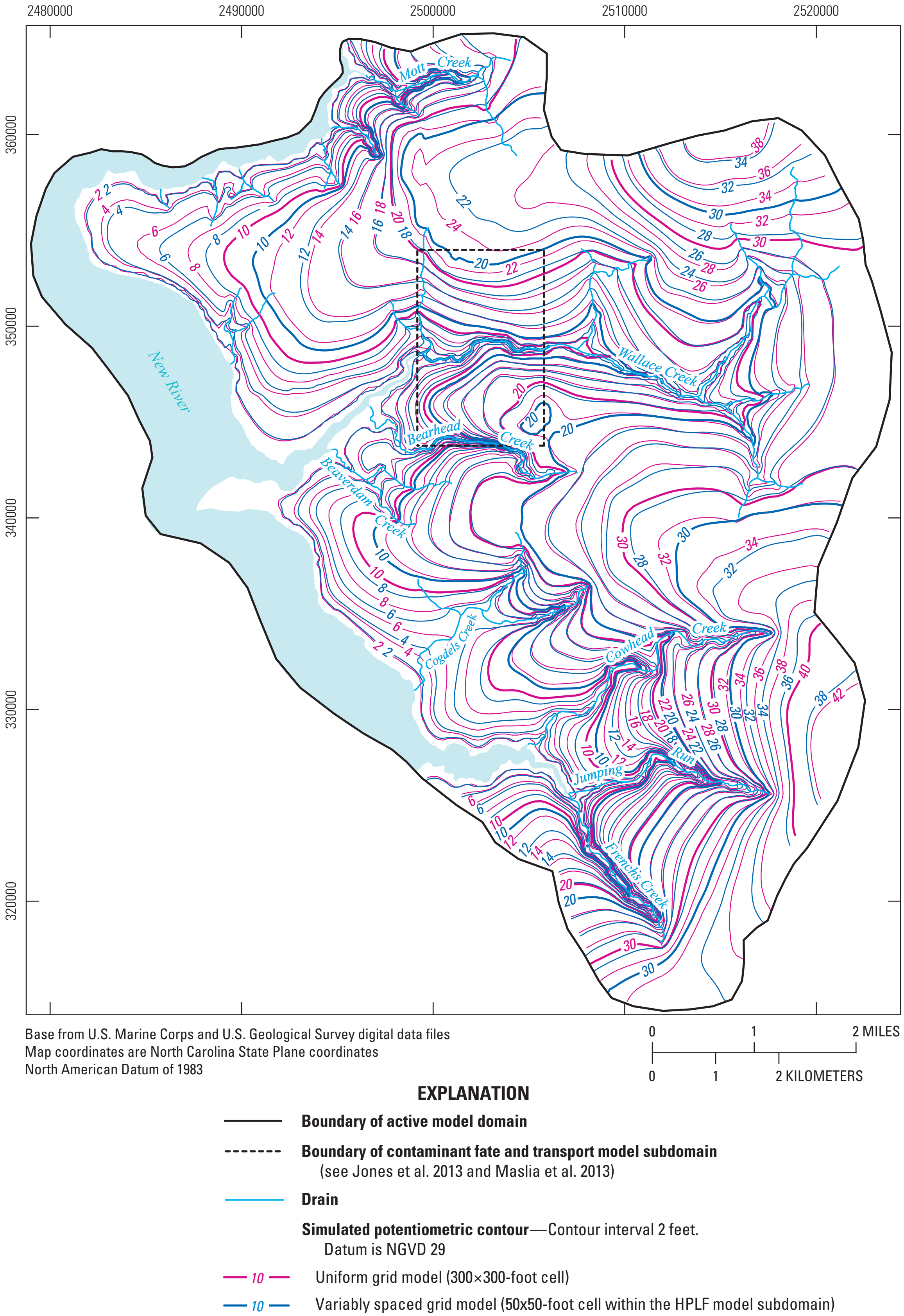

Figure S4.19. Simulated potentiometric levels for layer 1 for the uniform grid model and the Hadnot Point landfill (HPLF) area variably spaced grid model, Hadnot Point–Holcomb Boulevard study area, U.S. Marine Corps Base Camp Lejeune, North Carolina.

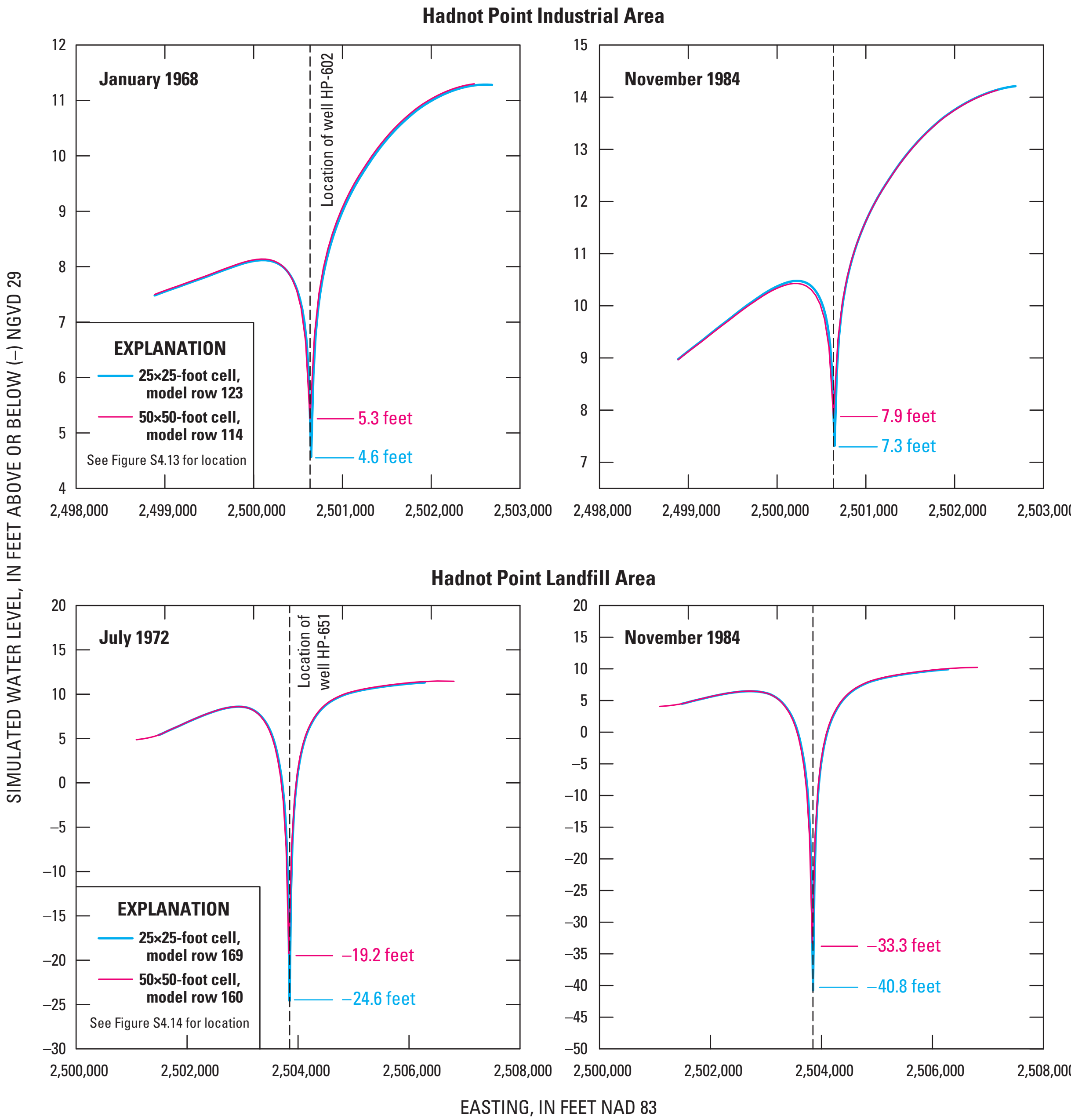

Figure S4.20. Simulated water levels along designated model row containing water-supply wells HP-602 and HP-651 using finite-difference cell dimensions of 50 feet per side and 25 feet per side, Hadnot Point–Holcomb Boulevard study area, U.S. Marine Corps Base Camp Lejeune, North Carolina.

Discussion

Analyses and interpretations of the groundwater-flow model results should be considered in the context of model limitations and accuracy of water-level data. Results from the calibrated groundwater-flow model are used to estimate contaminant concentrations in groundwater; therefore, it is also important to consider the accuracy of the flow model results in the context of contaminant fate and transport results. Analyses of the variability of contaminant concentration due to changes in groundwater-flow model (i.e., horizontal hydraulic conductivity and recharge) are presented by Jones et al. (2013).

Measured Water-Level Data

More than 13,000 static water-level measurements were obtained from various documents published to summarize results of CERCLA and RCRA groundwater contaminant investigations (Faye et al. 2010, 2012). Water-level data used for calibration and analyses in this report are further described by Faye et al. (2013). Water-level measurements analyzed and used for model calibration include (1) static water-level measurements, which were used for steady-state model assessment and calibration, and (2) continuous water-level measurements, which were used for transient-state model calibration. In general, measured water-level data used in this study are subjected to errors due to, among others, the following: (1) uncertainty of measurement datum (vertical), (2) uncertainty of well location, and (3) measurement and reporting errors. Some of these errors can be minimized or recognized by comparing data from multiple sources when available. For example, land-surface altitude—which is commonly used to determine water-level altitude—was obtained on some occasions from multiple sources, including drillers' reports, topographic maps, and DEMs. The discrepancies observed among land-surface altitudes from these multiple sources were generally less than 1 ft; the most reliable source was selected. Measurement errors also were minimized by using a filtering process described in Faye et al. (2013). Reporting errors were noted in some instances and were corrected during the data-entry process. For example, on some occasions, the water depth was reported as water altitude. Many supply wells were equipped with tubing to obtain airline measurements, which are known to be less accurate than sounders or tape measurements (Driscoll 1986). To minimize measurement errors, airline measurements were not used. The period of available data in some instances was limited. Measured water-level data used for steady-state model calibration were only available for partial periods of time; for example, more than 75 percent of static water-level measurements were obtained after January 1985. Predevelopment conditions occurred in the 1940s when most supply wells were not available; therefore, some static water-level measurements could have been affected by nearby pumping wells (Faye et al. 2013).

Transient model calibration should be considered within the context of the available data. Most of the reliable (e.g., tape measurements) water-level measurements for supply wells were obtained during maintenance operations when wells were out of service or turned off. Water-level measurements during pumping were airline measurements and are considered to be poor data. Therefore, water-level data at most supply wells do not represent—or poorly represent—pumping conditions. In addition, continuous water-level data were spatially limited to only a few locations (Faye 2012); however, daily data from 1988 to 2008 were available for well X24S6. Continuous water-level data obtained during aquifer tests were available for many supply wells; however, the periods of these tests are minutes, and the model results are interpreted to represent monthly mean values.

When comparing simulated water levels to measured water levels, several aspects should be considered. For example, the time scale of the measurement should be taken into account because some field measurements represent conditions of short duration (e.g., minutes to days) whereas simulated values represent monthly mean values. Therefore, the model formulation and results are not applicable to events of short duration—this would include short periods of high recharge due to high intensity rainfall. Also, certain hydrogeologic features (e.g., perched water table) are not represented in the model, and these features may be the cause of discrepancies between simulated and measured values.

Model Limitations

The groundwater-flow model described in this supplement was constructed using the MODFLOW family of finite-difference codes. Because no natural boundary conditions exist near the sites of interest—HPIA and HPLF—a uniform grid model extending to the natural hydrologic boundaries was constructed. In cases like this, finite-difference analysis has the disadvantage of using large grids that are not easily refined for additional analysis—such as contaminant fate and transport. Another disadvantage of a coarse grid is that stressed simulated water levels may not be comparable with measured water levels. In other words, the simulated drawdown obtained using a coarse model grid usually underestimates the measured drawdown value. Because the calibration process did not include comparing simulated and observed drawdown levels, the effect of the calibration performance due to the coarse grid is limited.

Vertical discretization of the model was based on limited geophysical data. From 931 data points available to describe the hydrogeologic framework, only 6 data points contained information for the top of the Lower Castle Hayne confining unit (layer 7). Therefore, the thickness of hydrogeologic units should be considered an approximation. In addition, multiple hydrogeologic units were combined into multiple layers. For example, layers 1 and 5 contain multiple hydrogeologic units (Table S4.1). However, contaminant transport model results typically are more sensitive than groundwater-flow model results to the combination of multiple hydrogeologic units in a model layer.

Drains (simulated using the DRN package in MODFLOW) were used to simulate groundwater discharge to various creeks and streams, including sections of Wallace Creek. Drains can only be used to remove water from the aquifer. Historical aerial images show the prevalence of surface water over time in upstream areas of Wallace Creek. Although there is no information to correctly determine if Wallace Creek behaved as a losing stream at times, the assumption that Wallace Creek always behaves as a gaining stream is probably appropriate.

A specified-head boundary was used in MODFLOW to simulate New River. The sections of New River included in the model are a tidal estuary of the Atlantic Ocean, and the long-term average water level resembles sea level. Data from a stream station (U.S. Geological Survey site 0209303205) located at New River near Highway 17 indicate that the water level varies about 1–2 ft (U.S. Geological Survey 2011). However, this station is located in a section of New River that is probably more affected by river conditions than the estuary conditions; therefore, variability of head in the estuary is probably lower. The assumption that sea level (specified-head boundary) was constant is probably appropriate.

No-flow (zero flux) boundaries were used to represent groundwater divides that coincide with topographic divides. These no-flow boundaries probably shifted over time due to pumping and seasonal effects (e.g., slight changes in recharge). Although the boundary locations change over time, probably the long-term average location is relatively fixed.

Model calibration in this study was accomplished by using trial-and-error and parameter estimation methods in a complementary manner. Parameter estimation was used to extract maximum information from the data. For example, more than 700 water-level measurements were available to calibrate the steady-state model. Most of the water-level measurements correspond to layers 1, 3, and 5. In addition, soil data were available for estimation of areas of low and high infiltration. Therefore, parameter estimation was appropriate for the steady-state model calibration phase to determine recharge and hydraulic conductivity for layers 1, 3, and 5. Because water-level measurements representing layer 7 were scarce, hydraulic conductivity for layer 7 was not modified from initial estimates that were based on available data from aquifer tests. Other parameters, including specific yield and specific storage, were not varied from initial estimates, which were based on values provided by Faye and Valenzuela (2007). Additional analyses, in which these parameters were varied, indicate no effect on specific discharge or velocity values, which in turn are necessary for fate and transport simulations. More rigourous sensitivity analyses could be conducted by computing the covariance matrix. However, initial simulations indicated that computing the covariance matrix using parameter estimation was time prohibited in terms of computational times using equipment available to authors at the time model calibration and sensitivity analyses were conducted.

Acknowledgment

Authors acknowledge the assistance of Robert E. Faye, consultant to Eastern Research Group, Inc., for review and analyses of water-level data, review of the groundwater-flow model calibration, and review of this supplement in its entirety.

References

Anderson MP and Woessner WW. Applied Groundwater Modeling: Simulation of Flow and Advective Transport: Academic Press, Inc.; 1992.

Baker Environmental, Inc. Final Feasibility Study for Operable Unit No. 1 (Sites 21, 24, and 78), Marine Corps Base Camp Lejeune, North Carolina; 1994. Contract Task Order 0177, Contract No.: N62470-89-D-4814 (CERCLA Administrative Record File #1256).

Baker Environmental, Inc. Basewide Remediation Assessment Groundwater Study (BRAGS), Marine Corps Base Camp Lejeune, North Carolina; 1998a. Contract Task Order 0140, Contract No.: N62470-89-D-4814 (CERCLA Administrative Record File #02013).

Baker Environmental, Inc. Groundwater Modeling Report, Operable Unit No. 9, Site 73—Amphibious Vehicle Maintenance Facility, Marine Corps Base Camp Lejeune, North Carolina; 1998b. Contract Task Order 0312, Contract No.: N62470-89-D-4814 (CERCLA Administrative Record File #02583).

Bear J. Hydraulics of Groundwater. McGraw-Hill, Inc.; 1979.

Cardinell AP, Berg SA, and Lloyd OB Jr. Hydrogeologic Framework of U.S. Marine Corps Base at Camp Lejeune, North Carolina. U.S. Geological Survey Water-Resources Investigations Report 93–4049; 1993.

CH2M HILL. Final Site Management Plan, Fiscal Year 2006, Marine Corps Base (MCB) Camp Lejeune, North Carolina. Norfolk, VA: Naval Facilities Engineering Command, Atlantic Division; 2006. Contract No.: N62470-03-D-4186.

Doherty J. PEST: Model Independent Parameter Estimation: User Manual; 2010. [cited 2012 July 24]; Available from *http://www.pesthomepage.org/Downloads.php*.

Doherty J. MODFLOW-ASP: Using MODFLOW-2000 with PEST-ASP; 2011. [cited 2011 December 2]; Available from *http://www.pesthomepage.org/getfiles.php?file=mf2pest.pdf*.

Doherty JE, Fienen MN, and Hunt RJ. Approaches to Highly Parameterized Inversion: Pilot-Point Theory, Guidelines, and Research Directions: U.S. Geological Survey Scientific Investigations Report 2010–5168; 2010, 36 p.

Driscoll FG. Groundwater and Wells. 2nd ed. Johnson Division; 1986.

Faye RE. Analyses of Groundwater Flow, Contaminant Fate and Transport, and Distribution of Drinking Water at Tarawa Terrace and Vicinity, U.S. Marine Corps Base Camp Lejeune, North Carolina: Historical Reconstruction and Present-Day Conditions—Chapter B: Geohydrologic Framework of the Castle Hayne Aquifer System. Atlanta, GA: Agency for Toxic Substances and Disease Registry; 2007.

Faye RE. Analyses of Groundwater Flow, Contaminant Fate and Transport, and Distribution of Drinking Water at Tarawa Terrace and Vicinity, U.S. Marine Corps Base Camp Lejeune, North Carolina: Historical Reconstruction and Present-Day Conditions—Chapter F: Simulation of the Fate and Transport of Tetrachloroethylene (PCE). Atlanta, GA: Agency for Toxic Substances and Disease Registry; 2008.

Faye RE. Analyses and Historical Reconstruction of Groundwater Flow, Contaminant Fate and Transport, and Distribution of Drinking Water Within the Service Areas of the Hadnot Point and Holcomb Boulevard Water Treatment Plants and Vicinities, U.S. Marine Corps Base Camp Lejeune, North Carolina—Chapter B: Geohydrologic Framework of the Brewster Boulevard and Castle Hayne Aquifer Systems and the Tarawa Terrace Aquifer and Confining Unit. Atlanta, GA: Agency for Toxic Substances and Disease Registry; 2012.

Faye RE, Anderson BA, Suárez-Soto RJ, and Sautner JB. Analyses and Historical Reconstruction of Groundwater Flow, Contaminant Fate and Transport, and Distribution of Drinking Water Within the Service Areas of the Hadnot Point and Holcomb Boulevard Water Treatment Plants and Vicinities, U.S. Marine Corps Base Camp Lejeune, North Carolina—Chapter C: Occurrence of Selected Contaminants in Groundwater at Installation Restoration Program Sites. Atlanta, GA: Agency for Toxic Substances and Disease Registry; 2010.

Faye RE, and Green JW Jr. Analyses of Groundwater Flow, Contaminant Fate and Transport, and Distribution of Drinking Water at Tarawa Terrace and Vicinity, U.S. Marine Corps Base Camp Lejeune, North Carolina: Historical Reconstruction and Present-Day Conditions—Chapter E: Occurrence of Contaminants in Groundwater. Atlanta, GA: Agency for Toxic Substances and Disease Registry; 2007.

Faye RE, Jones LE, and Suárez-Soto RJ. Descriptions and Characterizations of Water-Level Data and Groundwater Flow for the Brewster Boulevard and Castle Hayne Aquifer Systems and the Tarawa Terrace Aquifer—Supplement 3. In: Maslia ML, Suárez-Soto RJ, Sautner JB, Anderson BA, Jones LE, Faye RE, Aral MM, Guan J, Jang W, Telci IT, Grayman WM, Bove FJ, Ruckart PZ, and Moore, SM. Analyses and Historical Reconstruction of Groundwater Flow, Contaminant Fate and Transport, and Distribution of Drinking Water Within the Service Areas of the Hadnot Point and Holcomb Boulevard Water Treatment Plants and Vicinities, U.S. Marine Corps Base Camp Lejeune, North Carolina—Chapter A: Summary and Findings. Atlanta, GA: Agency for Toxic Substances and Disease Registry; 2013.

Faye RE, Suárez-Soto RJ, and Maslia ML. Analyses and Historical Reconstruction of Groundwater Flow, Contaminant Fate and Transport, and Distribution of Drinking Water Within the Service Areas of the Hadnot Point and Holcomb Boulevard Water Treatment Plants and Vicinities, U.S. Marine Corps Base Camp Lejeune, North Carolina—Chapter D: Occurrence of Selected Contaminants in Groundwater at Above-Ground and Underground Storage Tank (AST/UST) Sites. Atlanta, GA: Agency for Toxic Substances and Disease Registry; 2012.

Faye RE and Valenzuela C. Analyses of Groundwater Flow, Contaminant Fate and Transport, and Distribution of Drinking Water at Tarawa Terrace and Vicinity, U.S. Marine Corps Base Camp Lejeune, North Carolina: Historical Reconstruction and Present-Day Conditions—Chapter C: Simulation of Groundwater Flow. Atlanta, GA: Agency for Toxic Substances and Disease Registry; 2007.

Freeze RA and Witherspoon PA. Theoretical Analysis of Regional Groundwater Flow—1. Analytical and Numerical Solutions to the Mathematical Model: Water Resources Research. 1966;2(4).

Freeze RA and Witherspoon PA. Theoretical Analysis of Regional Groundwater Flow—2. Effect of Water-Table Configuration and Subsurface Permeability Variation: Water Resources Research. 1967;3(2).

Geophex, Ltd. Final Report on Groundwater Resource Evaluation at Marine Corps Air Station, New River, Engineering Study 93–09; 1994.

Geophex, Ltd. Geophysical Investigation at Building 645 Site, MCB Camp Lejeune, NC, Final Report, 2001 (UST Management Web Portal File #720).

Geophex, Ltd. Geophysical Investigation at the Former Fuel Facility and Surrounding Areas, Hadnot Point, MCB Camp Lejeune, NC, Volume I: Interim report; 2002 (Leaking Underground Storage Tank Program File #450).

Giese GL, Eimers JL, and Coble RW. Simulation of Ground-Water Flow in the Coastal Plain Aquifer System of North Carolina. U.S. Geological Survey Professional Paper 1404-M; 1997.

Harbaugh AW. MODFLOW-2005, The U.S. Geological Survey Modular Ground-Water Model—The Ground-Water Flow Process. U.S. Geological Survey Techniques and Methods 6-A16; 2005.

Harbaugh AW, Banta ER, Hill MC, and McDonald MG. MODFLOW-2000, The U.S. Geological Survey Modular Ground-Water Model—User Guide to Modularization Concepts and the Ground-Water Flow Process. U.S. Geological Survey Open-File Report 00–92; 2000, 121 p.

Harned DA, Lloyd OB Jr, and Treece MW Jr. Assessment of Hydrologic and Hydrogeologic Data at Camp Lejeune Marine Corps Base, North Carolina. Raleigh, NC: U.S. Geological Survey Water-Resources Investigations Report 89–4006; 1989.

Hubbard MK. The Theory of Groundwater Motion, Part 1, Part 2. The Journal of Geology. 1940; XLVIII.

Jang W, Anderson BA, Suárez-Soto RJ, Aral MM, and Maslia ML. Source Characterization and Simulation of the Migration of Light Nonaqueous Phase Liquids (LNAPLs) in the Vicinity of the Hadnot Point Industrial Area—Supplement 7. In: Maslia ML, Suárez-Soto RJ, Sautner JB, Anderson BA, Jones LE, Faye RE, Aral MM, Guan J, Jang W, Telci IT, Grayman WM, Bove FJ, Ruckart PZ, and Moore SM. Analyses and Historical Reconstruction of Groundwater Flow, Contaminant Fate and Transport, and Distribution of Drinking Water Within the Service Areas of the Hadnot Point and Holcomb Boulevard Water Treatment Plants and Vicinities, U.S. Marine Corps Base Camp Lejeune, North Carolina—Chapter A: Summary and Findings. Atlanta, GA: Agency for Toxic Substances and Disease Registry; 2013.

Jang W and Aral MM. Analyses of Groundwater Flow, Contaminant Fate and Transport, and Distribution of Drinking Water at Tarawa Terrace and Vicinity, U.S. Marine Corps Base Camp Lejeune, North Carolina: Historical Reconstruction and Present-Day Conditions—Chapter G: Simulation of Three-Dimensional Multispecies, Multiphase Mass Transport of Tetrachloroethylene (PCE) and Associated Degradation By-Products. Atlanta, GA: Agency for Toxic Substances and Disease Registry; 2008.

Jones LE, Suárez-Soto RJ, Anderson BA, and Maslia ML. Source Characterization and Simulation of Fate and Transport of Selected Volatile Organic Compounds in the Vicinities of the Hadnot Point Industrial Area and Landfill—Supplement 6. In: Maslia ML, Suárez-Soto RJ, Sautner JB, Anderson BA, Jones LE, Faye RE, Aral MM, Guan J, Jang W, Telci IT, Grayman WM, Bove FJ, Ruckart PZ, and Moore SM. Analyses and Historical Reconstruction of Groundwater Flow, Contaminant Fate and Transport, and Distribution of Drinking Water Within the Service Areas of the Hadnot Point and Holcomb Boulevard Water Treatment Plants and Vicinities, U.S. Marine Corps Base Camp Lejeune, North Carolina—Chapter A: Summary and Findings. Atlanta, GA: Agency for Toxic Substances and Disease Registry; 2013.

Konikow LF, Hornberger GZ, Halford KJ, and Hanson RT. Revised Multi-Node Well (MNW2) Package for MODFLOW Ground-Water Flow Model. U.S. Geological Survey Techniques and Methods 6-A30; 2009, 67 p.

Kresic N. Hydrogeology and Groundwater Modeling. CRC Press LLC; 1997.

Maslia ML, Sautner JB, Faye RE, Suárez-Soto RJ, Aral MM, Grayman WM, Jang W, Wang J, Bove FJ, Ruckart PZ, Valenzuela C, Green JW Jr, and Krueger, AL. Analyses of Groundwater Flow, Contaminant Fate and Transport, and Distribution of Drinking Water at Tarawa Terrace and Vicinity, U.S. Marine Corps Base Camp Lejeune, North Carolina: Historical Reconstruction and Present-Day Conditions—Chapter A: Summary of Findings. Atlanta, GA: Agency for Toxic Substances and Disease Registry; 2007.

Maslia ML, Aral MM, Faye RE, Suárez-Soto RJ, Sautner JB, Wang J, Jang W, Bove FJ, and Ruckart PZ. Reconstructing Historical Exposures to Volatile Organic Compound-Contaminated Drinking Water at a U.S. Military Base. Water Quality, Exposure and Health. 2009a; 1(1):49–68.

Maslia ML, Suárez-Soto RJ, Wang J, Aral MM, Sautner JB, and Valenzuela C. Analyses of Groundwater Flow, Contaminant Fate and Transport, and Distribution of Drinking Water at Tarawa Terrace and Vicinity, U.S. Marine Corps Base Camp Lejeune, North Carolina: Historical Reconstruction and Present-Day Conditions—Chapter I: Parameter Sensitivity, Uncertainty, and Variability Associated with Model Simulations of Groundwater Flow, Contaminant Fate and Transport, and Distribution of Drinking Water. Atlanta, GA: Agency for Toxic Substances and Disease Registry; 2009b.

Maslia ML, Suárez-Soto RJ, Sautner JB, Anderson BA, Jones LE, Faye RE, Aral MM, Guan J, Jang W, Telci IT, Grayman WM, Bove FJ, Ruckart PZ, and Moore SM. Analyses and Historical Reconstruction of Groundwater Flow, Contaminant Fate and Transport, and Distribution of Drinking Water Within the Service Areas of the Hadnot Point and Holcomb Boulevard Water Treatment Plants and Vicinities, U.S. Marine Corps Base Camp Lejeune, North Carolina—Chapter A: Summary and Findings. Atlanta, GA: Agency for Toxic Substances and Disease Registry; 2013.

McDonald MG, and Harbaugh AW. A Modular Three-Dimensional Finite-Difference Groundwater-Flow Model. U.S. Geological Survey Open-File Report 83–875; 1984.

National Oceanic and Atmospheric Administration. Marine Geophysical Trackline Data; 2008. [cited 2008 December]; Available from *http://www.ngdc.noaa.gov/mgg/geodas/trackline.html*.

Saltelli A, Chan K, and Scott EM, eds. Sensitivity Analysis. Chichester, England: John Wiley & Sons, Ltd; 2000.

Sautner JB, Suárez-Soto RJ, Anderson BA, and Maslia ML. Descriptions and Characterizations of Data Pertinent to Water-Supply Well Capacities, Histories, and Operations—Supplement 1. In: Maslia ML, Suárez-Soto RJ, Sautner JB, Anderson BA, Jones LE, Faye RE, Aral MM, Guan J, Jang W, Telci IT, Grayman WM, Bove FJ, Ruckart PZ, and Moore SM. Analyses and Historical Reconstruction of Groundwater Flow, Contaminant Fate and Transport, and Distribution of Drinking Water Within the Service Areas of the Hadnot Point and Holcomb Boulevard Water Treatment Plants and Vicinities, U.S. Marine Corps Base Camp Lejeune, North Carolina—Chapter A: Summary and Findings. Atlanta, GA: Agency for Toxic Substances and Disease Registry; 2013.

Schwartz FW and Zhang H. Fundamentals of Ground Water. New York, NY: John Wiley and Sons, Inc.; 2003.

Soil Survey Staff, Natural Resources Conservation Service, United States Department of Agriculture. Soil Survey Geographic (SSURGO) Database for Onslow County, North Carolina; 2009. [cited 2010 November 4]; Available from *http://soildatamart.nrcs.usda.gov*.

Telci IT, Sautner JB, Suárez-Soto RJ, Anderson BA, Maslia ML, and Aral MM. Development and Application of a Methodology to Characterize Present-Day and Historical Water-Supply Well Operations—Supplement 2. In: Maslia ML, Suárez-Soto RJ, Sautner JB, Anderson BA, Jones LE, Faye RE, Aral MM, Guan J, Jang W, Telci IT, Grayman WM, Bove FJ, Ruckart PZ, and Moore SM. Analyses and Historical Reconstruction of Groundwater Flow, Contaminant Fate and Transport, and Distribution of Drinking Water Within the Service Areas of the Hadnot Point and Holcomb Boulevard Water Treatment Plants and Vicinities, U.S. Marine Corps Base Camp Lejeune, North Carolina—Chapter A: Summary and Findings. Atlanta, GA: Agency for Toxic Substances and Disease Registry; 2013.

Toth JA. Theoretical Analysis of Groundwater Motion in Small Drainage Basins in Central Alberta, Canada. Journal of Geophysical Research. 1962;67(11).

Toth JA. Theoretical Analysis of Groundwater Motion in Small Drainage Basins. Journal of Geophysical Research. 1963;68(16).

U.S. Army Engineer Research and Development Center. Department of Defense Groundwater Modeling System (GMS), version 8. Vicksburg, MS: U.S. Army Corps of Engineers, Engineer Research and Development Center; 2008. [cited 2012 March 2]; Available from *http://chl.erdc.usace.army.mil/gms*.

U.S. Geological Survey. National Elevation Dataset, Seamless Server; 2010. [cited 2010 August 18]; Available from *http://ned.usgs.gov/*.

U.S. Geological Survey. National Water Information System, Web Interface for USGS 0209303205 New River Below HWY17 Bridge at Jacksonville, NC; 2011. [cited 2011 June 5]; Available from *http://waterdata.usgs.gov/nwis/inventory/?site_no=0209303205&agency_cd=USGS&amp*.

Winston RB. ModelMuse—A Graphical User Interface for MODFLOW–2005 and PHAST. U.S. Geological Survey Techniques and Methods 6–A29; 2009.

Tables S4.6 and S4.8

Table S4.6. Simulation stress period and corresponding month and year, Hadnot Point–Holcomb Boulevard study area, U.S. Marine Corps Base Camp Lejeune, North Carolina.

[Jan., January; Feb., February; Mar., March; Apr., April; Aug., August; Sept., September; Oct., October; Nov., November; Dec., December]

Stress period	Month and year	Stress period	Month and year	Stress period	Month and year	Stress period	Month and year
1	Jan. 1942	49	Jan. 1946	97	Jan. 1950	145	Jan. 1954
2	Feb. 1942	50	Feb. 1946	98	Feb. 1950	146	Feb. 1954
3	Mar. 1942	51	Mar. 1946	99	Mar. 1950	147	Mar. 1954
4	Apr. 1942	52	Apr. 1946	100	Apr. 1950	148	Apr. 1954
5	May 1942	53	May 1946	101	May 1950	149	May 1954
6	June 1942	54	June 1946	102	June 1950	150	June 1954
7	July 1942	55	July 1946	103	July 1950	151	July 1954
8	Aug. 1942	56	Aug. 1946	104	Aug. 1950	152	Aug. 1954
9	Sept. 1942	57	Sept. 1946	105	Sept. 1950	153	Sept. 1954
10	Oct. 1942	58	Oct. 1946	106	Oct. 1950	154	Oct. 1954
11	Nov. 1942	59	Nov. 1946	107	Nov. 1950	155	Nov. 1954
12	Dec. 1942	60	Dec. 1946	108	Dec. 1950	156	Dec. 1954
13	Jan. 1943	61	Jan. 1947	109	Jan. 1951	157	Jan. 1955
14	Feb. 1943	62	Feb. 1947	110	Feb. 1951	158	Feb. 1955
15	Mar. 1943	63	Mar. 1947	111	Mar. 1951	159	Mar. 1955
16	Apr. 1943	64	Apr. 1947	112	Apr. 1951	160	Apr. 1955
17	May 1943	65	May 1947	113	May 1951	161	May 1955
18	June 1943	66	June 1947	114	June 1951	162	June 1955
19	July 1943	67	July 1947	115	July 1951	163	July 1955
20	Aug. 1943	68	Aug. 1947	116	Aug. 1951	164	Aug. 1955
21	Sept. 1943	69	Sept. 1947	117	Sept. 1951	165	Sept. 1955
22	Oct. 1943	70	Oct. 1947	118	Oct. 1951	166	Oct. 1955
23	Nov. 1943	71	Nov. 1947	119	Nov. 1951	167	Nov. 1955
24	Dec. 1943	72	Dec. 1947	120	Dec. 1951	168	Dec. 1955
25	Jan. 1944	73	Jan. 1948	121	Jan. 1952	169	Jan. 1956
26	Feb. 1944	74	Feb. 1948	122	Feb. 1952	170	Feb. 1956
27	Mar. 1944	75	Mar. 1948	123	Mar. 1952	171	Mar. 1956
28	Apr. 1944	76	Apr. 1948	124	Apr. 1952	172	Apr. 1956
29	May 1944	77	May 1948	125	May 1952	173	May 1956
30	June 1944	78	June 1948	126	June 1952	174	June 1956
31	July 1944	79	July 1948	127	July 1952	175	July 1956
32	Aug. 1944	80	Aug. 1948	128	Aug. 1952	176	Aug. 1956
33	Sept. 1944	81	Sept. 1948	129	Sept. 1952	177	Sept. 1956
34	Oct. 1944	82	Oct. 1948	130	Oct. 1952	178	Oct. 1956
35	Nov. 1944	83	Nov. 1948	131	Nov. 1952	179	Nov. 1956
36	Dec. 1944	84	Dec. 1948	132	Dec. 1952	180	Dec. 1956
37	Jan. 1945	85	Jan. 1949	133	Jan. 1953	181	Jan. 1957
38	Feb. 1945	86	Feb. 1949	134	Feb. 1953	182	Feb. 1957
39	Mar. 1945	87	Mar. 1949	135	Mar. 1953	183	Mar. 1957
40	Apr. 1945	88	Apr. 1949	136	Apr. 1953	184	Apr. 1957
41	May 1945	89	May 1949	137	May 1953	185	May 1957
42	June 1945	90	June 1949	138	June 1953	186	June 1957
43	July 1945	91	July 1949	139	July 1953	187	July 1957
44	Aug. 1945	92	Aug. 1949	140	Aug. 1953	188	Aug. 1957
45	Sept. 1945	93	Sept. 1949	141	Sept. 1953	189	Sept. 1957
46	Oct. 1945	94	Oct. 1949	142	Oct. 1953	190	Oct. 1957
47	Nov. 1945	95	Nov. 1949	143	Nov. 1953	191	Nov. 1957
48	Dec. 1945	96	Dec. 1949	144	Dec. 1953	192	Dec. 1957

Table S4.6. Simulation stress period and corresponding month and year, Hadnot Point–Holcomb Boulevard study area, U.S. Marine Corps Base Camp Lejeune, North Carolina.—Continued

[Jan., January; Feb., February; Mar., March; Apr., April; Aug., August; Sept., September; Oct., October; Nov., November; Dec., December]

Stress period	Month and year	Stress period	Month and year	Stress period	Month and year	Stress period	Month and year
193	Jan. 1958	241	Jan. 1962	289	Jan. 1966	337	Jan. 1970
194	Feb. 1958	242	Feb. 1962	290	Feb. 1966	338	Feb. 1970
195	Mar. 1958	243	Mar. 1962	291	Mar. 1966	339	Mar. 1970
196	Apr. 1958	244	Apr. 1962	292	Apr. 1966	340	Apr. 1970
197	May 1958	245	May 1962	293	May 1966	341	May 1970
198	June 1958	246	June 1962	294	June 1966	342	June 1970
199	July 1958	247	July 1962	295	July 1966	343	July 1970
200	Aug. 1958	248	Aug. 1962	296	Aug. 1966	344	Aug. 1970
201	Sept. 1958	249	Sept. 1962	297	Sept. 1966	345	Sept. 1970
202	Oct. 1958	250	Oct. 1962	298	Oct. 1966	346	Oct. 1970
203	Nov. 1958	251	Nov. 1962	299	Nov. 1966	347	Nov. 1970
204	Dec. 1958	252	Dec. 1962	300	Dec. 1966	348	Dec. 1970
205	Jan. 1959	253	Jan. 1963	301	Jan. 1967	349	Jan. 1971
206	Feb. 1959	254	Feb. 1963	302	Feb. 1967	350	Feb. 1971
207	Mar. 1959	255	Mar. 1963	303	Mar. 1967	351	Mar. 1971
208	Apr. 1959	256	Apr. 1963	304	Apr. 1967	352	Apr. 1971
209	May 1959	257	May 1963	305	May 1967	353	May 1971
210	June 1959	258	June 1963	306	June 1967	354	June 1971
211	July 1959	259	July 1963	307	July 1967	355	July 1971
212	Aug. 1959	260	Aug. 1963	308	Aug. 1967	356	Aug. 1971
213	Sept. 1959	261	Sept. 1963	309	Sept. 1967	357	Sept. 1971
214	Oct. 1959	262	Oct. 1963	310	Oct. 1967	358	Oct. 1971
215	Nov. 1959	263	Nov. 1963	311	Nov. 1967	359	Nov. 1971
216	Dec. 1959	264	Dec. 1963	312	Dec. 1967	360	Dec. 1971
217	Jan. 1960	265	Jan. 1964	313	Jan. 1968	361	Jan. 1972
218	Feb. 1960	266	Feb. 1964	314	Feb. 1968	362	Feb. 1972
219	Mar. 1960	267	Mar. 1964	315	Mar. 1968	363	Mar. 1972
220	Apr. 1960	268	Apr. 1964	316	Apr. 1968	364	Apr. 1972
221	May 1960	269	May 1964	317	May 1968	365	May 1972
222	June 1960	270	June 1964	318	June 1968	366	June 1972
223	July 1960	271	July 1964	319	July 1968	367	July 1972
224	Aug. 1960	272	Aug. 1964	320	Aug. 1968	368	Aug. 1972
225	Sept. 1960	273	Sept. 1964	321	Sept. 1968	369	Sept. 1972
226	Oct. 1960	274	Oct. 1964	322	Oct. 1968	370	Oct. 1972
227	Nov. 1960	275	Nov. 1964	323	Nov. 1968	371	Nov. 1972
228	Dec. 1960	276	Dec. 1964	324	Dec. 1968	372	Dec. 1972
229	Jan. 1961	277	Jan. 1965	325	Jan. 1969	373	Jan. 1973
230	Feb. 1961	278	Feb. 1965	326	Feb. 1969	374	Feb. 1973
231	Mar. 1961	279	Mar. 1965	327	Mar. 1969	375	Mar. 1973
232	Apr. 1961	280	Apr. 1965	328	Apr. 1969	376	Apr. 1973
233	May 1961	281	May 1965	329	May 1969	377	May 1973
234	June 1961	282	June 1965	330	June 1969	378	June 1973
235	July 1961	283	July 1965	331	July 1969	379	July 1973
236	Aug. 1961	284	Aug. 1965	332	Aug. 1969	380	Aug. 1973
237	Sept. 1961	285	Sept. 1965	333	Sept. 1969	381	Sept. 1973
238	Oct. 1961	286	Oct. 1965	334	Oct. 1969	382	Oct. 1973
239	Nov. 1961	287	Nov. 1965	335	Nov. 1969	383	Nov. 1973
240	Dec. 1961	288	Dec. 1965	336	Dec. 1969	384	Dec. 1973

Table S4.6. Simulation stress period and corresponding month and year, Hadnot Point–Holcomb Boulevard study area, U.S. Marine Corps Base Camp Lejeune, North Carolina.—Continued

[Jan., January; Feb., February; Mar., March; Apr., April; Aug., August; Sept., September; Oct., October; Nov., November; Dec., December]

Stress period	Month and year	Stress period	Month and year	Stress period	Month and year	Stress period	Month and year
385	Jan. 1974	433	Jan. 1978	481	Jan. 1982	529	Jan. 1986
386	Feb. 1974	434	Feb. 1978	482	Feb. 1982	530	Feb. 1986
387	Mar. 1974	435	Mar. 1978	483	Mar. 1982	531	Mar. 1986
388	Apr. 1974	436	Apr. 1978	484	Apr. 1982	532	Apr. 1986
389	May 1974	437	May 1978	485	May 1982	533	May 1986
390	June 1974	438	June 1978	486	June 1982	534	June 1986
391	July 1974	439	July 1978	487	July 1982	535	July 1986
392	Aug. 1974	440	Aug. 1978	488	Aug. 1982	536	Aug. 1986
393	Sept. 1974	441	Sept. 1978	489	Sept. 1982	537	Sept. 1986
394	Oct. 1974	442	Oct. 1978	490	Oct. 1982	538	Oct. 1986
395	Nov. 1974	443	Nov. 1978	491	Nov. 1982	539	Nov. 1986
396	Dec. 1974	444	Dec. 1978	492	Dec. 1982	540	Dec. 1986
397	Jan. 1975	445	Jan. 1979	493	Jan. 1983	541	Jan. 1987
398	Feb. 1975	446	Feb. 1979	494	Feb. 1983	542	Feb. 1987
399	Mar. 1975	447	Mar. 1979	495	Mar. 1983	543	Mar. 1987
400	Apr. 1975	448	Apr. 1979	496	Apr. 1983	544	Apr. 1987
401	May 1975	449	May 1979	497	May 1983	545	May 1987
402	June 1975	450	June 1979	498	June 1983	546	June 1987
403	July 1975	451	July 1979	499	July 1983	547	July 1987
404	Aug. 1975	452	Aug. 1979	500	Aug. 1983	548	Aug. 1987
405	Sept. 1975	453	Sept. 1979	501	Sept. 1983	549	Sept. 1987
406	Oct. 1975	454	Oct. 1979	502	Oct. 1983	550	Oct. 1987
407	Nov. 1975	455	Nov. 1979	503	Nov. 1983	551	Nov. 1987
408	Dec. 1975	456	Dec. 1979	504	Dec. 1983	552	Dec. 1987
409	Jan. 1976	457	Jan. 1980	505	Jan. 1984	553	Jan. 1988
410	Feb. 1976	458	Feb. 1980	506	Feb. 1984	554	Feb. 1988
411	Mar. 1976	459	Mar. 1980	507	Mar. 1984	555	Mar. 1988
412	Apr. 1976	460	Apr. 1980	508	Apr. 1984	556	Apr. 1988
413	May 1976	461	May 1980	509	May 1984	557	May 1988
414	June 1976	462	June 1980	510	June 1984	558	June 1988
415	July 1976	463	July 1980	511	July 1984	559	July 1988
416	Aug. 1976	464	Aug. 1980	512	Aug. 1984	560	Aug. 1988
417	Sept. 1976	465	Sept. 1980	513	Sept. 1984	561	Sept. 1988
418	Oct. 1976	466	Oct. 1980	514	Oct. 1984	562	Oct. 1988
419	Nov. 1976	467	Nov. 1980	515	Nov. 1984	563	Nov. 1988
420	Dec. 1976	468	Dec. 1980	516	Dec. 1984	564	Dec. 1988
421	Jan. 1977	469	Jan. 1981	517	Jan. 1985	565	Jan. 1989
422	Feb. 1977	470	Feb. 1981	518	Feb. 1985	566	Feb. 1989
423	Mar. 1977	471	Mar. 1981	519	Mar. 1985	567	Mar. 1989
424	Apr. 1977	472	Apr. 1981	520	Apr. 1985	568	Apr. 1989
425	May 1977	473	May 1981	521	May 1985	569	May 1989
426	June 1977	474	June 1981	522	June 1985	570	June 1989
427	July 1977	475	July 1981	523	July 1985	571	July 1989
428	Aug. 1977	476	Aug. 1981	524	Aug. 1985	572	Aug. 1989
429	Sept. 1977	477	Sept. 1981	525	Sept. 1985	573	Sept. 1989
430	Oct. 1977	478	Oct. 1981	526	Oct. 1985	574	Oct. 1989
431	Nov. 1977	479	Nov. 1981	527	Nov. 1985	575	Nov. 1989
432	Dec. 1977	480	Dec. 1981	528	Dec. 1985	576	Dec. 1989

Table S4.6. Simulation stress period and corresponding month and year, Hadnot Point–Holcomb Boulevard study area, U.S. Marine Corps Base Camp Lejeune, North Carolina.—Continued

[Jan., January; Feb., February; Mar., March; Apr., April; Aug., August; Sept., September; Oct., October; Nov., November; Dec., December]

Stress period	Month and year	Stress period	Month and year	Stress period	Month and year	Stress period	Month and year
577	Jan. 1990	625	Jan. 1994	673	Jan. 1998	721	Jan. 2002
578	Feb. 1990	626	Feb. 1994	674	Feb. 1998	722	Feb. 2002
579	Mar. 1990	627	Mar. 1994	675	Mar. 1998	723	Mar. 2002
580	Apr. 1990	628	Apr. 1994	676	Apr. 1998	724	Apr. 2002
581	May 1990	629	May 1994	677	May 1998	725	May 2002
582	June 1990	630	June 1994	678	June 1998	726	June 2002
583	July 1990	631	July 1994	679	July 1998	727	July 2002
584	Aug. 1990	632	Aug. 1994	680	Aug. 1998	728	Aug. 2002
585	Sept. 1990	633	Sept. 1994	681	Sept. 1998	729	Sept. 2002
586	Oct. 1990	634	Oct. 1994	682	Oct. 1998	730	Oct. 2002
587	Nov. 1990	635	Nov. 1994	683	Nov. 1998	731	Nov. 2002
588	Dec. 1990	636	Dec. 1994	684	Dec. 1998	732	Dec. 2002
589	Jan. 1991	637	Jan. 1995	685	Jan. 1999	733	Jan. 2003
590	Feb. 1991	638	Feb. 1995	686	Feb. 1999	734	Feb. 2003
591	Mar. 1991	639	Mar. 1995	687	Mar. 1999	735	Mar. 2003
592	Apr. 1991	640	Apr. 1995	688	Apr. 1999	736	Apr. 2003
593	May 1991	641	May 1995	689	May 1999	737	May 2003
594	June 1991	642	June 1995	690	June 1999	738	June 2003
595	July 1991	643	July 1995	691	July 1999	739	July 2003
596	Aug. 1991	644	Aug. 1995	692	Aug. 1999	740	Aug. 2003
597	Sept. 1991	645	Sept. 1995	693	Sept. 1999	741	Sept. 2003
598	Oct. 1991	646	Oct. 1995	694	Oct. 1999	742	Oct. 2003
599	Nov. 1991	647	Nov. 1995	695	Nov. 1999	743	Nov. 2003
600	Dec. 1991	648	Dec. 1995	696	Dec. 1999	744	Dec. 2003
601	Jan. 1992	649	Jan. 1996	697	Jan. 2000	745	Jan. 2004
602	Feb. 1992	650	Feb. 1996	698	Feb. 2000	746	Feb. 2004
603	Mar. 1992	651	Mar. 1996	699	Mar. 2000	747	Mar. 2004
604	Apr. 1992	652	Apr. 1996	700	Apr. 2000	748	Apr. 2004
605	May 1992	653	May 1996	701	May 2000	749	May 2004
606	June 1992	654	June 1996	702	June 2000	750	June 2004
607	July 1992	655	July 1996	703	July 2000	751	July 2004
608	Aug. 1992	656	Aug. 1996	704	Aug. 2000	752	Aug. 2004
609	Sept. 1992	657	Sept. 1996	705	Sept. 2000	753	Sept. 2004
610	Oct. 1992	658	Oct. 1996	706	Oct. 2000	754	Oct. 2004
611	Nov. 1992	659	Nov. 1996	707	Nov. 2000	755	Nov. 2004
612	Dec. 1992	660	Dec. 1996	708	Dec. 2000	756	Dec. 2004
613	Jan. 1993	661	Jan. 1997	709	Jan. 2001	757	Jan. 2005
614	Feb. 1993	662	Feb. 1997	710	Feb. 2001	758	Feb. 2005
615	Mar. 1993	663	Mar. 1997	711	Mar. 2001	759	Mar. 2005
616	Apr. 1993	664	Apr. 1997	712	Apr. 2001	760	Apr. 2005
617	May 1993	665	May 1997	713	May 2001	761	May 2005
618	June 1993	666	June 1997	714	June 2001	762	June 2005
619	July 1993	667	July 1997	715	July 2001	763	July 2005
620	Aug. 1993	668	Aug. 1997	716	Aug. 2001	764	Aug. 2005
621	Sept. 1993	669	Sept. 1997	717	Sept. 2001	765	Sept. 2005
622	Oct. 1993	670	Oct. 1997	718	Oct. 2001	766	Oct. 2005
623	Nov. 1993	671	Nov. 1997	719	Nov. 2001	767	Nov. 2005
624	Dec. 1993	672	Dec. 1997	720	Dec. 2001	768	Dec. 2005

Table S4.6. Simulation stress period and corresponding month and year, Hadnot Point–Holcomb Boulevard study area, U.S. Marine Corps Base Camp Lejeune, North Carolina.—Continued

[Jan., January; Feb., February; Mar., March; Apr., April; Aug., August; Sept., September; Oct., October; Nov., November; Dec., December]

Stress period	Month and year	Stress period	Month and year	Stress period	Month and year
769	Jan. 2006	781	Jan. 2007	793	Jan. 2008
770	Feb. 2006	782	Feb. 2007	794	Feb. 2008
771	Mar. 2006	783	Mar. 2007	795	Mar. 2008
772	Apr. 2006	784	Apr. 2007	796	Apr. 2008
773	May 2006	785	May 2007	797	May 2008
774	June 2006	786	June 2007	798	June 2008
775	July 2006	787	July 2007		
776	Aug. 2006	788	Aug. 2007		
777	Sept. 2006	789	Sept. 2007		
778	Oct. 2006	790	Oct. 2007		
779	Nov. 2006	791	Nov. 2007		
780	Dec. 2006	792	Dec. 2007		

Table S4.8. Simulated and observed predevelopment water levels in wells within the Hadnot Point–Holcomb Boulevard study area, U.S. Marine Corps Base Camp Lejeune, North Carolina.

Site name	Water level, in feet above NGVD 29		Residual, in feet
	Simulated	Observed[1]	
Layer 1			
01-GW02	8	7.8	–0.2
01-GW03	8.2	7.7	–0.5
01-GW05	8.2	7.5	–0.7
01-GW08	7.5	5.4	–2.1
01-GW09	7.4	5.4	–2
01-GW10	7.6	6	–1.6
01-GW15	8.1	7.8	–0.3
01-GW17	8.7	8.2	–0.5
02-GW01	21.3	25.6	4.3
02-GW02	21.1	21.9	0.8
02-GW03	21.6	26.4	4.8
02-GW04	21.5	23.3	1.8
02-GW05	21.1	24	2.9
02-GW10	21.4	26.6	5.2
02-GW12	21.6	25.9	4.3
03-MW02	19	26.2	7.2
03-MW03	20.3	21.8	1.5
03-MW06	16.9	20	3.1
03-MW08	20.7	24.8	4.1
03-MW09	21.2	26.2	5
03-MW10	20.4	27.6	7.2
03-MW11	17.3	12	–5.3
03-MW12	18.4	11.7	–6.7
03-MW13	17.3	10.8	–6.5
06-GW01S	14	19.8	5.8
06-GW02S	19.3	25.7	6.4
06-GW03	13.8	15.5	1.7
06-GW06	18.2	19.2	1
06-GW07S	14	12.3	–1.7
06-GW08	15.9	16	0.1
06-GW09	11.4	12.1	0.7
06-GW11	13.7	16.3	2.6
06-GW12	14.3	12.7	–1.6
06-GW15S	15.7	19.4	3.7
06-GW18	19	21.8	2.8
06-GW20	16.9	19.9	3
06-GW21	14.5	17	2.5
06-GW22	17.9	19.1	1.2
06-GW23	17.4	19	1.6
Layer 1—Continued			
06-GW25	19.8	22.9	3.1
06-GW26	10.7	12	1.3
06-GW31	14	16.5	2.5
09-GW01	17.5	21.7	4.2
09-GW02	16.6	19.3	2.7
09-GW03	14.9	16.7	1.8
09-GW04	19.7	22.8	3.1
09-GW05	16.8	21.1	4.3
09-GW06	17.1	21.4	4.3
09-GW07S	15.7	18.2	2.5
09-GW08	17.1	21	3.9
10-MW02	15.2	17.4	2.2
10-MW03	15.5	16.1	0.6
10-MW04	13.7	13.1	–0.6
10-MW08	12.6	12.6	0
10-TW02 (new)	15.2	20.8	5.6
10-TW07	12.8	16.5	3.7
21-GW01	20	21.1	1.1
21-GW02	20	21	1
21-GW03	19.5	21.9	2.4
21-GW04	18.4	20.9	2.5
22-MW01	19.6	20.3	0.7
22-MW02	20.1	19.5	–0.6
22-MW03	19.7	20.7	1
22-MW04	20.2	21.5	1.3
22-MW05	19.2	21.9	2.7
22-MW06	19.8	20.7	0.9
22-MW07	19.3	20.9	1.6
22-MW08	19.1	20.6	1.5
22-MW09	19.1	19.4	0.3
22-MW10	20	20.5	0.5
22-MW11	18.8	20.6	1.8
22-MW12	19	20.6	1.6
22-MW13	19.7	21.3	1.6
22-MW14	18.7	19.6	0.9
22-MW15	19.1	20.7	1.6
22-MW16	19.4	18.7	–0.7
22-MW17	19.5	19.9	0.4
22-MW18	19.9	19.9	0

Table S4.8. Simulated and observed predevelopment water levels in wells within the Hadnot Point–Holcomb Boulevard study area, U.S. Marine Corps Base Camp Lejeune, North Carolina.—Continued

Site name	Water level, in feet above NGVD 29		Residual, in feet
	Simulated	Observed[1]	
Layer 1—Continued			
22-MW19	20.3	20.1	–0.2
22-MW22	18.9	20.4	1.5
22-MW23	19.5	20.9	1.4
22-RW01	19.2	19	–0.2
22-RW02	19.6	17.7	–1.9
24-GW02	11.2	9.5	–1.7
24-GW03	11	10.4	–0.6
24-GW04	11.6	10.2	–1.4
24-GW05	13.7	14.1	0.4
24-GW07 (new)	16.1	14.6	–1.5
24-GW09	10	9.9	–0.1
24-GW10	9	7.8	–1.2
28-GW04	3.7	2.7	–1
28-GW05	4.1	4	–0.1
28-GW06	0	2.3	2.3
28-GW08 (new)	2.8	1	–1.8
28-GW08 (old)	2.8	1	–1.8
74-GW02	22.4	26.1	3.7
74-GW04	22.8	22.2	–0.6
74-GW05	22.2	27	4.8
78-Bldg902_P01	20.8	23.9	3.1
78-GW01	12.1	12.2	0.1
78-GW02	12	23.2	11.2
78-GW03	11.3	8.2	–3.1
78-GW04-1	13	11.4	–1.6
78-GW05	13.7	17.1	3.4
78-GW06	13.8	13.7	–0.1
78-GW07	14.6	13.2	–1.4
78-GW08	15.5	15.2	–0.3
78-GW09-1 (old)	14.3	12.2	–2.1
78-GW10	15.5	15.5	0
78-GW11	14.7	14.5	–0.2
78-GW12	16.8	17.8	1
78-GW13	15.1	13.4	–1.7
78-GW14	16.2	16.9	0.7
78-GW15	17.3	18.3	1
78-GW16	18.8	19.7	0.9
78-GW17-1	18.3	18.5	0.2
78-GW18	17.3	16.6	–0.7
78-GW19	17.3	20.3	3
78-GW20	17.3	16.1	–1.2
78-GW21	20.6	22.9	2.3
78-GW23	20.7	22.9	2.2
78-GW24-1	20.9	25.5	4.6
78-GW25	21.2	24	2.8
78-GW26	16.4	22.8	6.4
78-GW29	8.7	9.8	1.1
78-GW33	21.5	22.5	1
78-GW35	18.2	18.2	0
78-GW36	16.3	16.5	0.2
78-GW37	12.4	10.4	–2
78-GW39	6.5	4	–2.5
78-GW40	20.6	20.5	–0.1
78-GW41	20.9	22.8	1.9
78-GW42	12.8	10.5	–2.3
78-GW43	20.7	19.7	–1
78-GW44	20.8	20.2	–0.6
78-GW45	20.1	20.2	0.1
78-GW46	20.9	20.2	–0.7
78-GW47	20.7	19.8	–0.9
78-GW48	20.7	20.6	–0.1
78-GW49	13.8	12.8	–1
78-GW50	12.6	10.9	–1.7
78-GW51	13.6	11	–2.6
78-GW52	13.4	10.8	–2.6
78-GW53	13.2	10.9	–2.3
78-GW54	11.9	10.4	–1.5
78-GW55	11.7	10.3	–1.4
78-GW56	11.5	10.4	–1.1
78-GW57	12.6	10.7	–1.9
78-GW59	11.6	10.2	–1.4
78-GW60	14.3	12.5	–1.8
78-GW61	10	9.2	–0.8
78-GW63	10	8.6	–1.4
78-GW64	10.3	7.4	–2.9
78-GW65	10.2	8.8	–1.4
78-GW66	10.7	9.3	–1.4
78-GW67	10.8	9.2	–1.6

Table S4.8. Simulated and observed predevelopment water levels in wells within the Hadnot Point–Holcomb Boulevard study area, U.S. Marine Corps Base Camp Lejeune, North Carolina.—Continued

Site name	Water level, in feet above NGVD 29		Residual, in feet
	Simulated	Observed[1]	
Layer 1—Continued			
78-GW68	11.2	9.4	–1.8
78-RW-10N	20.9	21.7	0.8
82-MW03	10	8.6	–1.4
82-MW30	14.3	22.4	8.1
84-MW17 (Baker)	5.2	5.9	0.7
84-MW18 (Baker)	6.9	15.1	8.2
84-MW19 (Baker)	5.1	4.4	–0.7
84-MW20 (Baker)	4.1	3.2	–0.9
84-MW21 (Baker)	5.9	12.1	6.2
84-MW22 (Baker)	5.6	4.7	–0.9
84-MW23 (Baker)	1.5	2	0.5
88-MW01	11.1	19.4	8.3
88-MW02	10.8	16.4	5.6
88-MW02IW	10.8	8.7	–2.1
88-MW03	10.8	17.9	7.1
88-MW03IW	10.8	9.6	–1.2
88-MW04	10.8	10.1	–0.7
88-MW04IW	10.8	10	–0.8
88-MW05	10.6	17.2	6.6
88-MW05IW	10.6	9.6	–1
88-MW06	10.6	10.7	0.1
88-MW06IW	10.6	9.5	–1.1
88-MW07	10.1	14.3	4.2
88-MW07IW	10.1	9.4	–0.7
88-MW08	10	14.7	4.7
88-MW08IW	10	9.6	–0.4
88-MW09	10.4	12.9	2.5
88-MW09IW	10.4	9.8	–0.6
88-MW10IW	10.8	8.5	–2.3
88-TW20	10.5	12.3	1.8
88-TW21	10.4	10.6	0.2
88-TW23	10.5	9.7	–0.8
88-TW25	10.3	10	–0.3
88-TW26	10.7	9.8	–0.9
94Bldg1613_ GW01	14	15.4	1.4
94Bldg1613_ GW02	14.4	17.6	3.2
94Bldg1613_ GW03	14.3	14	–0.3
94Bldg1613_ GW04	13.6	19.5	5.9
94Bldg1613_ GW05	13.5	18	4.5
94Bldg1613_ GW06	13.7	14.6	0.9
94Bldg1613_ GW07	14.8	17.3	2.5
94Bldg1613_ GW09	13.6	20.2	6.6
94Bldg1613_ GW10	14.1	14	–0.1
94Bldg1613_ GW11	13.7	13.6	–0.1
94Bldg1613_ GW12	13.9	14.3	0.4
94Bldg1613_ GW13	14.7	14.6	–0.1
94Bldg1613_ GW14	14.1	14.7	0.6
94Bldg1613_ GW16	14.1	13.4	–0.7
94Bldg1613_ GW17	13.8	13.9	0.1
94Bldg1613_ GW18	13.8	12.9	–0.9
94Bldg1613_ GW19	13.8	13.4	–0.4
94Bldg1613_ GW20	14.1	13.4	–0.7
94Bldg1613_ GW21	13.8	13.9	0.1
94Bldg1613_ GW22	13.9	13.5	–0.4
Bldg20_MW01	9.6	16.1	6.5
Bldg21_DW01	3	2	–1
Bldg21_DW02	3	2	–1
Bldg21_DW04	2.7	1.9	–0.8
Bldg21_MW01	2.9	2.4	–0.5
Bldg21_MW02	2.9	3.1	0.2
Bldg21_MW03	3.1	2.3	–0.8
Bldg21_MW04	2.9	2.4	–0.5
Bldg21_MW05	2.8	1.5	–1.3
Bldg21_MW06	2.8	2.2	–0.6

Table S4.8. Simulated and observed predevelopment water levels in wells within the Hadnot Point–Holcomb Boulevard study area, U.S. Marine Corps Base Camp Lejeune, North Carolina.—Continued

Site name	Water level, in feet above NGVD 29		Residual, in feet
	Simulated	Observed[1]	
Layer 1—Continued			
Bldg21_MW08	3	1.6	–1.4
Bldg21_MW09	3	2.5	–0.5
Bldg21_RW01	2.9	2	–0.9
Bldg24_MW01	5	10.6	5.6
Bldg33_MW01	19	23.2	4.2
Bldg33_MW02	19	23.3	4.3
Bldg33_MW03	18.9	23.1	4.2
Bldg33_MW04	19.4	26.4	7
Bldg33_MW05	18.8	25.4	6.6
Bldg33_MW06	19.7	26.8	7.1
Bldg33_MW07	18.7	25.4	6.7
Bldg33_MW08	18.7	25.5	6.8
Bldg33_MW11	19	25.6	6.6
Bldg45_MW01 (ATEC)	6.8	16.3	9.5
Bldg45_MW01 (Wright)	5.8	12.2	6.4
Bldg45_MW02 (ATEC)	6.7	15.6	8.9
Bldg45_MW02 (Wright)	5.8	7.8	2
Bldg45_MW03 (ATEC)	6.9	15.5	8.6
Bldg45_MW03 (Wright)	6.3	10.8	4.5
Bldg45_MW04 (Law)	6.7	18.2	11.5
Bldg45_MW04 (Wright)	4.8	4.7	–0.1
Bldg45_MW05 (Law)	6.5	13	6.5
Bldg45_MW07 (Law)	6.8	16.4	9.6
Bldg45_MW10 (Law)	6.6	15.2	8.6
Bldg45_MW12 (Law)	6.6	16.9	10.3
Bldg45_MW13 (Law)	6	13.8	7.8
Bldg45_MW14 (Law)	5.4	9.6	4.2
Bldg45_MW15 (Law)	5.6	11.2	5.6
Bldg45_MW16 (Law)	5.9	12.8	6.9
Bldg45_MW17 (Law)	6.5	14.3	7.8
Bldg45_MW18 (Law)	6.6	15.2	8.6
Bldg45_MW23 (E&E)	6.9	17.4	10.5
Bldg45_PW01 (Law)	6.7	14.3	7.6
Bldg61_MW01	11.7	21	9.3
Bldg61_MW02	11.7	22	10.3
Bldg61_MW03	11.7	21.6	9.9
Bldg311_MW06	8	8	0
Bldg331_MW01	7.7	6.7	–1
Bldg331_MW02	7.8	6.8	–1
Bldg331_MW03	7.9	6.9	–1
Bldg331_MW04	8	6.9	–1.1
Bldg331_MW06	8	6.7	–1.3
Bldg331_MW07	8.1	6.7	–1.4
Bldg331_MW08	7.7	6.4	–1.3
Bldg331_MW09	7.9	6.2	–1.7
Bldg331_MW10	8	6.4	–1.6
Bldg331_MW11	7.7	6.4	–1.3
Bldg331_MW12	7.9	6.9	–1
Bldg331_MW14	7.9	7.2	–0.7
Bldg331_MW15	7.7	7	–0.7
Bldg331_PW16	8	6.6	–1.4
Bldg575_MW01	6	3.3	–2.7
Bldg645_MW04	18	14.4	–3.6
Bldg645_MW06	19	17.5	–1.5
Bldg645_MW07	18.1	16.1	–2
Bldg645_MW08	18.3	16.6	–1.7
Bldg645_MW12	18.3	20.3	2
Bldg645_MW19	17.8	16.4	–1.4
Bldg645_MW24	18	19.7	1.7
Bldg645_MW25	18.2	16.4	–1.8
Bldg820_MW02	13	18	5
Bldg820_MW03	13	17.2	4.2
Bldg820_MW04	13	18.5	5.5

Table S4.8. Simulated and observed predevelopment water levels in wells within the Hadnot Point–Holcomb Boulevard study area, U.S. Marine Corps Base Camp Lejeune, North Carolina.—Continued

Site name	Water level, in feet above NGVD 29		Residual, in feet
	Simulated	Observed[1]	
Layer 1—Continued			
Bldg820_MW05	13.1	19.7	6.6
Bldg820_MW06	12.9	16.6	3.7
Bldg820_MW08	12.6	12.3	–0.3
Bldg820_MW10	12.8	18	5.2
Bldg820_MW11	13.2	18.3	5.1
Bldg820_MW12	12.9	17.4	4.5
Bldg820_MW13	12.9	16	3.1
Bldg820_MW14	13.1	16.6	3.5
Bldg820_MW15	13.4	18	4.6
Bldg820_MW16	13.1	19.1	6
Bldg820_MW18	12.8	18.3	5.5
Bldg820_MW26	12.9	14.7	1.8
Bldg820_MW27	13.2	19.7	6.5
Bldg900_MW01	21	22.1	1.1
Bldg900_MW02	21.1	25.7	4.6
Bldg900_MW03	21	22.2	1.2
Bldg900_MW04	21	25.1	4.1
Bldg900_MW05	21.1	25.4	4.3
Bldg900_MW07	21.1	26	4.9
Bldg900_MW08	20.8	23.9	3.1
Bldg900_MW09	21	24.2	3.2
Bldg900_MW10	20.9	25	4.1
Bldg903_MW01	21.2	23.5	2.3
Bldg903_MW02	21.2	23.8	2.6
Bldg903_MW03	21.2	24	2.8
Bldg903_MW04	21.2	24.6	3.4
Bldg1101_MW01	18.4	19	0.6
Bldg1101_MW02	18.2	18.6	0.4
Bldg1101_MW03	18	18.5	0.5
Bldg1106_PZ01	19.2	22.9	3.7
Bldg1106_PZ02	19.2	22	2.8
Bldg1106_PZ03	19.2	23	3.8
Bldg1106_PZ04	19.3	21.2	1.9
Bldg1115_GT02	17.7	20	2.3
Bldg1115_GT03	17.5	20.2	2.7
Bldg1115_GT04	17.5	20.2	2.7
Bldg1115_GT05	17.5	19.6	2.1
Bldg1115_GT06	17.7	20.6	2.9
Bldg1115_GT07	17.9	19.7	1.8

Site name	Water level, in feet above NGVD 29		Residual, in feet
	Simulated	Observed[1]	
Layer 1—Continued			
Bldg1115_GT08	18.1	20.5	2.4
Bldg1115_GT09	18.2	20.6	2.4
Bldg1115_MW01	17.3	17.8	0.5
Bldg1115_MW02	16.9	17.6	0.7
Bldg1115_MW03	17.9	18.1	0.2
Bldg1115_MW05	17.5	20.8	3.3
Bldg1115_MW06	17.1	17.9	0.8
Bldg1115_MW07	18.3	18.9	0.6
Bldg1115_MW08	16.9	17.5	0.6
Bldg1115_MW09	17.7	18.2	0.5
Bldg1115_MW10	17.5	19.8	2.3
Bldg1115_MW11	17.4	18.9	1.5
Bldg1115_MW12	17.8	20.7	2.9
Bldg1115_MW13	17.5	16.9	–0.6
Bldg1115_MW14	17.4	17.1	–0.3
Bldg1115_MW15	17.8	17.5	–0.3
Bldg1115_MW16	17.5	18.1	0.6
Bldg1115_MW17	16.9	16	–0.9
Bldg1115_MW18	18.3	17.1	–1.2
Bldg1115_MW19	18.3	18.1	–0.2
Bldg1115_MW20	17.9	16.9	–1
Bldg1115_MW21	16.9	17	0.1
Bldg1310_MW02	17	16.7	–0.3
Bldg1310_MW03	17.1	16.9	–0.2
Bldg1323_MW01	14.2	15.3	1.1
Bldg1323_MW02	14.4	15.2	0.8
Bldg1323_TMW01	14.4	14.1	–0.3
Bldg1450_MW01	13.1	12.4	–0.7
Bldg1450_MW02	13.3	12.6	–0.7
Bldg1450_MW03	13.3	12.8	–0.5
Bldg1450_MW04	13.1	12.4	–0.7
Bldg1450_MW05	12.9	12.3	–0.6
Bldg1450_MW06	13.1	12.5	–0.6
Bldg1502_MW01 (new)	14.7	15.2	0.5
Bldg1502_MW01 (old)	15.5	14.9	–0.6
Bldg1502_MW02 (new)	14.2	15.1	0.9

Table S4.8. Simulated and observed predevelopment water levels in wells within the Hadnot Point–Holcomb Boulevard study area, U.S. Marine Corps Base Camp Lejeune, North Carolina.—Continued

Site name	Water level, in feet above NGVD 29		Residual, in feet
	Simulated	Observed[1]	
Layer 1—Continued			
Bldg1502_MW02 (old)	15.5	15	−0.5
Bldg1502_MW03	15.5	15	−0.5
Bldg1502_MW04	15.5	15	−0.5
Bldg1601_DP01	14.4	16.6	2.2
Bldg1601_DP02	14.4	16.8	2.4
Bldg1601_DP03	14.4	17	2.6
Bldg1601_DP04	14.3	16.9	2.6
Bldg1601_DP05	14.4	17	2.6
Bldg1601_DP06	14.4	16.5	2.1
Bldg1601_DP07	14.4	16.7	2.3
Bldg1601_DP08	14.4	16.9	2.5
Bldg1601_DP09	14.3	16.7	2.4
Bldg1601_DP10	14.4	17.3	2.9
Bldg1601_DP11	14.5	17.3	2.8
Bldg1601_DP12	14.5	16.8	2.3
Bldg1601_DP13	14.5	16.9	2.4
Bldg1601_DP14	14.4	15.5	1.1
Bldg1601_DP15	14.4	17.5	3.1
Bldg1601_DP16	14.4	17.8	3.4
Bldg1607_MW01	13.6	19.2	5.6
Bldg1607_MW02	13.6	19.9	6.3
Bldg1607_MW03	13.6	19.7	6.1
Bldg1854_MW01	6.9	4.8	−2.1
Bldg1854_MW02	6.9	4.6	−2.3
Bldg1854_MW06	6.9	4.6	−2.3
Bldg1854_MW08	6.7	4.5	−2.2
Bldg1919-1_MW01	2.4	2	−0.4
Bldg1919-1_MW02	2.4	2.1	−0.3
Bldg1919-1_MW03	2.4	2.1	−0.3
Bldg1932_MW01	4.3	4.3	0
Bldg1932_MW02	4.3	3.1	−1.2
Bldg1932_MW03	4.3	3	−1.3
BldgFC102_MW01 (new)	10	9.8	−0.2
BldgFC102_MW01 (old)	10	13	3
BldgFC102_MW02 (new)	10	9.6	−0.4
BldgFC102_MW02 (old)	9.9	14.3	4.4
BldgFC102_MW03 (new)	10	9.8	−0.2
BldgFC102_MW03 (old)	10	16	6
BldgFC201E_E01	11.9	13.8	1.9
BldgFC201E_E02	11.9	14.1	2.2
BldgFC201E_E03	11.9	13.6	1.7
BldgFC201E_MW04	11.8	13	1.2
BldgFC201E_MW05	12.1	13.2	1.1
BldgFC201E_MW07	11.9	13.2	1.3
BldgFC201E_MW10	11.8	12.8	1
BldgFC201E_MW13	12.3	13.4	1.1
BldgFC201E_MW14	12.1	13.1	1
BldgFC201E_MW15	11.7	12.9	1.2
BldgFC201E_MW16	11.4	13.2	1.8
BldgFC201W_MW01	11.6	13.2	1.6
BldgFC201W_MW02	11.6	14.2	2.6
BldgFC201W_MW03	11.6	13	1.4
BldgFC263_MW01	11.9	9.2	−2.7
BldgFC263_MW02	12.2	10.1	−2.1
BldgFC263_MW03	11.7	9.4	−2.3
BldgFC263_MW04	12.3	9.9	−2.4
BldgFC263_MW05	11.7	9.7	−2
BldgFC263_MW06	11.4	9.4	−2

Table S4.8. Simulated and observed predevelopment water levels in wells within the Hadnot Point–Holcomb Boulevard study area, U.S. Marine Corps Base Camp Lejeune, North Carolina.—Continued

Site name	Water level, in feet above NGVD 29		Residual, in feet
	Simulated	Observed[1]	
Layer 1—Continued			
BldgFC263_MW07	11.5	9.1	–2.4
BldgFC263_MW08	11.8	9.1	–2.7
BldgFC263_MW09	11.7	9	–2.7
BldgFC263_MW10	12.2	10.2	–2
BldgFC263_MW11	12.1	10	–2.1
BldgFC263_MW12	11.9	9.7	–2.2
BldgFC263_MW13	11.4	8.6	–2.8
BldgFC263_MW14	12.3	9.4	–2.9
BldgFC263_MW16	11.9	9.7	–2.2
BldgFC280_MW01	14.7	14.4	–0.3
BldgFC281_MW01	15.8	17	1.2
BldgH19_MW01	1.3	2.4	1.1
BldgH19_MW02	1.3	4.1	2.8
BldgH19_MW03	1.3	4	2.7
BldgH19_MW04	1.3	4	2.7
BldgH19_MW05	1.3	3.9	2.6
BldgH19_MW06	1.3	3.9	2.6
BldgH19_MW07	1.3	2.5	1.2
BldgH19_MW08	1.3	2.6	1.3
BldgH19_MW09	1.4	2.4	1
BldgH19_MW10	1.4	2.4	1
BldgH19_MW14	1.3	2.4	1.1
BldgH28_MW01	0.7	2.6	1.9
BldgH28_MW02	1	2.7	1.7
BldgH28_MW03	1.1	2.7	1.6
BldgH28_MW04	1.1	2.1	1
BldgH28_MW05	1.1	2.6	1.5
BldgH28_MW06	1	2.7	1.7
BldgH28_MW07	0.9	2.5	1.6
BldgH28_MW08	1	2.6	1.6
BldgH28_MW09	1	2.7	1.7
BldgH28_MW10	0.9	2.6	1.7
BldgH28_MW11	1	2.6	1.6
BldgH30_MW01	0.6	2.4	1.8
BldgH30_MW02	0.6	2.5	1.9
BldgH30_MW05	0.6	2.4	1.8
BldgH30_MW12	0.5	2.4	1.9
BldgHP100_PZ01	7.7	6.3	–1.4
BldgHP100_PZ03	7.7	6.4	–1.3
BldgHP100_PZ04	7.7	7.2	–0.5
BldgHP100_PZ06	7.6	7	–0.6
BldgHP100_PZ07	7.7	6.5	–1.2
BldgHP100_PZ08	7.7	7.4	–0.3
BldgHP250_MW01	4.8	10.7	5.9
BldgLCH4015_MW03	22.9	27.3	4.4
BldgLCH4015_MW04	23.2	27.4	4.2
BldgLCH4015_MW05	22.7	27.2	4.5
BldgLCH4015_MW06	22.6	26.7	4.1
BldgLCH4015_MW07	23.1	27.6	4.5
BldgLCH4015_MW08	23.1	26.9	3.8
BldgLCH4015_MW11	22.6	25.1	2.5
BldgLCH4015_MW12	22.7	25.4	2.7
BldgLCH4015_MW14	22.8	25.5	2.7
BldgLCH4015_MW15	23	25.7	2.7
BldgLCH4015_MW16	23.2	28	4.8
BldgLCH4015_MW18	22.9	28.3	5.4
BldgLCH4022_MW01	22.1	27.2	5.1
BldgLCH4022_MW03	22.2	27.1	4.9
BldgLCH4022_MW19	22.1	26.9	4.8

Table S4.8. Simulated and observed predevelopment water levels in wells within the Hadnot Point–Holcomb Boulevard study area, U.S. Marine Corps Base Camp Lejeune, North Carolina.—Continued

Site name	Water level, in feet above NGVD 29		Residual, in feet
	Simulated	Observed[1]	
Layer 1—Continued			
BldgPT5_MW02	11.1	11.8	0.7
BldgPT5_MW03	10.8	11	0.2
BldgPT5_MW04	10.8	11.5	0.7
BldgPT5_MW09	10.6	11.2	0.6
BldgPT37_MW01	5.4	4.9	–0.5
BldgS688_MW01	3	3.3	0.3
BldgS2633_MW02	5.2	1.7	–3.5
BldgSLCH4019_ MW05	22.2	26.8	4.6
BldgSLCH4019_ MW06	22.4	27	4.6
G-BP06	21.8	22.8	1
G-MW03S	15.5	21.2	5.7
G-MW04	14.4	16.3	1.9
G-MW05	18.4	22.1	3.7
G-MW08	20.7	22.2	1.5
G10-MW10	30.5	30.8	0.3
G10-MW7	35.1	38	2.9
G10-MW8	17.7	18.6	0.9
G10-MW9	19.4	18.9	–0.5
HP-585	35.7	31	–4.7
HP-708-4	28.2	31.9	3.7
HPFF_MW01	19.5	23.3	3.8
HPFF_MW02	19.8	22.7	2.9
HPFF_MW03	20.4	21.4	1
HPFF_MW04	20	21.5	1.5
HPFF_MW05	18.6	20.2	1.6
HPFF_MW06	20.1	20.1	0
HPFF_MW07	19.4	19	–0.4
HPFF_MW09	18.6	18.4	–0.2
HPFF_MW14	19	21.5	2.5
HPFF_MW15	19.4	21.1	1.7
HPFF_MW16	18.2	20.6	2.4
HPFF_MW17	18.7	19.4	0.7
HPFF_MW18	18	18.9	0.9
HPFF_MW19	19	20.9	1.9
HPFF_MW20	20.3	21	0.7
HPFF_MW21	18.9	22.8	3.9
HPFF_MW22	19.3	22.4	3.1
HPFF_MW23	18.5	18.4	–0.1
HPFF_MW24	18.5	20.1	1.6
HPFF_MW25	18.6	19.7	1.1
HPFF_MW26	18.3	19.1	0.8
HPFF_MW27	18.1	19.3	1.2
HPFF_MW28	18.9	20.8	1.9
HPFF_MW29	19.2	21.1	1.9
HPFF_MW30	19.2	22.2	3
HPFF_MW31	18.6	19.9	1.3
HPFF_MW32	18.4	19.8	1.4
HPFF_MW33	18	19.1	1.1
HPFF_MW34	17.7	18	0.3
HPFF_MW35	18.1	18.8	0.7
HPFF_MW36	17.8	18.8	1
HPFF_MW37	17.3	18.5	1.2
HPFF_MW38	20.1	22.8	2.7
HPFF_MW40	19.3	22.1	2.8
HPFF_MW41	19.1	21.2	2.1
HPFF_MW42	19	21.4	2.4
HPFF_MW44	15	14.1	–0.9
HPFF_MW47	16.2	15.1	–1.1
HPFF_MW48	16.9	17	0.1
HPFF_MW50	16.9	16.3	–0.6
HPFF_MW51	17.6	17.7	0.1
HPFF_MW53	18.4	17.7	–0.7
HPFF_MW57	17.3	16.8	–0.5
HPFF_MW61	19	17.6	–1.4
HPFF_MW63	18	15.9	–2.1
HPFF_MW64	19.4	18.3	–1.1
HPFF_MW66	19.1	18.3	–0.8
HPFF_MW68	19.2	20.8	1.6
HPFF_MW69	19.9	18.3	–1.6
HPFF_MW70	20	19.4	–0.6
HPGW22-1	19.4	20.6	1.2
HPGW22-2	18.3	20.4	2.1
TankS781_MW01 (O&G)	5.4	4.3	–1.1
TankS781_MW03 (O&G)	4.9	3.7	–1.2
TankS781_MW05 (O&G)	5.4	3.7	–1.7

Table S4.8. Simulated and observed predevelopment water levels in wells within the Hadnot Point–Holcomb Boulevard study area, U.S. Marine Corps Base Camp Lejeune, North Carolina.—Continued

Site name	Water level, in feet above NGVD 29		Residual, in feet
	Simulated	Observed[1]	
Layer 1—Continued			
TankS781_MW09 (O&G)	3	2.8	−0.2
TankS781_MW11 (O&G)	5.1	8.2	3.1
TankS781_MWA (D&D)	4.8	4.5	−0.3
TankS781_MWB (D&D)	4.9	4.6	−0.3
SOW3	17.3	9	−8.3
SOW2	7.2	9	1.8
M-1	24	22.8	−1.2
M-2	25.1	17.4	−7.7
Layer 2			
LCH-4007	24.9	13.4	−11.5
Layer 3			
01-GW16DW	7.7	6.5	−1.2
01-GW17DW	8.3	8.3	0
78-GW04-2	12.5	10.2	−2.3
78-GW09-2	13.6	12.8	−0.8
78-GW17-2	17.8	17.3	−0.5
78-GW24-2	19.6	20.3	0.7
78-GW30-2	19.2	18.1	−1.1
78-GW31-2	16.2	15.1	−1.1
78-GW32-2	18	17.1	−0.9
80-MW01	3.3	3.3	0
80-MW02	3.2	2.7	−0.5
80-MW03	4	5.1	1.1
80-MW04	4	3.2	−0.8
80-MW05	3.5	3.4	−0.1
80-MW06	3.1	3.2	0.1
80-MW07	4.2	3.9	−0.3
80-MW08	3.7	2.6	−1.1
84-MW16 (Baker)	5.5	5	−0.5
88-MW02DW	9.8	8.6	−1.2
88-MW03DW	9.8	9.4	−0.4
88-MW04DW	9.9	9.8	−0.1
88-MW05DW	9.6	9.4	−0.2

Site name	Water level, in feet above NGVD 29		Residual, in feet
	Simulated	Observed[1]	
Layer 3—Continued			
Bldg45_MW06 (Law)	6.4	5.3	−1.1
Bldg45_MW09 (Law)	6.3	5.2	−1.1
Bldg45_MW21 (Law)	5	5	0
Bldg45_MW22 (Law)	6.4	4	−2.4
Bldg645_MW01	17.6	16	−1.6
Bldg645_MW02	17.6	16.1	−1.5
Bldg645_MW03	17.6	16.1	−1.5
Bldg645_MW05	17.8	17	−0.8
Bldg645_MW09	17.7	16.1	−1.6
Bldg645_MW10	17.5	16.1	−1.4
Bldg645_MW11	17.7	16.3	−1.4
Bldg645_MW13	17.7	16.5	−1.2
Bldg645_MW14	17.5	16.1	−1.4
Bldg645_MW20	17.2	16.3	−0.9
Bldg645_MW23	17.7	18	0.3
Bldg820_MW07	12.3	12.7	0.4
Bldg820_MW09	12.6	11.2	−1.4
Bldg820_MW17	12.6	11.8	−0.8
Bldg820_MW19	12.4	11.9	−0.5
Bldg820_MW21	12.1	11.7	−0.4
Bldg820_MW23	11.9	13	1.1
Bldg820_MW25	11.9	13	1.1
Bldg1115_MW22	16.3	15.7	−0.6
Bldg1115_MW23	17.6	17.1	−0.5
Bldg1115_MW24	16.3	15.8	−0.5
Bldg1115_MW25	16.9	16.4	−0.5
BldgH19_MW11	0.9	2.6	1.7
BldgH19_MW13	0.9	2.6	1.7
BldgLCH4015_MW13	20.5	10.5	−10
BldgLCH4015_MW19	20.8	6.6	−14.2
BldgLCH4015_MW20	20.7	6.4	−14.3

Table S4.8. Simulated and observed predevelopment water levels in wells within the Hadnot Point–Holcomb Boulevard study area, U.S. Marine Corps Base Camp Lejeune, North Carolina.—Continued

Site name	Water level, in feet above NGVD 29		Residual, in feet
	Simulated	Observed[1]	
Layer 3—Continued			
BldgLCH4015_MW21	20.8	7.8	−13
BldgLCH4015_MW22	20.7	7.7	−13
BldgLCH4015_MW23	20.9	7.8	−13.1
BldgS2633_MW06DW	4.6	3.4	−1.2
BldgSLCH4019_MW04	20.3	3.2	−17.1
BldgSLCH4019_MW10	20.1	2.6	−17.5
HP-609	16	18.7	2.7
HP-620	19.9	14	−5.9
HPFF_MW10	18.7	18.2	−0.5
HPFF_MW43	14.2	13.2	−1
HPFF_MW45	15.6	15.2	−0.4
HPFF_MW49	16.3	15.8	−0.5
HPFF_MW55	17.6	18.4	0.8
HPFF_MW58	17.6	17.4	−0.2
HPFF_MW59	18.4	18.4	0
HPFF_MW65	18.5	18.1	−0.4
HPFF_MW67	18.2	17.3	−0.9
HPFF_MW71	18.9	17.9	−1
TankS781_MW02 (O&G)	5.1	3.8	−1.3
TankS781_MW04 (O&G)	4.6	3.6	−1
TankS781_MW06 (O&G)	5.2	3.5	−1.7
TankS781_MW08 (O&G)	3.5	2.9	−0.6
TankS781_MW10 (O&G)	3	2.7	−0.3
TankS781_MW12 (O&G)	4.8	4.3	−0.5
TankS781_MW14 (O&G)	3	2.7	−0.3
SOW5	7.4	9	1.6

Site name	Water level, in feet above NGVD 29		Residual, in feet
	Simulated	Observed[1]	
Layer 4			
06-GW01D	12.5	12	−0.5
06-GW02DW	16	15.7	−0.3
06-GW36D	12.9	12.4	−0.5
G-MW03D	14.1	15.3	1.2
HP-37	0.7	0.9	0.2
HPFF_MW11	18	18.3	0.3
HPFF_MW12	17.5	17.6	0.1
Layer 5			
06-GW07DW	13.4	13.1	−0.3
06-GW15D	13.1	7	−6.1
06-GW27DW	9.7	9.3	−0.4
06-GW28DW	10	9.6	−0.4
06-GW30DW	11.3	10.1	−1.2
06-GW35D	9.1	9.1	0
06-GW37DW	7.9	9.1	1.2
06-GW40DW	11	6.2	−4.8
06-GW43DW	7.6	7	−0.6
09-GW07D	15.6	13.4	−2.2
28-GW01DW	3	1.4	−1.6
28-GW07DW	3.7	2.3	−1.4
28-GW09DW	3.9	2.5	−1.4
78-642-1	19.8	21	1.2
78-642-2	19.3	20	0.7
78-GW04-3	11.3	10.5	−0.8
78-GW09-3	12.5	14.4	1.9
78-GW17-3	16.4	18	1.6
78-GW24-3	18.7	20	1.3
78-GW30-3	18.3	17.9	−0.4
78-GW31-3	14.6	15.4	0.8
78-GW32-3	16.5	17.4	0.9
80-MW03IW	3.7	2.8	−0.9
Bldg645_MW15	17.1	15.1	−2
Bldg645_MW16	16.9	15.7	−1.2
Bldg645_MW17	16.8	15.5	−1.3
Bldg645_MW18	17.6	18.5	0.9

Table S4.8. Simulated and observed predevelopment water levels in wells within the Hadnot Point–Holcomb Boulevard study area, U.S. Marine Corps Base Camp Lejeune, North Carolina.—Continued

Site name	Water level, in feet above NGVD 29		Residual, in feet
	Simulated	Observed[1]	
Layer 5—Continued			
Bldg645_MW21	16.9	16	–0.9
Bldg645_MW22	17.2	15.6	–1.6
Bldg645_MW26	17.3	15.6	–1.7
Bldg645_MW27	17.8	14.8	–3
Bldg645_MW28	17.2	15	–2.2
Bldg645_MW29	17.6	14.7	–2.9
Bldg645_MW30	17.9	23.2	5.3
Bldg645_MW31	17.6	13.1	–4.5
Bldg645_MW32	17.6	15	–2.6
Bldg820_MW09D	11.7	12.4	0.7
HP-650	24.4	26.9	2.5
HP-651	12.6	13.7	1.1
HP-652	24.3	26.5	2.2
HP-699	8.2	8	–0.2
HP-700	6.6	4.5	–2.1
HP-705	23.5	16	–7.5
HP-708	27.4	31.1	3.7
HP-709	16.6	13	–3.6
HPFF_MW13	15.1	15.9	0.8
HPFF_MW46	14.2	15	0.8
HPFF_MW52	16.4	18.2	1.8
HPFF_MW56	15.1	17.1	2
HPFF_MW60	16.7	18.1	1.4
HPFF_MW62	16.5	15.1	–1.4
LCH-4009	22.1	16.8	–5.3
R(1950)	4	8	4
S190A	6.7	2	–4.7
SOW4	15.9	15	–0.9
X24S1	4.6	3.6	–1
X24S6	6.3	5.8	–0.5

Site name	Water level, in feet above NGVD 29		Residual, in feet
	Simulated	Observed[1]	
Layer 7			
06-GW01DA	12.1	10.3	–1.8
06-GW01DB	12.4	7.5	–4.9
06-GW27DA	10.6	7.1	–3.5
06-GW38D	11.7	8.7	–3
06-GW39D	8.7	5.9	–2.8
06-GW40DA	11.9	11.5	–0.4
Multilayer			
HP-557	28	26	–2
HP-558	29.2	28	–1.2
HP-595	32.5	33	0.5
HP-596	33.7	34	0.3
HP-601	13.2	15.4	2.2
HP-602	15.5	14.1	–1.4
HP-603	11.5	11.6	0.1
HP-604	14.8	16	1.2
HP-605	19.8	19	–0.8
HP-606	17.6	17.3	–0.3
HP-607 (new)	15	8	–7
HP-607 (old)	15.5	15	–0.5
HP-608	11.4	10.2	–1.2
HP-610	13.8	12.4	–1.4
HP-611 (new)	29.3	33.6	4.3
HP-611 (old)	13.2	15.5	2.3
HP-612 (new)	30.7	32.9	2.2
HP-612 (old)	15.3	15	–0.3
HP-613	17.1	9.3	–7.8
HP-614 (new)	26.3	28	1.7
HP-614 (old)	13.8	13.4	–0.4
HP-615	16	14.7	–1.3
HP-616	19.1	13.3	–5.8

Table S4.8. Simulated and observed predevelopment water levels in wells within the Hadnot Point–Holcomb Boulevard study area, U.S. Marine Corps Base Camp Lejeune, North Carolina.—Continued

Site name	Water level, in feet above NGVD 29		Residual, in feet
	Simulated	Observed[1]	
Multilayer—Continued			
HP-618 (new)	25.2	20	–5.2
HP-619 (new)	26.1	30	3.9
HP-621 (new)	21.5	8	–13.5
HP-622	13.7	16.1	2.4
HP-623	13.1	14.6	1.5
HP-625	12	9	–3
HP-627 (new)	20.9	19	–1.9
HP-628 (new)	12.8	10	–2.8
HP-628 (old)	15	4.5	–10.5
HP-629 (old)	25.1	23.7	–1.4
HP-630	15.9	16	0.1
HP-631	24.4	25.8	1.4
HP-633	9.4	7.6	–1.8
HP-634	19.4	20.3	0.9
HP-635	16.2	17	0.8
HP-636	17	15.8	–1.2
HP-637	15.1	14.2	–0.9
HP-638	8.2	5.8	–2.4
HP-641	20.5	15.2	–5.3
HP-642	19.7	22.7	3
HP-643	12	13.2	1.2
HP-644	14.2	10.4	–3.8
HP-645	17.1	10.1	–7
HP-646	18	8	–10
HP-647	21.6	10.3	–11.3
HP-648	23.5	23.1	–0.4
HP-649	23.3	20.9	–2.4
HP-653	16.7	14.9	–1.8
HP-654	20.6	19.2	–1.4
HP-660	12.9	11.5	–1.4
HP-661	13.8	16	2.2
HP-662	14.7	14	–0.7
HP-663	21.3	19	–2.3
HP-698	9.8	10	0.2
HP-701	6.7	5	–1.7
HP-703	13.4	9	–4.4
HP-704	8.8	6	–2.8
HP-706	24.2	19	–5.2
HP-707	11.5	10	–1.5
HP-710	15.6	13.5	–2.1
HP-711	17.4	17.5	0.1
HP-5186	16.5	12	–4.5

[1] See Faye et al. (2013, Table S3.4) for data sources and additional details. Table S3.4 (Faye et al. 2013) uses the term “estimated potentiometric level” instead of “observed” water level.

Statistics:

Minimum residual = –17.5 feet
Maximum residual = 11.5 feet
Average residual = 0.5 feet
Standard deviation = 3.3 feet
Root-mean-square residual = 3.39 feet

ATSDR
AGENCY FOR TOXIC SUBSTANCES
AND DISEASE REGISTRY

Analyses and Historical Reconstruction of Groundwater Flow, Contaminant Fate and Transport, and Distribution of Drinking Water Within the Service Areas of the Hadnot Point and Holcomb Boulevard Water Treatment Plants and Vicinities, U.S. Marine Corps Base Camp Lejeune, North Carolina—Chapter A–Supplement 4: Simulation of Three-Dimensional Groundwater Flow